

AD-A194 789

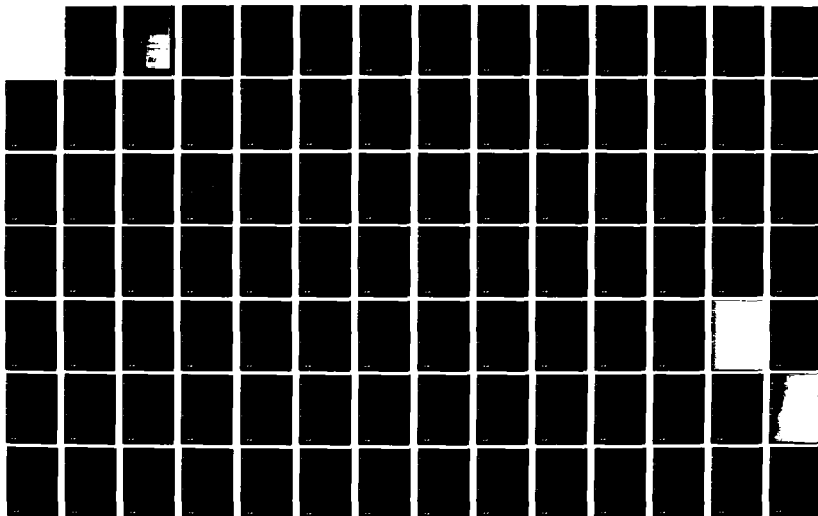
FISCAL YEAR 1986 PROGRAM 26802 - TASK 28 ADM TEST
RESULTS(U) MECHANICAL TECHNOLOGY INC LATHAM NY STIRLING
ENGINE SYSTEMS DIV M DHAR FEB 87 MTI-87SESD37
DRAK78-82-C-0255

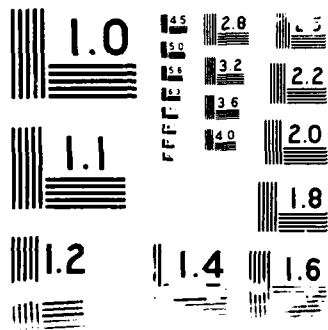
1/1

UNCLASSIFIED

F/G 21/7

NL

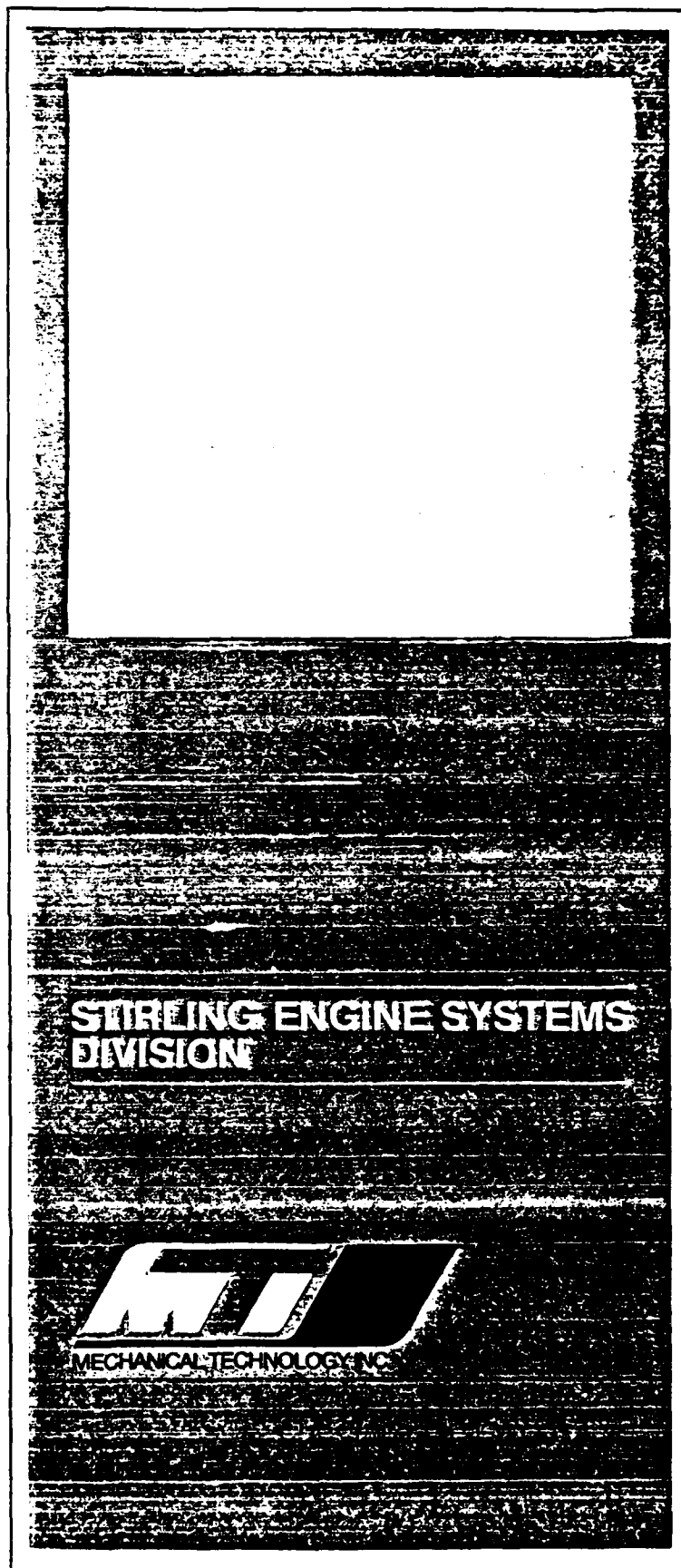




AD-A194 709

DTIC
SELECTE
MAY 11 1988
D

DISTRIBUTION STATEMENT A
Approved for public release
Distribution Unlimited



1

MTI 87SESD37

**FY86 IR&D PROGRAM 26802 - TASK 2.0
ADM TEST RESULTS**

**Prepared by:
M. Dhar**

February 1987

DTIC
ELECTE
S MAY 11 1988 **D**
GoD

DISTRIBUTION STATEMENT A

**Approved for public release
Distribution Unlimited**

**MECHANICAL TECHNOLOGY INCORPORATED
968 Albany-Shaker Road
Latham, New York 12110**

MTI 87SED37

FY86 IR&D PROGRAM 26802 - TASK 2.0

ADM TEST RESULTS



Prepared by:

M. Dhar

February 1987

Accession For	
NDS CRASH	<input checked="" type="checkbox"/>
DTC TAB	<input type="checkbox"/>
Unarmoured	<input type="checkbox"/>
Justified	
per ltr	
Date	
Author	
Title	
Subject	
A-1	

MECHANICAL TECHNOLOGY INCORPORATED
968 Albany-Shaker Road
Latham, New York 12110

Table of Contents

	<u>PAGE</u>
List of Figures	iii
List of Tables	vii
Background	1
Task Objective	1
Executive Summary	1
Introduction	3
ADM Engine with Monolithic Head	3
Instrumentation	6
Tests Performed	11
Test 1 - Baseline Configuration Test	12
Test 2 - Without Stator O-Ring	25
Test 3 - Repeat Baseline Configuration Engine Test With Stator O-Ring In	32
Test 4 - Locked Displacer Test	32
Performance Prediction of ADM Monolithic Head at Larger Piston Amplitudes	37
ADM Hardware Modification	53
APPENDIX A: HISTORICAL DESCRIPTION OF THE ADM ENGINE DIAGNOSTIC TESTS	A-1
APPENDIX B: TUBED HEAD ADM ENGINE TEST	B-1
APPENDIX C: SEAL CLEARANCE SUMMARY AND INSPECTION REPORTS	C-1
APPENDIX D: TRANSDUCER CALIBRATION REPORTS	D-1



LIST OF FIGURES

<u>NUMBER</u>	<u>PAGE</u>
1 ADM Monolithic Head Power Module	2
2 ADM Engine Configuration	4
3 Bearing Supply and Piston Offset Control Scheme	7
4 Slope/Intercept Plot; Head Temperature = 760°C, Piston Stroke = 14 mm, Displacer Phase Angle = 66°	13
5 Slope/Intercept Plot; Head Temperature = 660°C, Piston Stroke = 14 mm, Displacer Phase Angle = 66°	14
6 Slope/Intercept Plot; Head Temperature = 560°C, Piston Stroke = 14 mm, Displacer Phase Angle = 66°	15
7 Slope Comparison of Slope/Intercept Curve; Head Temperature = 660°C, Piston Stroke = 14 mm, Displacer Phase Angle = 66°	16
8 Slope Comparison of Slope/Intercept Curve; Head Temperature = 560°C, Piston Stroke = 14 mm, Displacer Phase Angle = 66°	17
9 PV Power Comparison for FY84 and FY86 (O-Ring In) Engine Builds; Head Temperature = 660°C	19
10 PV Power Comparison for FY84 and FY86 (O-Ring In) Engine Builds; Head Temperature = 560°C	20
11 Regenerator Temperatures with O-Ring In; Head Temperature = 660°C . . .	21
12 Regenerator Temperatures with O-Ring In; Head Temperature = 560°C . . .	22
13 Predicted and Measured Regenerator Temperatures; Head Temperature = 660°C	23
14 Predicted and Measured Regenerator Temperatures; Head Temperature = 560°C	24
15 PV Power With and Without Stator O-Ring; Head Temperature = 660°C . . .	26
16 PV Power With and Without Stator O-Ring; Head Temperature = 560°C . . .	27
17 PV Power Comparison for FY84 and FY86 (O-Ring Out) Engine Build; Head Temperature = 660°C	28
18 PV Power Comparison for FY84 and FY86 (O-Ring Out) Engine Build; Head Temperature = 560°C	29
19 Regenerator Temperatures with O-Ring Out; Head Temperature = 660°C . .	30
20 Regenerator Temperatures with O-Ring Out; Head Temperature = 560°C . .	31
21 PV Power Repeat Test with Stator O-Ring In; Head Temperature = 660°C .	33



LIST OF FIGURES (Continued)

NUMBER	PAGE
22 PV Power Repeat Test with Stator O-Ring In; Head Temperature = 560°C . .	34
23 Regenerator Temperatures; Repeat Test with Stator O-Ring In; Head Temperature = 660°C	35
24 Regenerator Temperatures; Repeat Test with Stator O-Ring In; Head Temperature = 560°C	36
25 Locked-Displacer Test; Comparison of CFAST Code Predictions and Measured Test Data	38
26 Locked-Displacer Test; Comparison of HFAST Code Predictions and Measured Test Data	39
27 Comparison of Test Data with Modified HFAST Code Predictions	40
28 Plot of Measured PV Power versus Piston Amplitude Square	41
29 HFAST-Predicted PV Power at 9-mm Piston Amplitude; Temperature Ratio = 760/50°C; Leakage Coefficient = $1.343 \cdot 10^{-13} \text{ m}^3$	43
30 HFAST-Predicted PV Power at 9-mm Piston Amplitude; Temperature Ratio = 660/50°C; Leakage Coefficient = $1.343 \cdot 10^{-13} \text{ m}^3$	44
31 HFAST-Predicted Heater Head Heat Input; 9-mm Piston Amplitude; Temperature Ratio = 760/50°C; Leakage Coefficient = $1.343 \cdot 10^{-13} \text{ m}^3$. .	45
32 HFAST-Predicted Heater Head Heat Input; 9-mm Piston Amplitude; Temperature Ratio = 660/50°C; Leakage Coefficient = $1.343 \cdot 10^{-13} \text{ m}^3$. .	46
33 HFAST-Predicted PV Power at 9-mm Displacer Amplitude; Temperature Ratio = 760/50°C; Leakage Coefficient = $1.343 \cdot 10^{-13} \text{ m}^3$	47
34 HFAST-Predicted PV Power at 9-mm Displacer Amplitude; Temperature Ratio = 660/50°C; Leakage Coefficient = $1.343 \cdot 10^{-13} \text{ m}^3$	48
35 HFAST-Predicted Heater Head Heat Input; Displacer Amplitude = 9-mm; Temperature Ratio = 760/50°C; Leakage Coefficient = $1.343 \cdot 10^{-13} \text{ m}^3$. .	49
36 HFAST-Predicted Heater Head Heat Input; Displacer Amplitude = 9-mm; Temperature Ratio = 660/50°C; Leakage Coefficient = $1.343 \cdot 10^{-13} \text{ m}^3$. .	50
37 Leakage Loss as a Function of Piston Amplitude; Displacer Amplitude = 9-mm; Temperature Ratio = 660/50°C; Leakage Coefficient = $1.343 \cdot 10^{-13} \text{ m}^3$	51



LIST OF FIGURES (Continued)

<u>NUMBER</u>	<u>PAGE</u>
38 Pressure Amplitude as a Function of Piston Amplitude; Displacer Amplitude = 9 mm; Temperature Ratio = 760/50°C; Leakage Coefficient $1.343 \cdot 10^{-13} \text{ m}^3$	52
39 PV Power as a Function of Piston Amplitude; Displacer Amplitude = 9 mm; Temperature Ratio = 760/50°C; Leakage Coefficient = $7.7668 \cdot 10^{-14} \text{ m}^3$.	54
40 PV Power as a Function of Piston Amplitude; Displacer Amplitude = 9 mm; Temperature Ratio = 660/50°C; Leakage Coefficient = $7.7668 \cdot 10^{-14} \text{ m}^3$.	55
41 Heater Head Input as a Function of Piston Amplitude; Displacer Amplitude = 9 mm; Temperature Ratio = 760/50°C; Leakage Coefficient = $7.7688 \cdot 10^{-14} \text{ m}^3$	56
42 Heater Head Input as a Function of Piston Amplitude; Displacer Amplitude = 9 mm; Temperature Ratio = 660/50°C; Leakage Coefficient = $7.7688 \cdot 10^{-14} \text{ m}^3$	57



List of Tables

<u>NUMBER</u>		<u>PAGE</u>
1	Configuration Differences Between Present and Earlier ADM Builds . . .	5
2	Instrumentation: FPSE Test Cell No. 2	8
3	Monolithic Heater Head Thermocouples Type K; 40-mil Thick	9
4	Regenerator Thermocouples Type K; 20-mil Thick	10



Background

The Advanced Development Model (ADM) engine testing performed in 1984 showed that the thermodynamic power of the engine was much lower than thermodynamic code predictions. Also, the ADM engine when tested under the engineering model (EM) operating conditions, yielded lower thermodynamic power than was previously achieved by the EM performance engine which, to the first order, is thermodynamically similar to the ADM.

Task Objective

The objective of Task 2.0 of IR&D program 26802 was to identify and understand the cause for thermodynamic power shortfall in the ADM engine.

Executive Summary

In FY84, ADM diagnostic tests confirmed that the power shortfall in the ADM engine was not due to higher than expected parasitic losses (losses associated with the engine pressure wave), but was due to an inadequate power generating capability of the engine with increasing displacer stroke. It was concluded from the FY84 tests that the power discrepancy was due to some deficiency in the upper end of the ADM engine (see Figure 1).

In FY85, IR&D test results narrowed the probable causes for the power shortfall to the following:

- Inadequate external heat transfer capability of the cooler
- Large dead volume in the compression space causing some unknown loss
- Clearance seal between the displacer liner and motor stator.

In early FY86, IR&D test results indicated that the primary cause for the power shortfall was the inadequate seal between the displacer liner and the motor stator. Late in FY86, the ADM engine was tested with an O-ring installed between the motor stator and the displacer liner. Good repeatable performance was achieved and the test results were similar to code predictions. This established the clearance seal between the displacer liner and



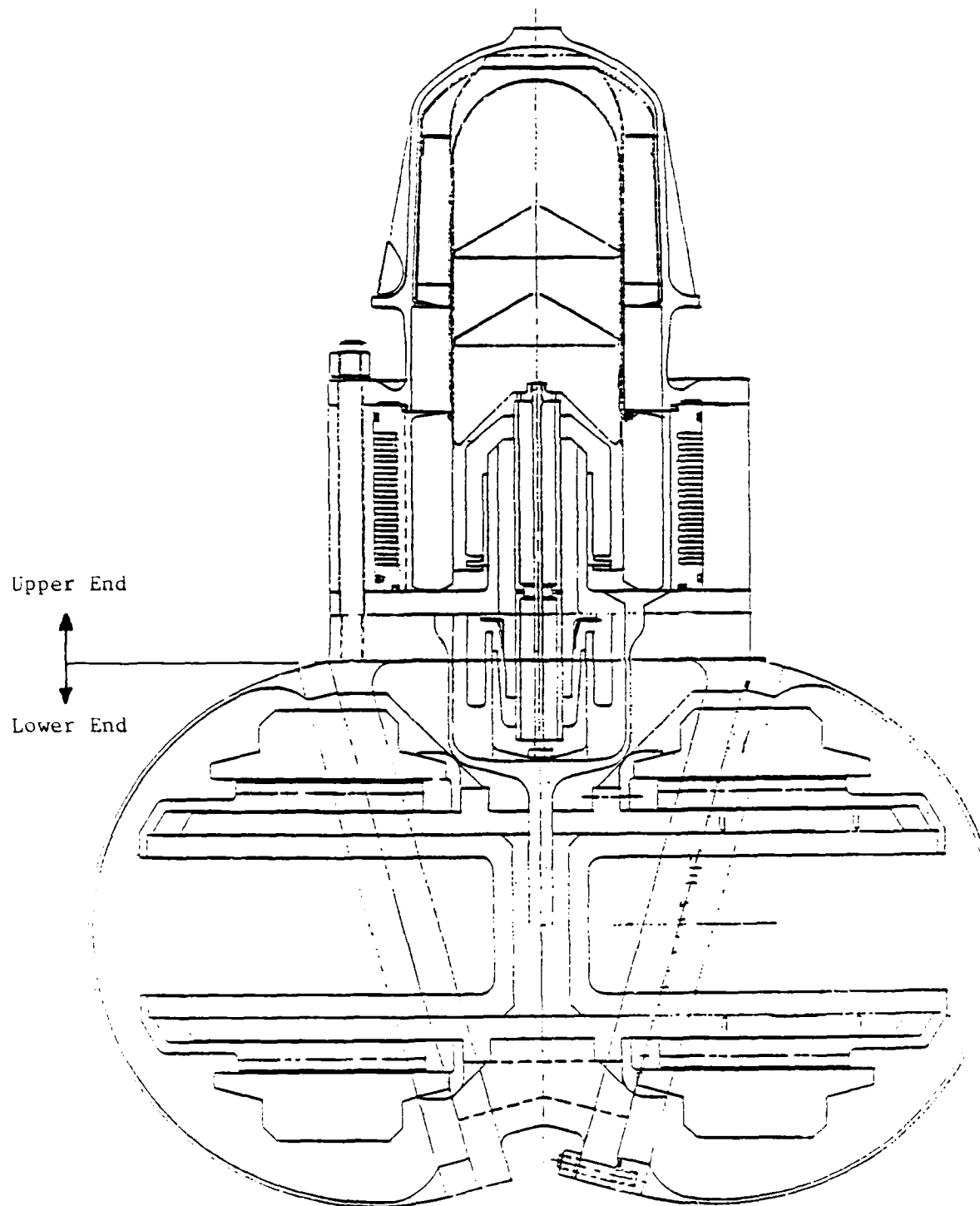


Fig. 1 ADM Monolithic Head Power Module

the motor stator as the main cause for the earlier poor thermodynamic performance of the ADM engine.

Introduction

A detailed historical description of the diagnostic tests performed in FY84 and FY85 and the conclusions reached is given in Appendix A.

In FY86, under IR&D program 26802, Task 2.0, the ADM engine was tested with both tubed and monolithic heads. Results obtained from the tubed head testing are documented in Appendix B. The configuration and the test results of the engine build with monolithic head are described below. ←

ADM Engine with Monolithic Head

A detailed description of the ADM monolithic head engine/alternator configuration is contained in the design report 84SESD17. A general layout of the engine is shown in Figure 2. The only significant hardware change for the test engine from the configuration shown in Figure 2 was the incorporation of a thermocouple adapter plate between the heater head and the cooler housing. This modification was required to connect the regenerator matrix thermocouples to the data acquisition system.

Critical seal components of the ADM engine were inspected for a dimension check. Inspection records and dimensional summary are included in Appendix C.

The baseline engine build configuration is given below. The differences between this configuration and the earlier tested (FY84) ADM configurations are listed in Table 1:

- Monolithic head No. 1
- ADM displacer drive
- 2.6-mil wire, 120-mesh, square-weave screen regenerator with 40-mil thick window plates on each end of the regenerator (375 wire screens with total weight of 832 g)



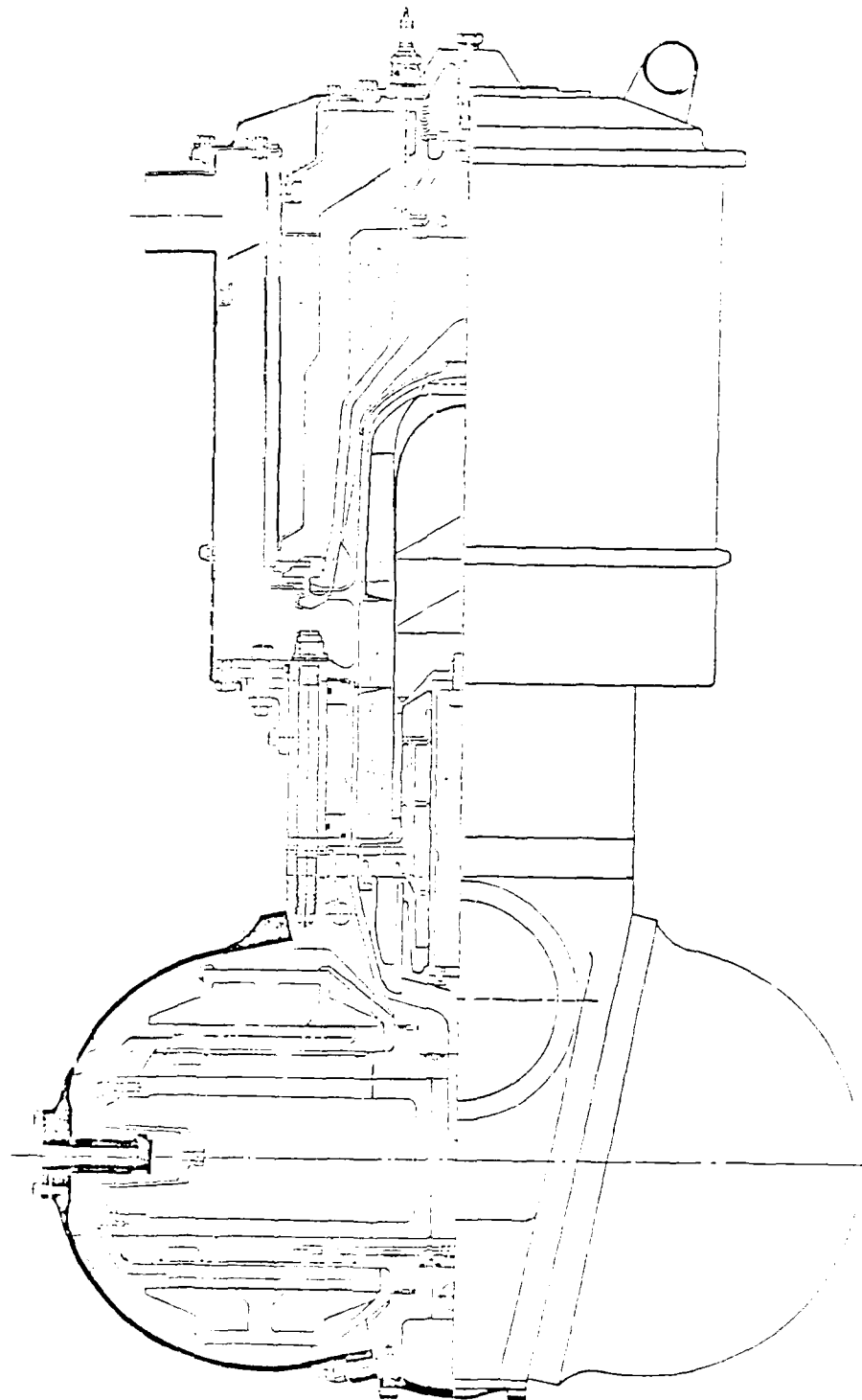


Fig. 2 ADM Engine Configuration

Table 1
Configuration Differences Between
Present and Earlier ADM Builds

Component	Present	Earlier
Monolithic Head	No. 1	No. 1, 3, and 16
Regenerator Screens	2.6-mil Square-Weave Wire Screens With Window Plates on Both Ends	3.7-mil Screens, 3.7-mil Metex, 1-mil Screen
Seal Between Liner and Motor Stator	O-Ring	Clearance
Cooler	EM Generation 3	ADM, EM Generation 2
Compression Space Ports	Closed	Open
Thermocouples		
Regenerator Expansion	Yes No	No Yes

- Generation 3 EM cooler (a detailed description is contained in IR&D report 87SESD36)
- O-ring between the displacer liner and motor stator
- ADM lower end
- Power piston cylinder compression space ports closed
- External bearing supply and piston offset control scheme (Figure 3).

Instrumentation

Instrumentation and appropriate signal conditioning devices for each transducer are listed in Table 2. Tables 3 and 4 list the locations of thermocouples for the heater head and the regenerator, respectively.

Two general comments regarding measurement uncertainties:

- Approximately 60-Hz noise was seen in the measurements of dynamic variables. The noise level was pronounced during slope/intercept testing when both the displacer motor and the alternators were connected to the power supply devices (Algars). During the load line test (only displacer motor connected to the Algar), the level of noise was lower. It is believed that the noise had negligibly small influence on the measurement accuracy. Enough time was not available to isolate the cause for this noise.
- Compression space pressure was measured at two locations: 1) lower compression space between the power pistons, and 2) upper compression space below the cooler (probe in the displacer flange). Both pressure probes were identical devices. During the engine operation upper probe indicated higher mean pressure than the lower probe. This difference was piston stroke (pressure amplitude) dependent. At zero piston stroke, mean pressure measurements were close. At 14-mm stroke, the upper probe indicated 2-bar higher mean pressure and 10% higher pressure amplitude. In a latter test, the location of the two probes was reversed and the lower probe then indicated a higher pressure reading. This concluded that the difference in measured pressures was not real but was caused by the instrumentation and the associated signal conditioning devices. The cause for this discrepancy has not been identified. Since the lower mean pressure measurement was consistent

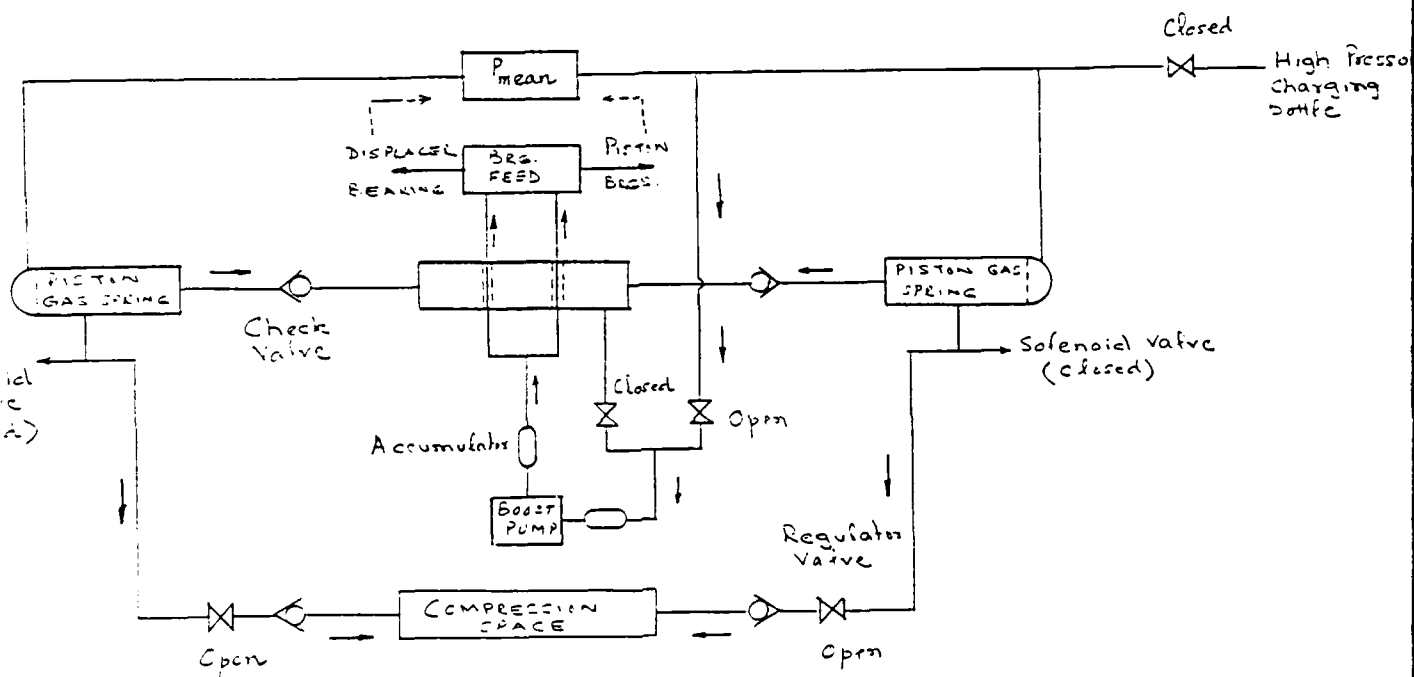


Fig. 3 Bearing Supply and Piston Offset Control Scheme

Table 2

Instrumentation: FPSE Test Cell No. 2

Parameter	Sensor	Range and Accuracy	Associated Devices
<u>Pressure</u>			
Displacer Gas Spring - Load Side	Druck PDCR 200, S/N 1902	100 bar, +1%	Analog, 2831J Signal Conditioner
Displacer Gas Spring - Head Side	Entran 9939, S/N 12W4X-M9-9	100 bar, +1%	Analog, 2831J Signal Conditioner
Piston Gas Spring No. 1	Druck PDCR 200, S/N 1901	100 bar, +1%	Analog, 2831J Signal Conditioner
Piston Gas Spring No. 2	Kulite XTM-190-2000, S/N 16-46	100 bar, +1%	Analog, 2831J Signal Conditioner
Compression Space Between Pistons	Kulite XTM-190-2000, S/N H6-84	100 bar, +1%	Analog, 2831J Signal Conditioner
Compression Space Above Hub	Kulite XTM-190-2000, S/N A5-32	100 bar, +1%	Analog, 2831J Signal Conditioner
Bearing Supply Pressure	Kulite XTM-190-2000, S/N B7-49	100 bar, +1%	Analog, 2831J Signal Conditioner
Combustor Air Pressure	Dynisco APT320J-25, S/N 142570	< +1%	None
Combustor Fuel Pressure	Dynisco APT320J-25, S/N 142571	< +1%	None
Supply Air Delta P	Validyne DP45-26, S/N 42706	< +1%	MTI-Made Conditioner
Supply Fuel Delta P	Validyne DP45-26, S/N 42705	< +1%	MTI-Made Conditioner
<u>Displacer</u>			
Displacer - Xd1	Kaman 2UB SPL	+2% Over 0.8-in. Stroke	Kaman KD-2310 Osc., S/N 0-33386
Displacer - Xd2	Kaman 2UB SPL	+2% Over 0.8-in. Stroke	Kaman KD-2310 Osc., S/N 0-33383
Piston - XA1p1	Kaman 2UB SPL	+2% Over 1.1-in. Stroke	Kaman KD-2310 Osc., S/N 0-33385
Piston - XA1p2	Kaman 2UB SPL	+2% Over 1.1-in. Stroke	Kaman KD-2310 Osc., S/N 0-33390
Piston - XA2p1	Kaman 2UB SPL	+2% Over 1.1-in. Stroke	Kaman KD-2310 Osc., S/N 0-33388
Piston - XA2p1	Kaman 2UB SPL	+2% Over 1.1-in. Stroke	Kaman KD-2310 Osc., S/N 0-33387
<u>Temperature</u>			
Coolant Thermistors	Omega 44033 Type	0 to 70 C, + 0.5 C	None
Thermocouples	Type K - ISA Standard	2.2 C or +7.5%	Hy-Cal 305B, 0 x Ref. Junction
<u>Coolant Flow Rates</u>			
Bearingless Flow Meter	B100, S/N 1205	800 Pulses/Liter = 0.5%	None
<u>Voltage, Current, Power</u>			
Alternator Terminal Voltage	Potential Transformers	< +1%	None
Alternator Current	CT and Burden Resistor	< +1%	None
Load Voltage	Potential Transformers	< +1%	None
Load Power	F.W. Bell Transducer	+3%	None
Displacer Motor Terminal Voltage	Potential Transformers	< +1%	None
Displacer Motor Current	CT and Burden Resistor	< +1%	None

Table 3
Monolithic Heater Head Thermocouples
Type K; 40-mil Thick

Channel Assignment	Side	Location*
34	Left	6.0
33	Left	4.3
28	Left	4.15
29	Left	3.6
36	Back	1.0
37	Back	2.0
38	Back	2.5
40	Back	3.0
2	Back	4.0
7	Back	4.5
9	Back	5.0
8	Back	6.0
3	Right	1.0
10	Right	1.5
11	Right	2.2
12	Right	3.0
16	Right	4.0
17	Right	4.3
18	Right	4.5
20	Right	5.0
24	Front	1.0
43	Front	1.5
31	Front	2.5
26	Front	3.0

Out of the above 24 thermocouples, 23 were active. Average heater head temperature was calculated from the average of the above active 23 thermocouple readings. The standard deviation of the measured temperatures was about 40°C.

*Distance from Base in inches.



Table 4
Regenerator Thermocouples
Type K; 20-mil Thick

Channel Assignment	Location	Symbol on Plots
1	Top Back	1
35	Top Left	2
13	Top Right	3
25	Top Front	Not Active
21	Middle Front	4
19	Middle Right	5
32	Middle Left	6
27	Bottom Front	7
15	Bottom Right	8
14	Bottom Back	9
44	Bottom Left	0

with the other pressure probes (piston and displacer gas spring probes), the lower pressure measurement was used to calculate the piston PV powers.

Displacement and pressure probes were calibrated prior to each engine build. A typical set of calibration tables are included in Appendix D.

Tests Performed

Four different tests were performed. The first test ran the baseline engine configuration under the September 1984 ADM test operating conditions, which were:

- Slope/intercept test format
- Mean pressure: 60 bar
- Operating frequency: 58 Hz
- Average heater head temperatures: 760°C, 660°C, 560°C
- Piston stroke (peak to peak): 14 mm
- Displacer-to-piston phase angle: 66°

The second test was performed without the O-ring between the displacer liner and the motor stator to evaluate the influence of stator O-ring on engine performance. Operating conditions and the rest of the build configuration were the same as for the first test.

The third test was performed with the stator O-ring back in the engine to confirm if the engine performance was repeatable.

The fourth test was performed with the displacer locked. Power pistons were motored without supplying heat to the heater head. The purpose of this test was to evaluate the parasitic losses in the engine (losses associated with the pressure wave in the engine).

The following describes the results of the above series of tests.

Test 1 - Baseline Configuration Test

This test was performed on 20 September 1986 using test data file TADMH4. Figure 4 shows the plot of piston PV power versus displacer amplitude at an average heater head temperature of 760°C. The test data compare favorably with the CFAST code prediction. The HFAST code overpredicts the power by essentially a constant magnitude of 300 W at all plotted points*. The plotted PV power is the sum of two power piston PV powers. Since both the HFAST and CFAST codes show similar correlation with EM performance engine test data, it can be concluded that the thermodynamic performance of the present ADM baseline configuration is similar to the performance of the EM performance engine.

The displacer amplitude was limited to 6 mm (design amplitude 10 mm) due to high displacer motor current (10-A rms versus 3-A design). High motor current was partly due to high load side displacer gas spring losses (pressure wave phase angle of 7° as compared to predicted value of 2.8°) and partly due to reactive motor power required to maintain displacer to piston phase angle of 66°.

Figures 5 and 6 show the plot of piston PV power versus displacer amplitude at average heater head temperatures of 660°C and 560°C, respectively. CFAST matches the data at lower displacer strokes well, but overpredicts the PV power at higher displacer strokes. Slope (PV versus XD) discrepancy in CFAST predictions increases with decreasing heater head average temperature. (This behavior was also seen in the earlier EM and ADM test results versus CFAST code predictions and was the primary reason for the development of the HFAST code.) Again, the HFAST code overpredicts the PV power by ~300 W (Figure 4). Figures 7 and 8 show the PV versus XD slope comparison between the test data and modified HFAST predictions (HFAST predictions are arbitrarily decreased by ~300 W at all points plotted). HFAST predicts the slope and curvature in

*The compression space dead volume for both CFAST and HFAST codes was adjusted for one data point for each test to match the predicted and the measured pressure amplitude. A detailed discussion regarding the need for volume correction is given in IR&D report 87SESD38.

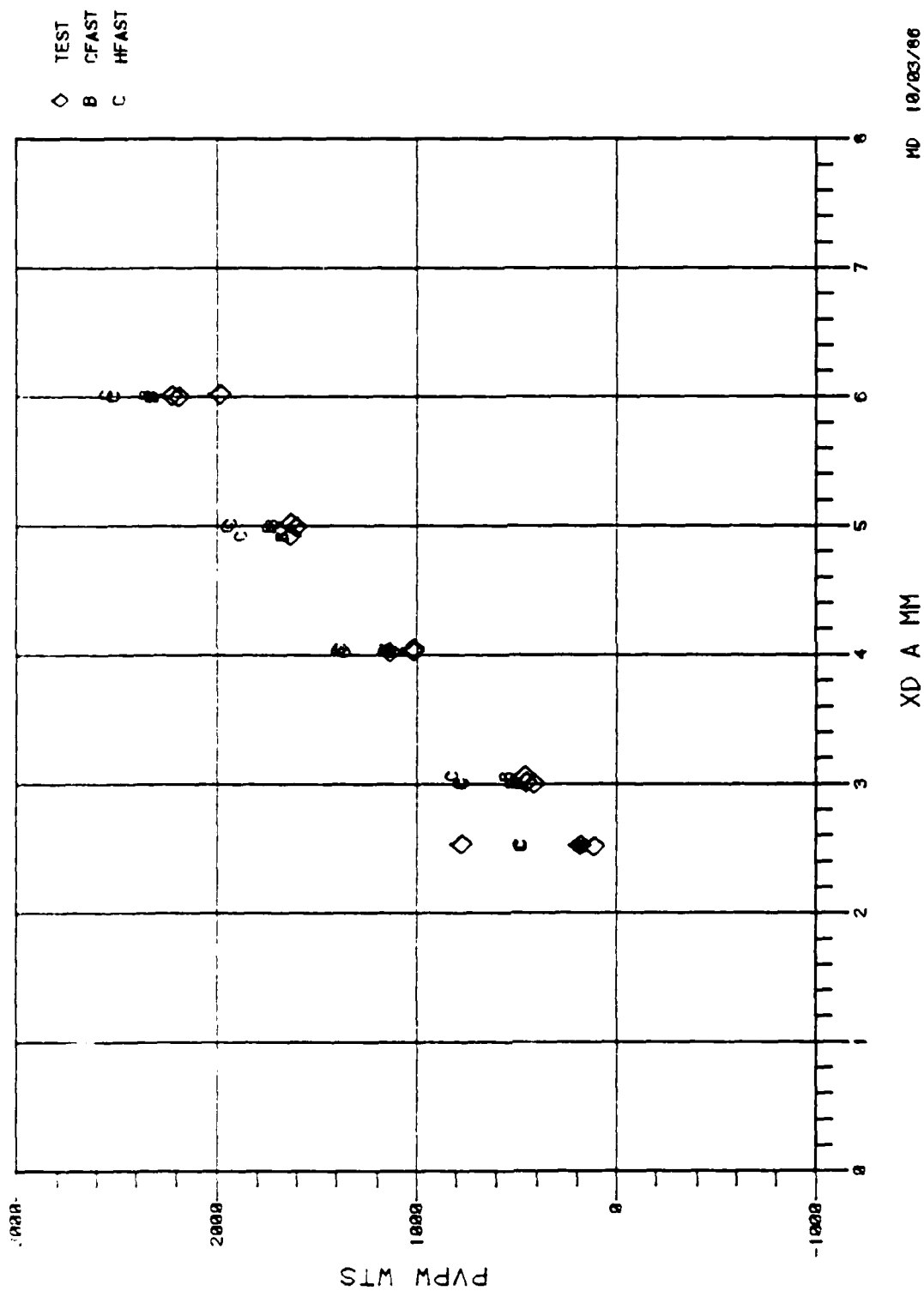


Fig. 4 Slope/Intercept Plot; Head Temperature = 760°C,
Piston Stroke = 14 mm, Displacer Phase Angle = 66°

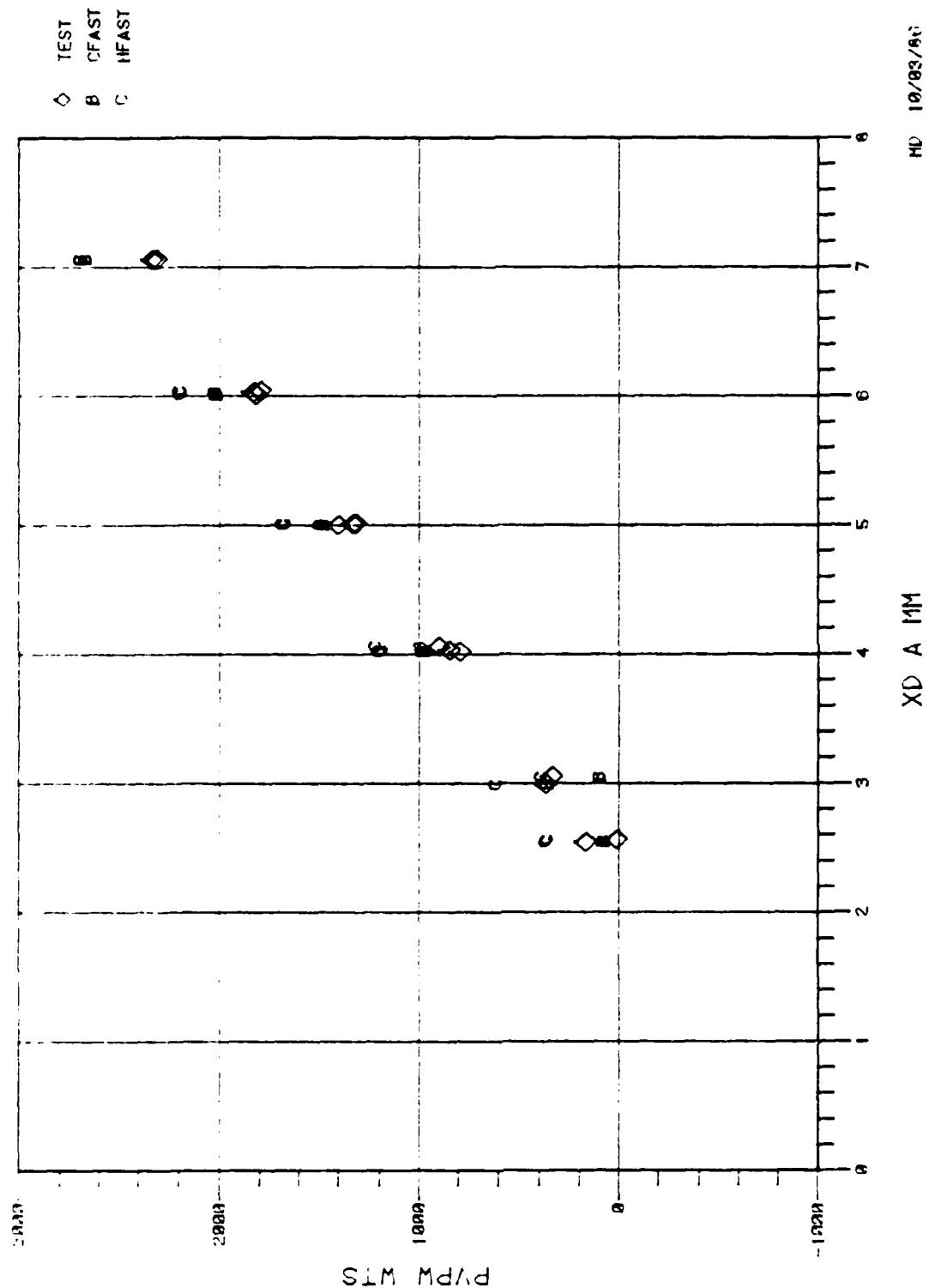


Fig. 5 Slope/Intercept Plot; Head Temperature = 660°C,
Piston Stroke = 14 mm, Displacer Phase Angle = 66°

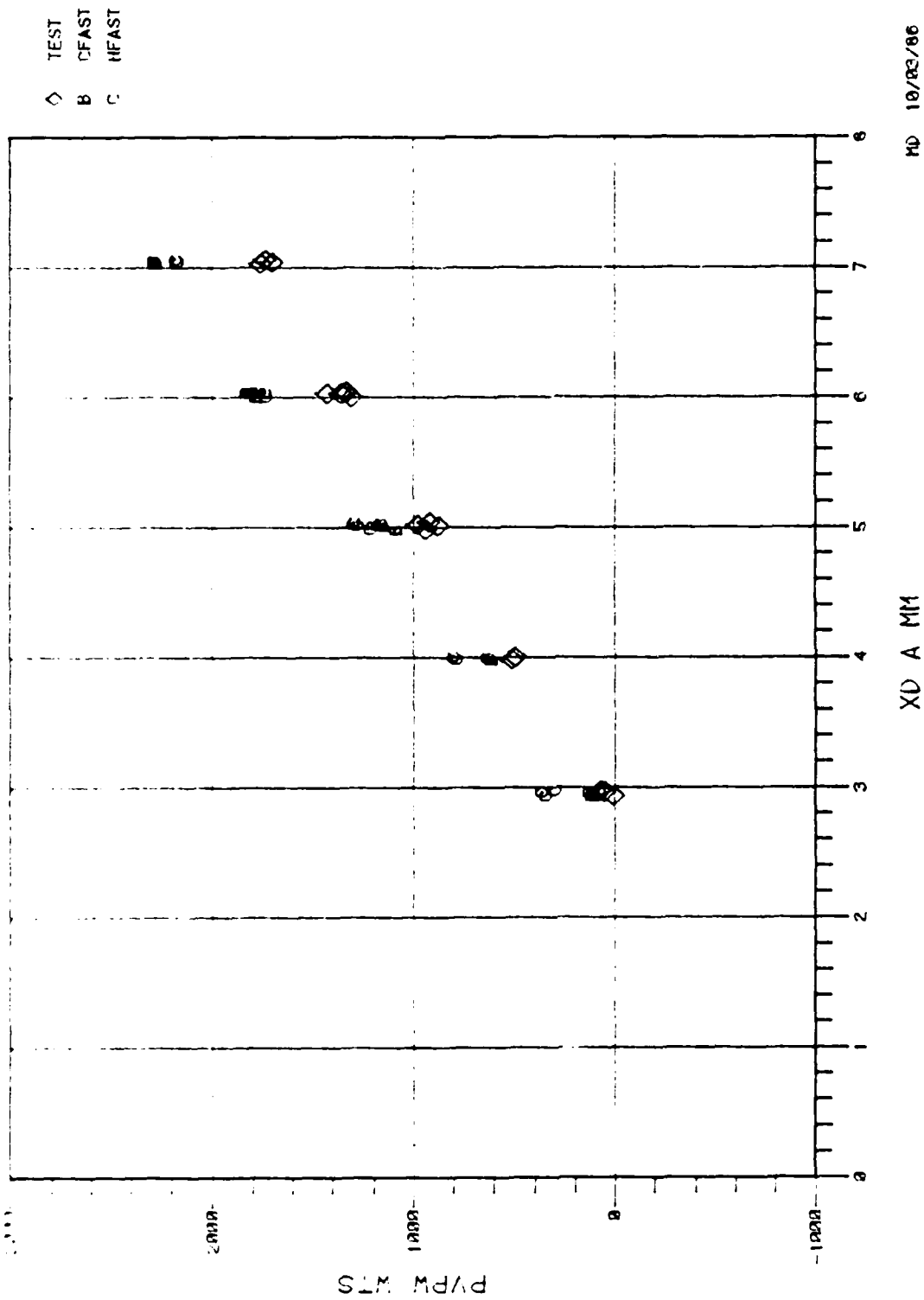


Fig. 6 Slope/Intercept Plot; Head Temperature = 560°C,
Piston Stroke = 14 mm, Displacer Phase Angle = 66°

MD 10/03/86

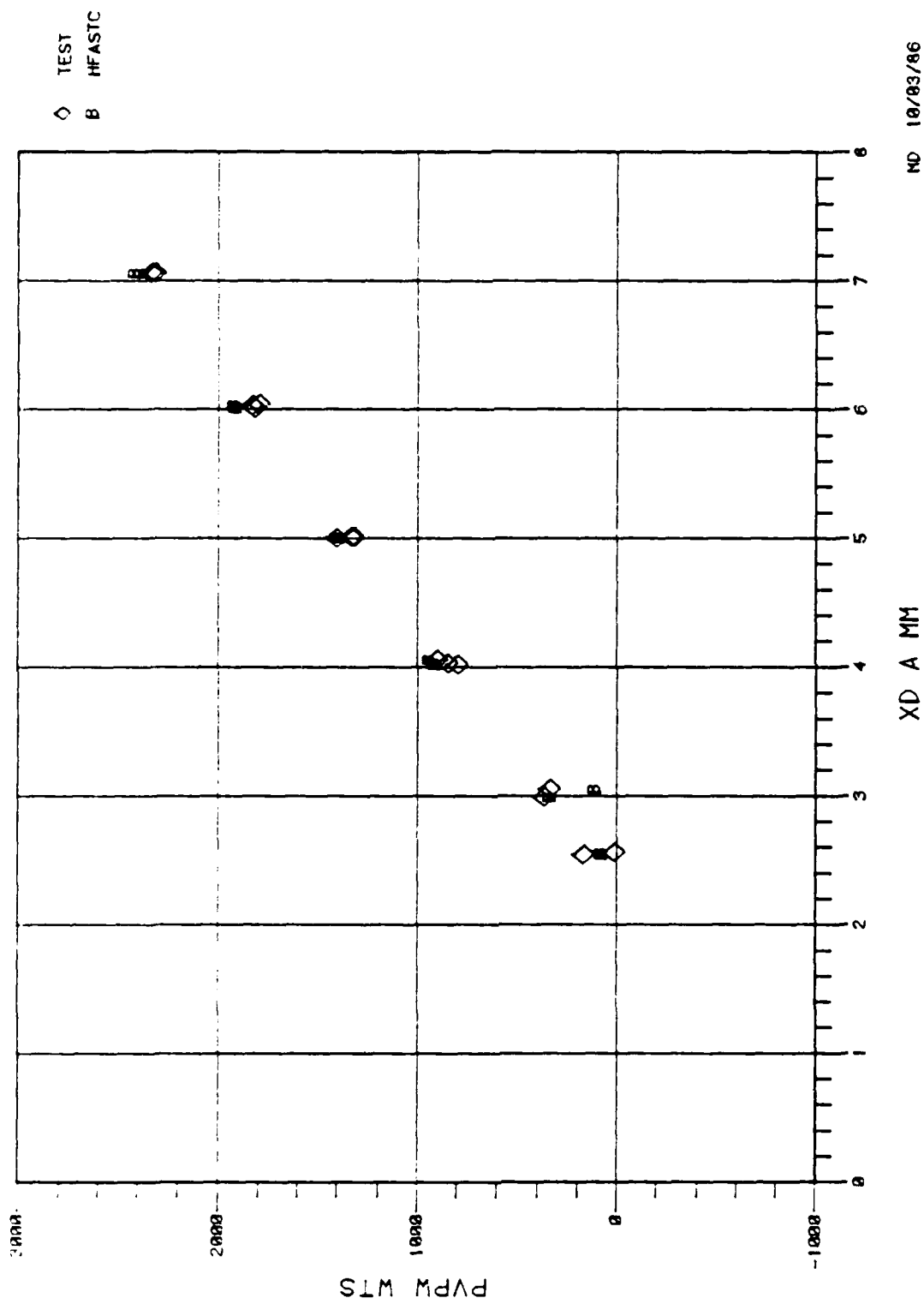


Fig. 7 Slope Comparison of Slope/Intercept Curve;
 Head Temperature = 660°C, Piston Stroke = 14 mm,
 Displacer Phase Angle = 66°

NO 10/03/86

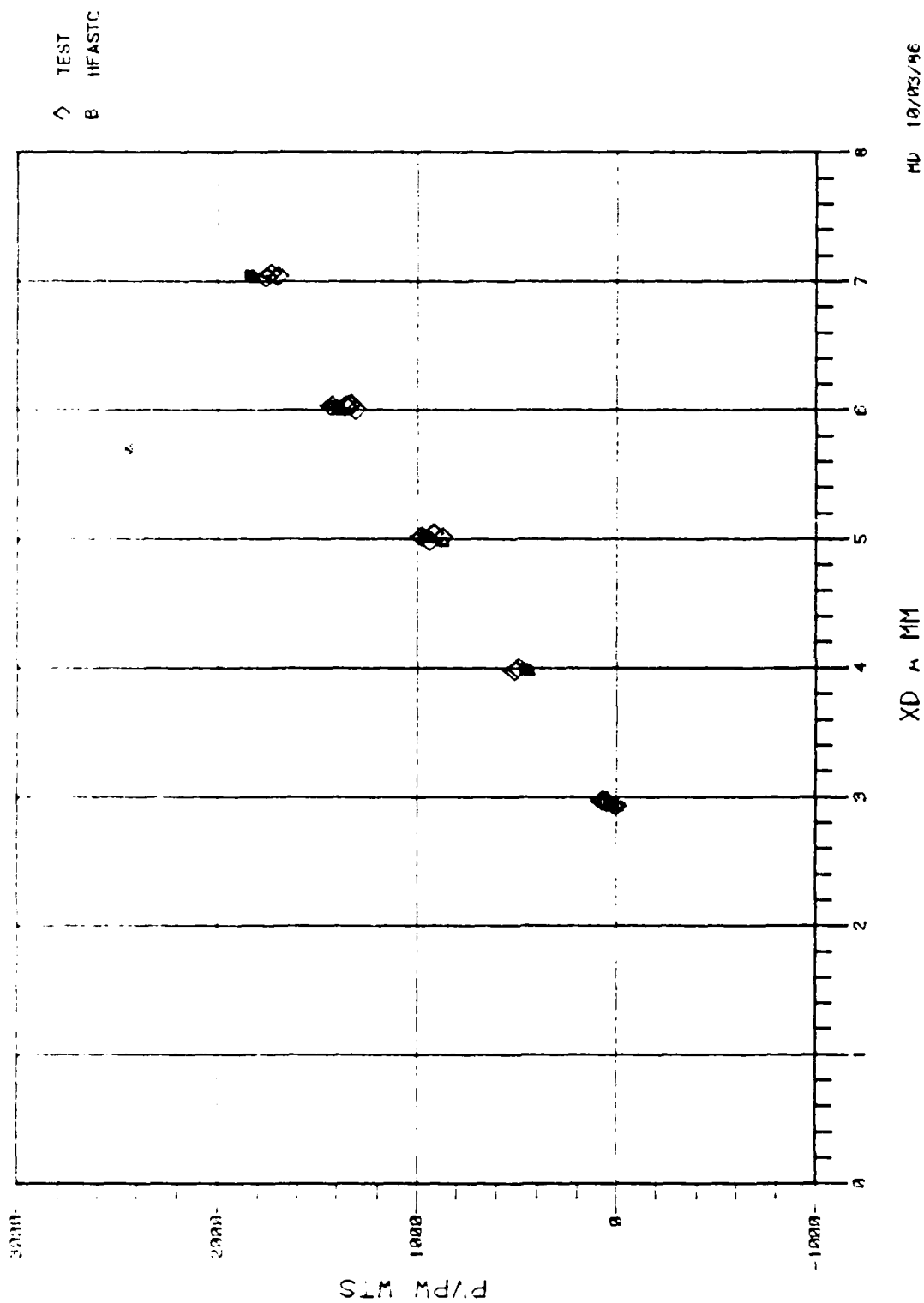


Fig. 8 Slope Comparison of Slope/Intercept Curve;
 Head Temperature = 560°C, Piston Stroke = 14 mm,
 Displacer Phase Angle = 66°

MD 10/03/96

the test data quite well. In summary, HFAST predicts the power generation with increasing displacer amplitude well, but underpredicts the parasitic losses.

In Figures 9 and 10, the above-measured PV power is compared to the PV power measured on 25 July 1984 ADM test. The present engine configuration yields about 40 to 50% more PV power at similar operating conditions than the 1984 ADM configuration.

Figures 11 and 12 show plots of measured regenerator temperatures at various displacer amplitudes. The engine was assembled with 375 square weave screens. Four thermocouples were placed at 90° to each other between the heater window plate and the first screen. After stacking 200 screens, three thermocouples were placed at 120° to each other. After stacking another set of 175 screens four more thermocouples were placed at 90° to each other between the last screen and the cooler window plate. The nonuniformity in the measured temperatures at the top of the regenerator reflects the circumferential temperature maldistribution in the heater head. This circumferential variation in heater head temperature is the result of imprecise mounting of combustor liner and ceramic heater head cap. Figures 13 and 14 show the comparison between the measured temperatures and code (CFAST and HFAST) predictions. HFAST predicts the top and bottom regenerator temperatures well but underpredicts the temperatures at the middle of the regenerator. HFAST regenerator temperature profile prediction has more curvature than in the test data.

In summary:

1. The present baseline ADM engine configuration has 40 to 50% more PV power at similar operating conditions than the 1984 ADM test configuration.
2. HFAST code predicts the power generation and regenerator top and bottom temperatures well. However, HFAST under predicts the parasitic losses by the following equation:

$$\Delta_{\text{parasitic loss}} \approx 4.4 \times \text{Pressure amplitude}^2$$



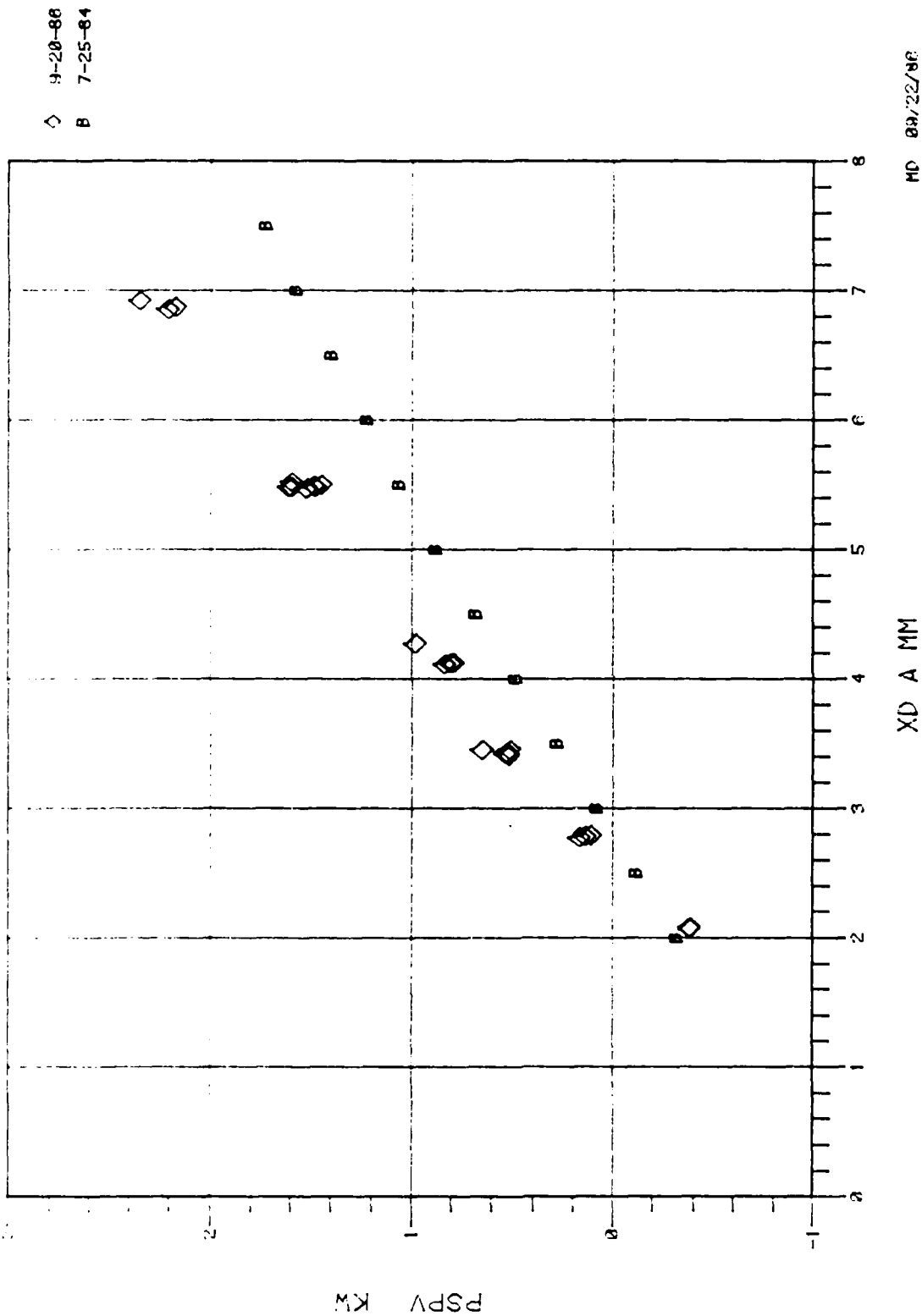


Fig. 9 PV Power Comparison for FY84 and FY86 (O-Ring In)
Engine Builds; lead Temperature = 660°C

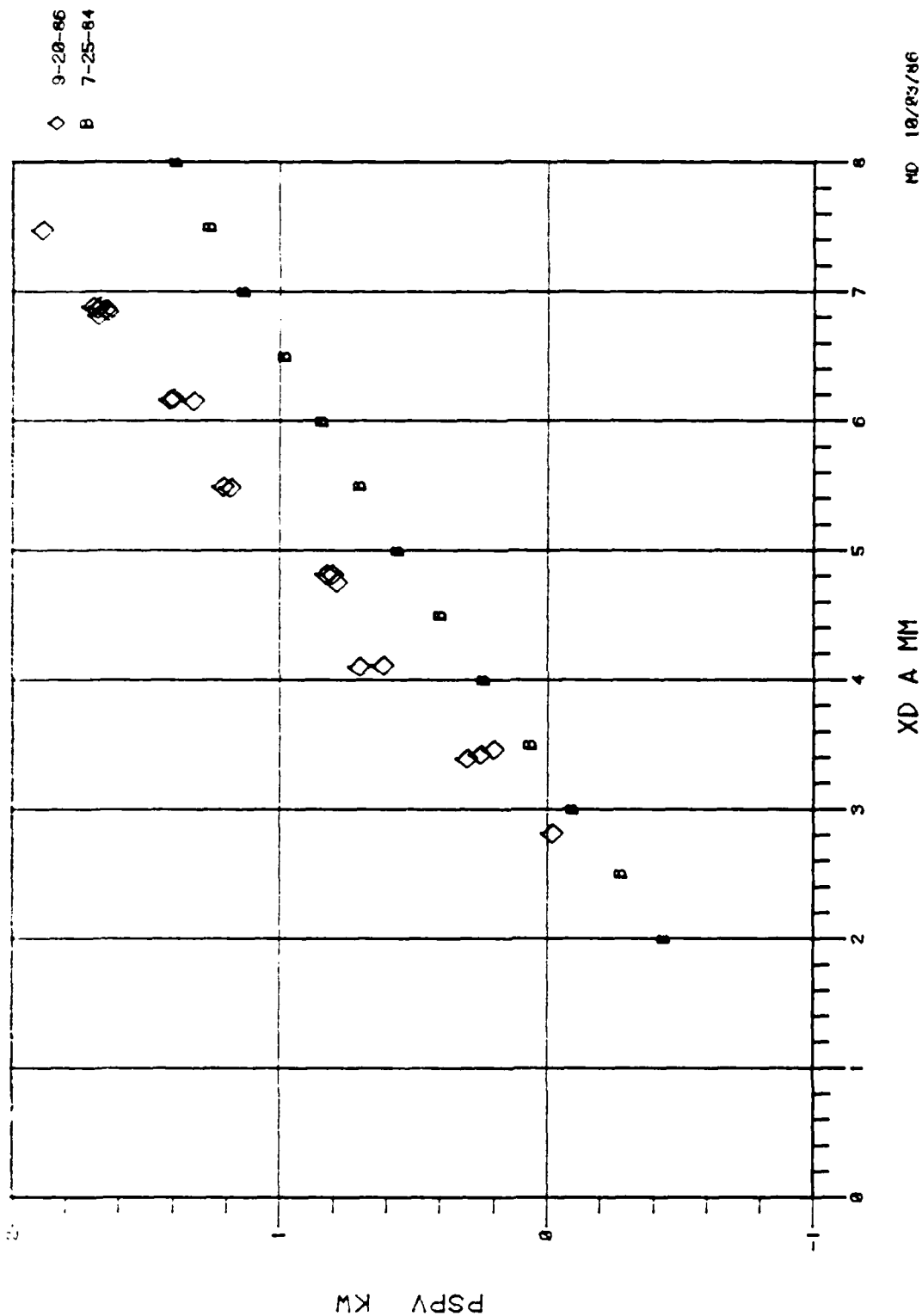


Fig. 10 PV Power Comparison for FY84 and FY86 (O-Ring In)
Engine Builds; Head Temperature = 560°C

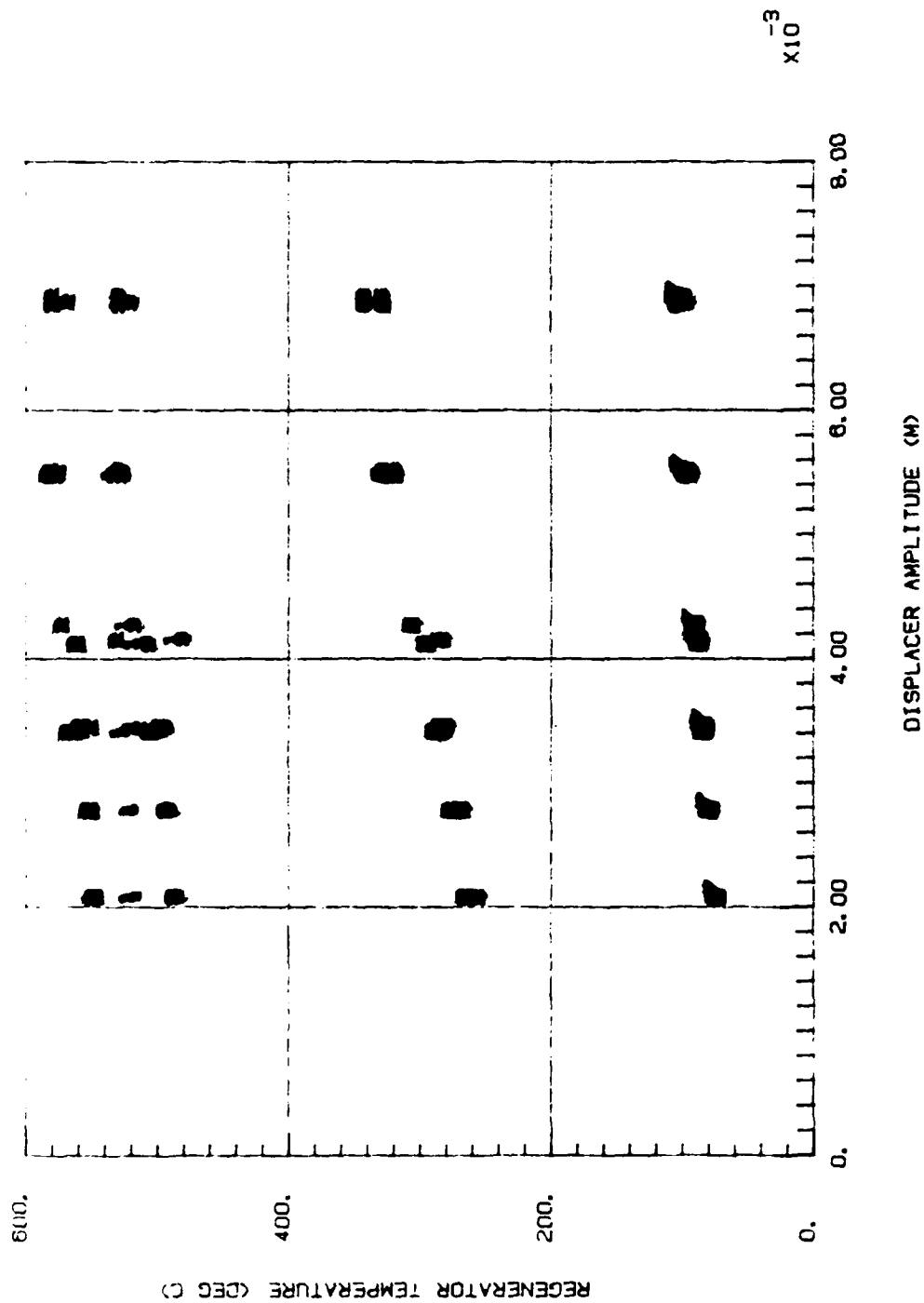


Fig. 11 Regenerator Temperatures with O-Ring In;
Head Temperature = 660°C

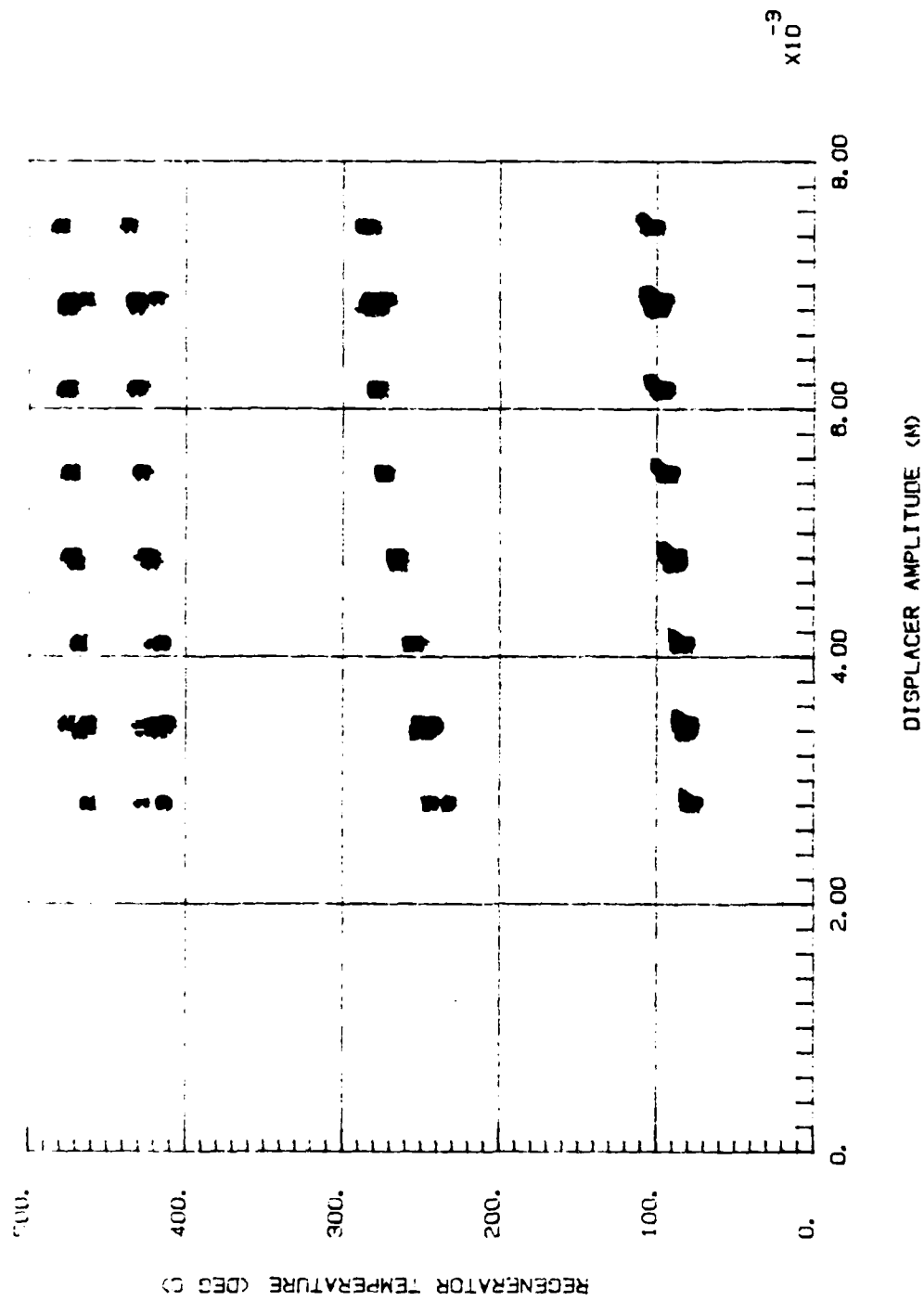
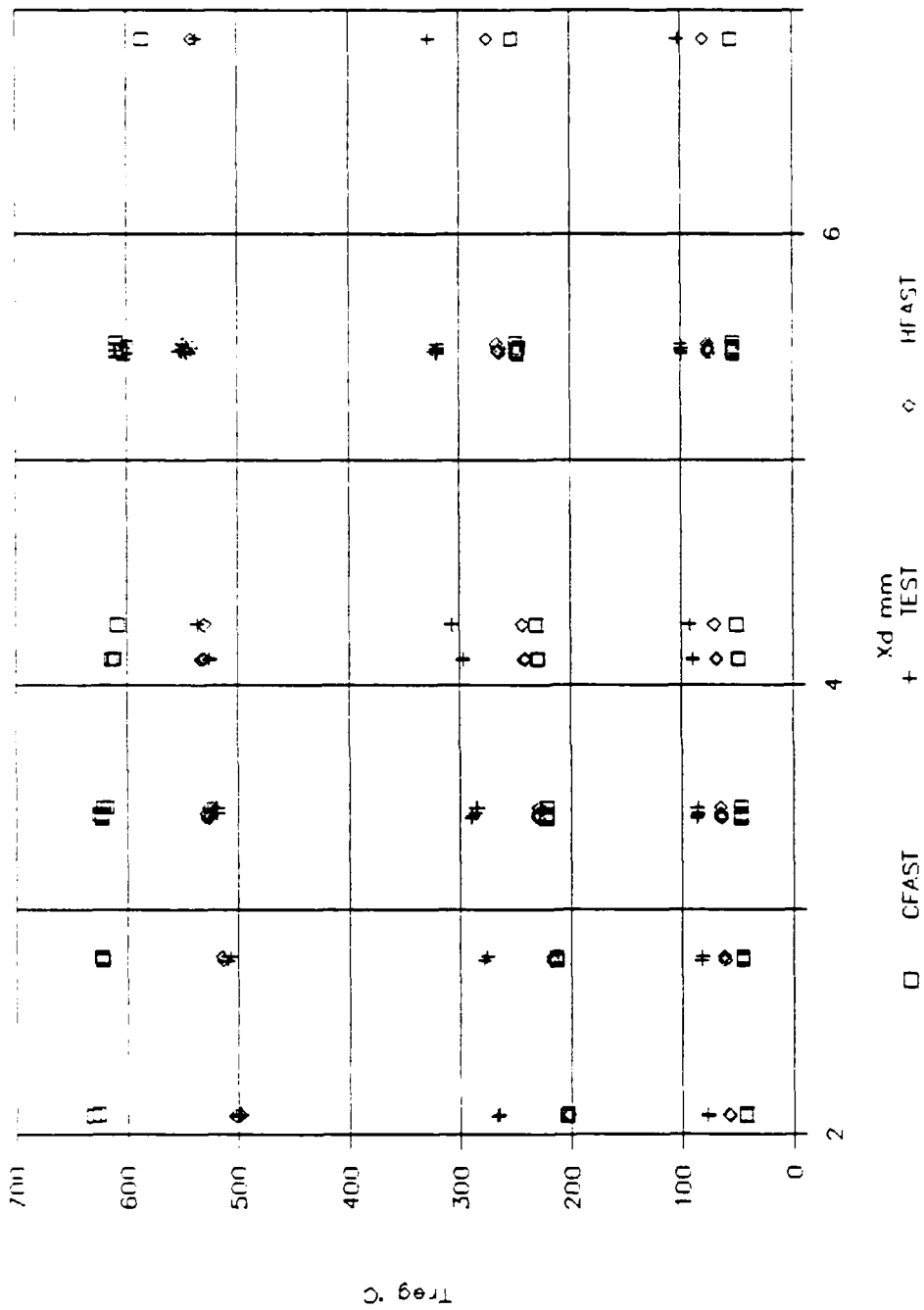


Fig. 12 Regenerator Temperatures with O-Ring In;
Head Temperature = 560°C



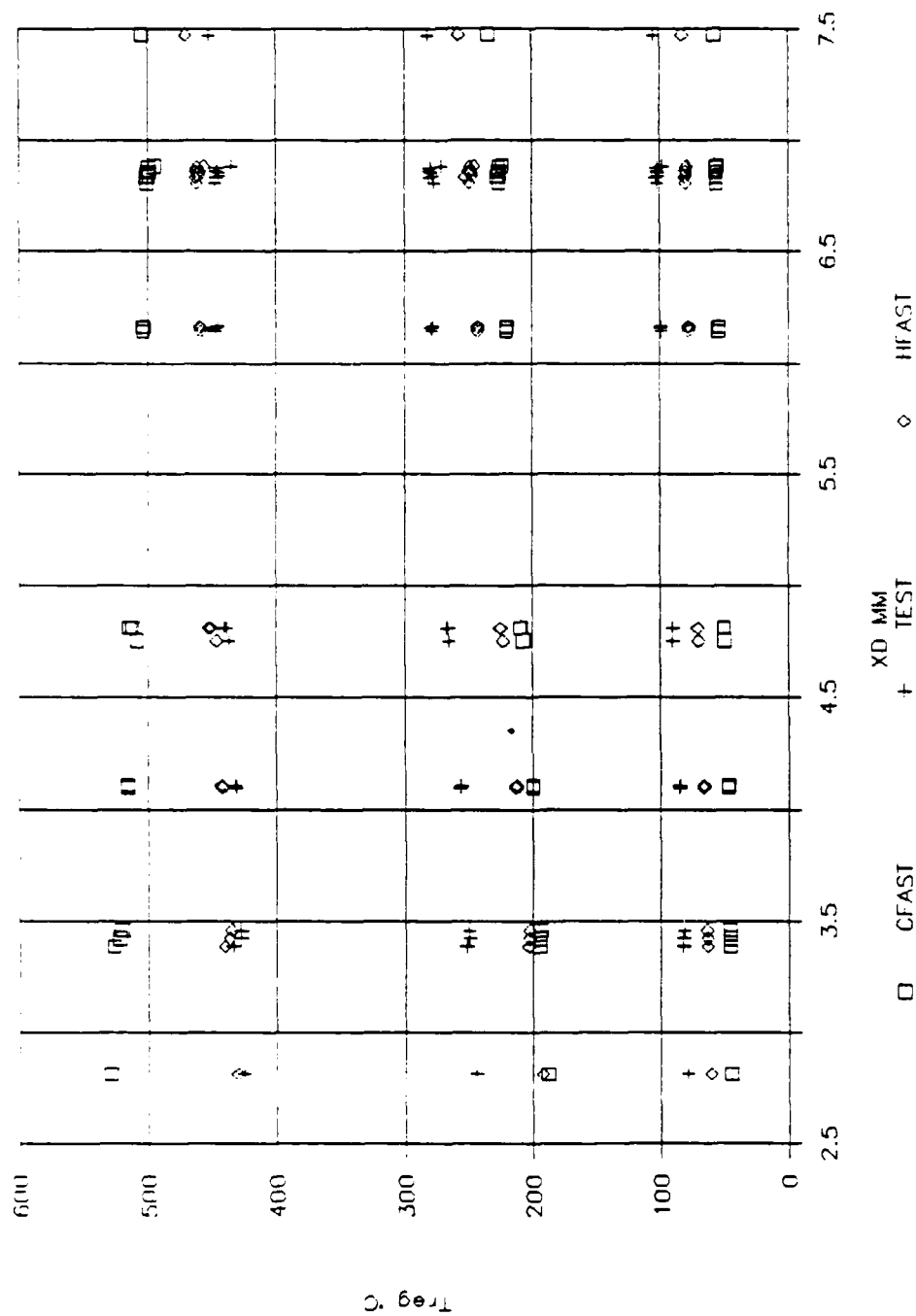


Fig. 14 Predicted and Measured Regenerator Temperature;
Head Temperature = 560°C

where parasitic loss is in watts, and pressure amplitude in bar.

3. HFAST test data correlation of the baseline ADM engine configuration is similar to the EM performance engine correlations.

Test 2 - Without Stator O-Ring

Other than removing the stator O-ring between the displacer liner and the motor stator, the engine had the same build and same operating conditions as the baseline engine configuration test. Testing was performed on 24 September 1986 using test data file TADMH5.

Figures 15 and 16 compare the measured PV power with and without the stator O-ring in the engine. PV power at low displacer amplitudes is similar; however, at high displacer amplitudes a significant drop in generated power is seen in the engine build with no stator O-ring.

Figures 17 and 18 compare the 24 September 1986 and 25 July 1984 engine test data. Although the two test configurations have many different components (see Table 1), the test results are similar. This establishes the fact that it is the sole presence of the stator O-ring that yields the considerable performance gain over the 1984 test results.

Figures 19 and 20 show the plot of measured regenerator temperatures at various displacer amplitudes. The following observations are made:

1. Regenerator top and bottom temperatures are similar with and without the stator O-ring in place.
2. More nonuniformity in regenerator top temperature measurement with O-ring out.
3. With increasing displacer amplitude, the temperature in the middle of the regenerator increases. This behavior can result from unequal working fluid flow in the regenerator during the hot and cold blows



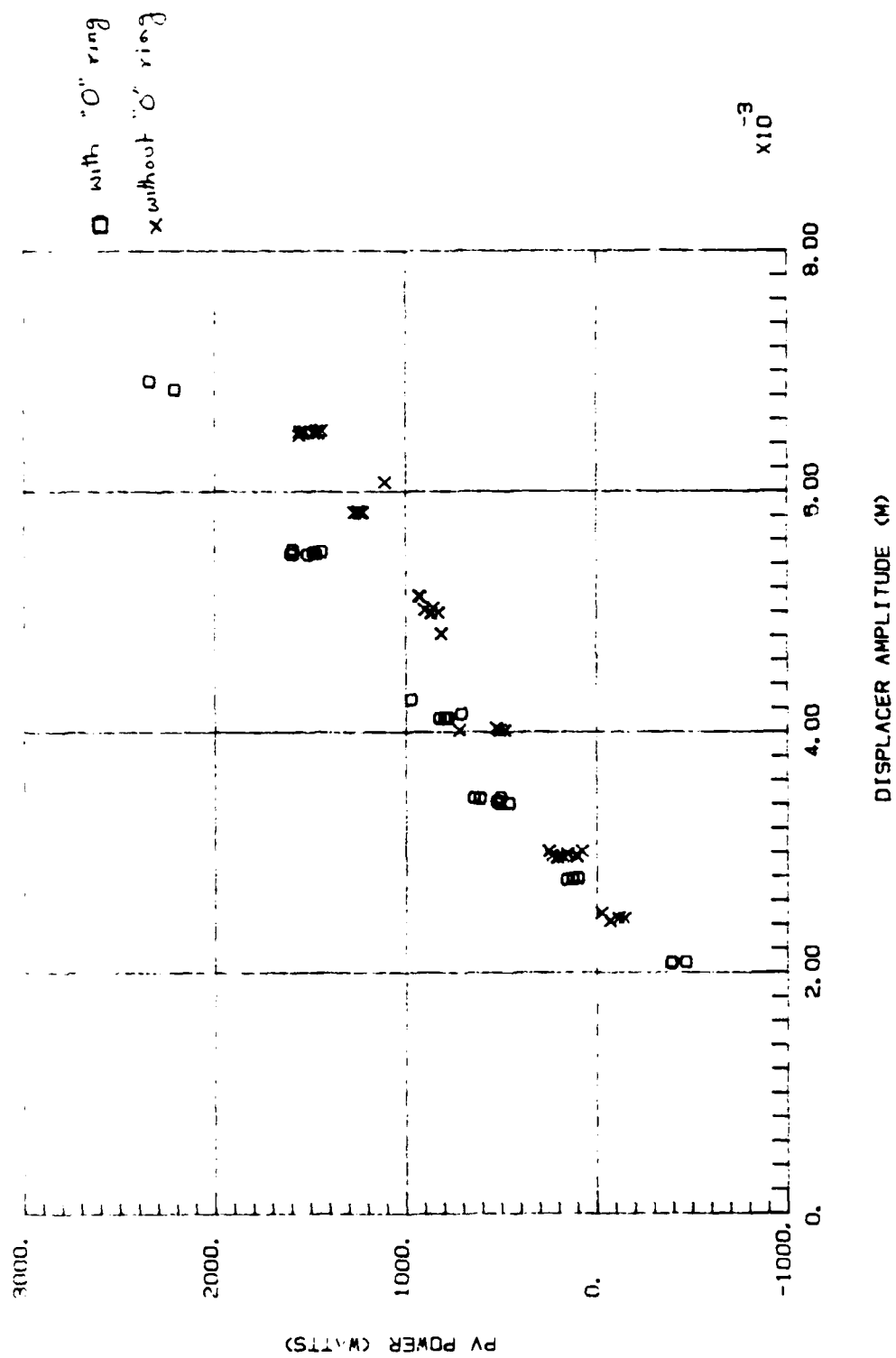


Fig. 15 PV Power With and Without Stator O-Ring;
Head Temperature = 660°C

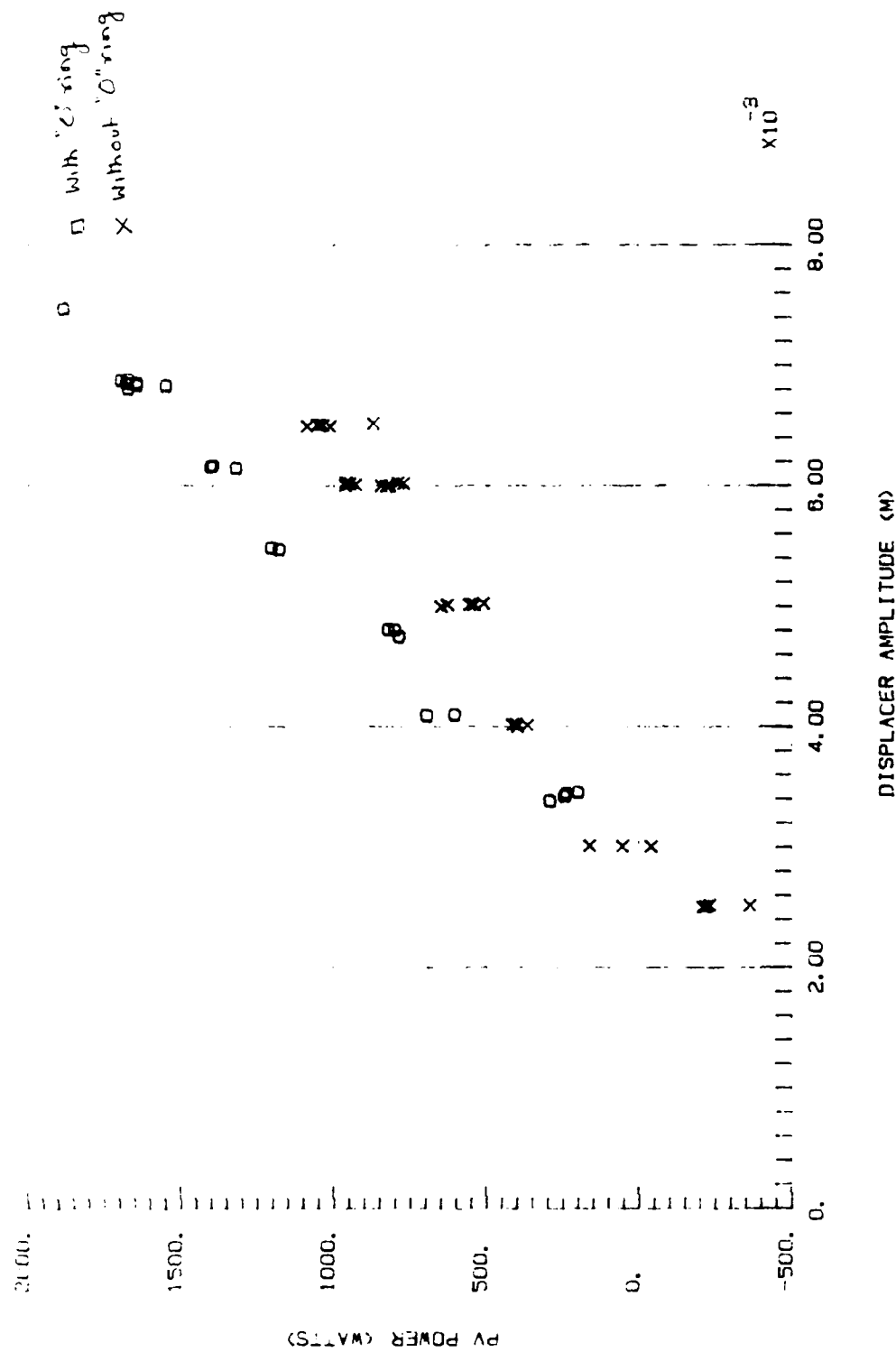


Fig. 16 PV Power With and Without Stator O-Ring;
Head Temperature = 560°C

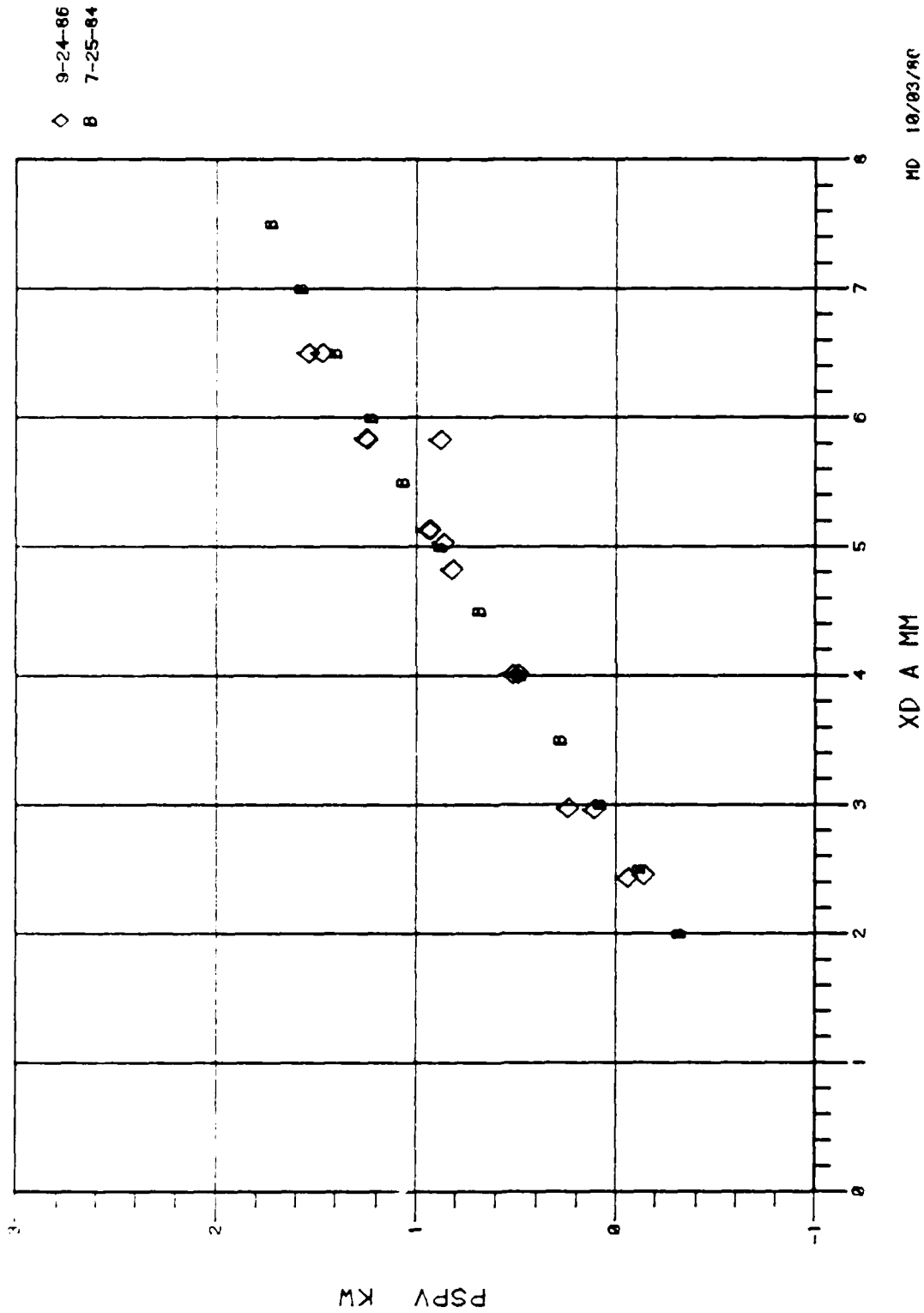


Fig. 17 PV Power Comparison for FY84 and FY86 (O-Ring Out)
Engine Build; Head Temperature = 660°C

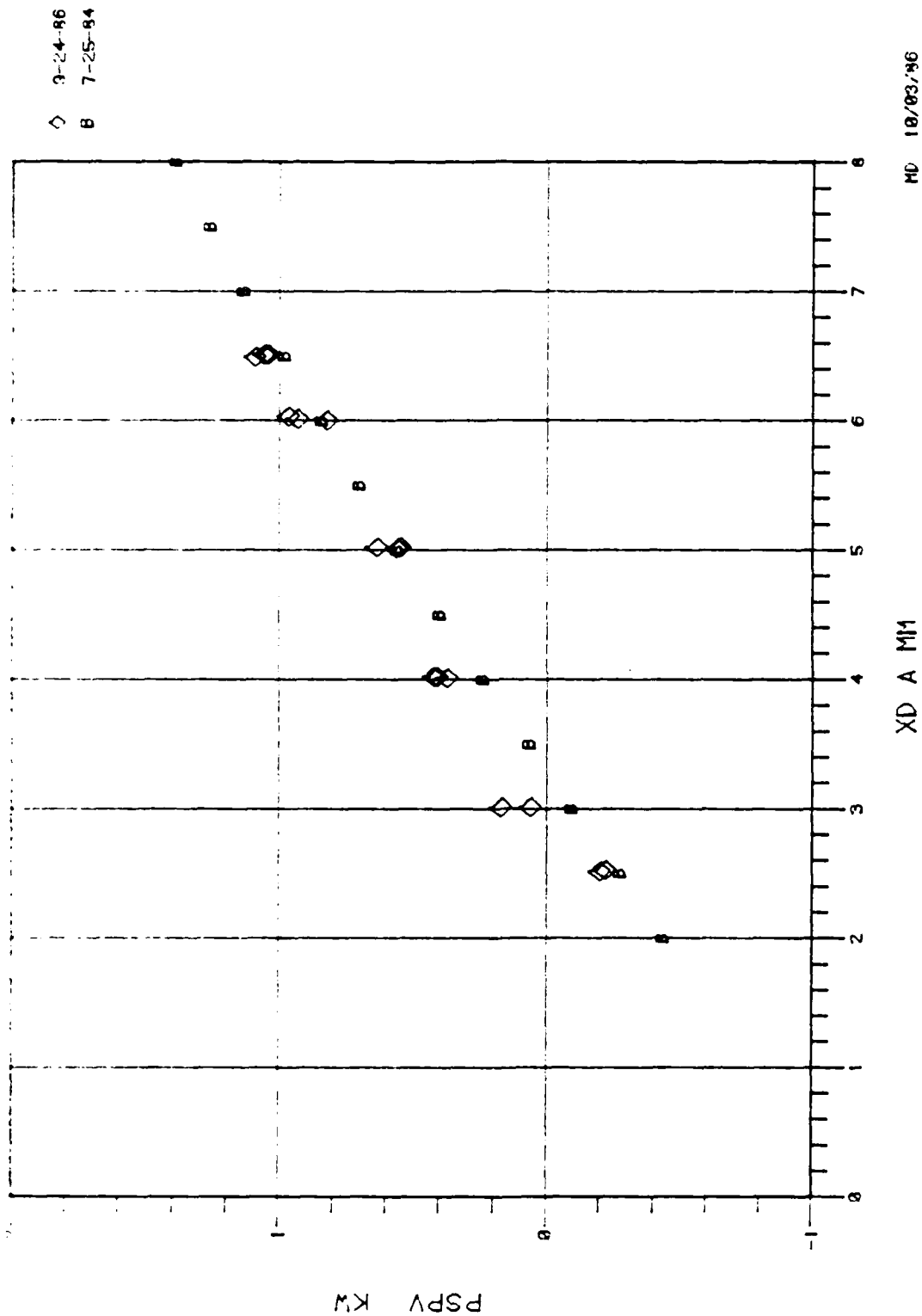


Fig. 18 PV Power Comparison for FY84 and FY86 (O-Ring Out)
Engine Builds; Head Temperature = 560°C

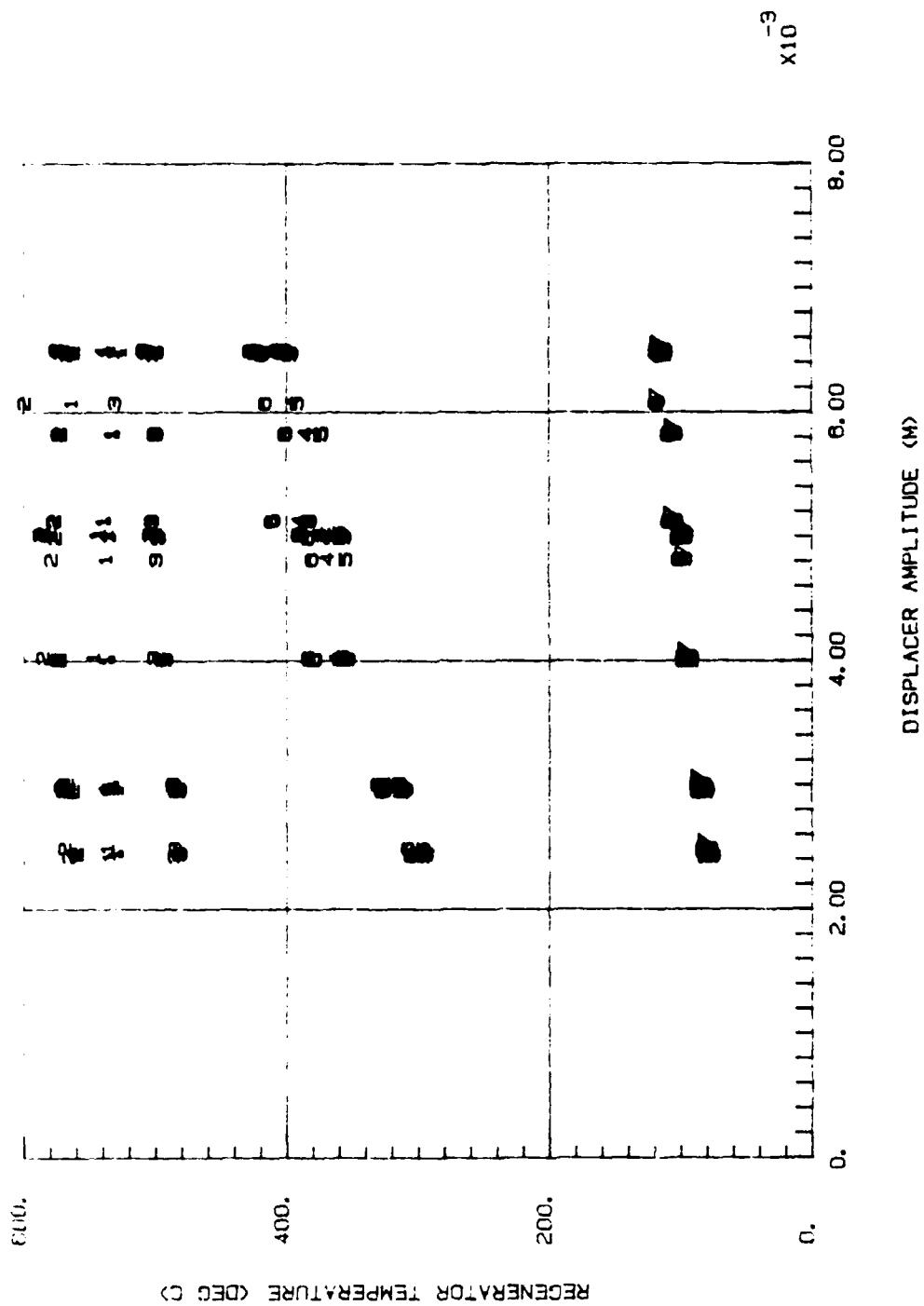


Fig. 19 Regenerator Temperatures with O-Ring Out;
Head Temperature = 660°C

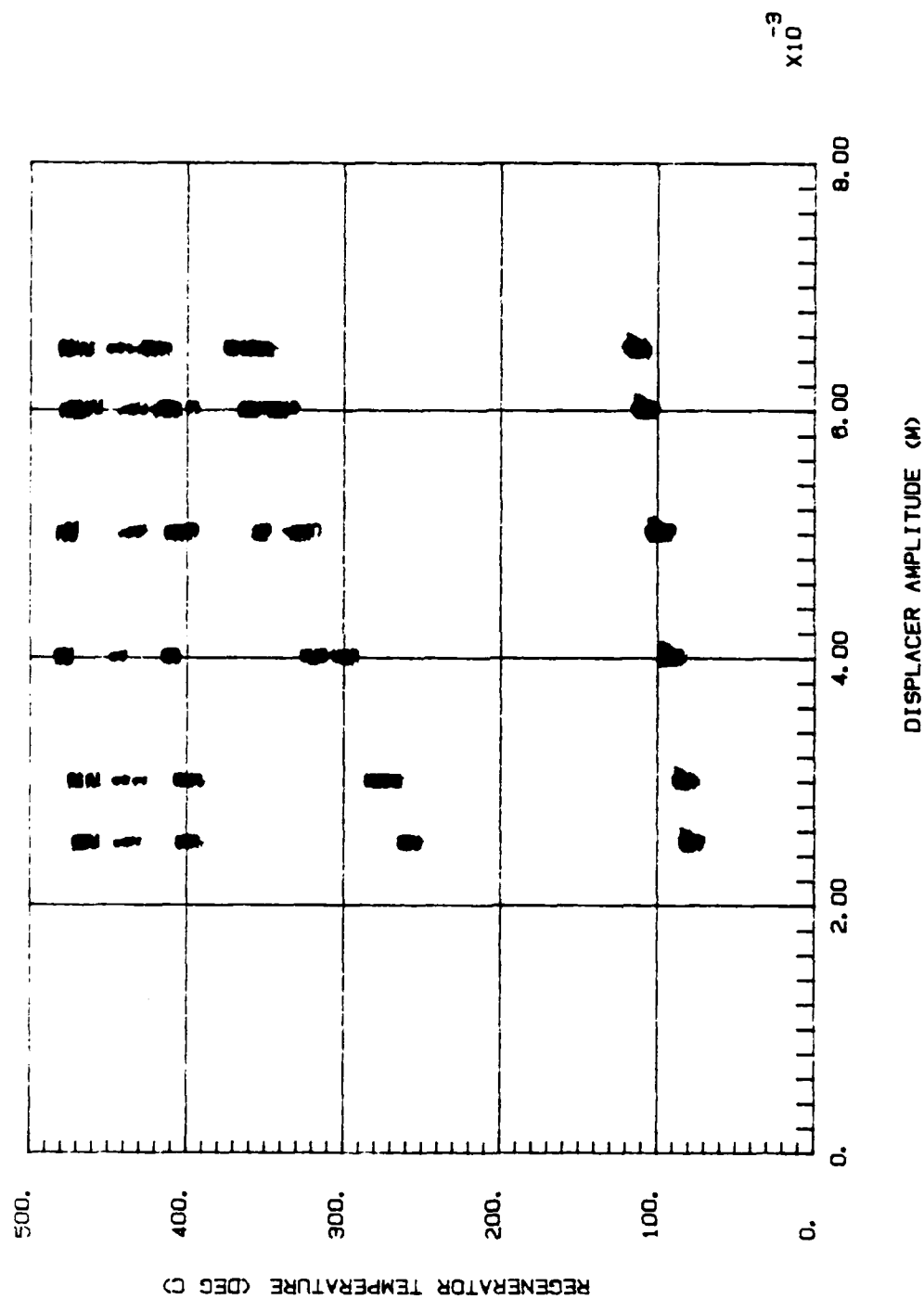


Fig. 20 Regenerator Temperatures with O-Ring Out;
Head Temperature = 560°C

(unequal bypass of working fluid through and around the appendix gap when the stator O-ring is removed).

In summary, the engine build without stator O-ring repeats the 1984 test data. The present hypothesis is that the clearance seal between the displacer liner and motor stator becomes large enough (during the engine operation) to cause significant bypass of flow through and around the appendix gap region.

Test 3 - Repeat Baseline Configuration Engine Test With Stator O-Ring In

Since the removal of stator O-ring from the engine build showed significant drop in engine performance and the engine performance was similar to the 1984 ADM test, it was decided to repeat the baseline configuration test with stator O-ring in. This test was performed on 27 September 1986 using test data file TADMH6.

Figures 21 and 22 show the comparison of PV power measured on engine builds with stator O-ring in, which were tested on 20 September 1986 and on 27 September 1986. Figures 23 and 24 show plots of regenerator temperatures at various displacer amplitudes for the 27 September 1986 test. Engine performance for the two builds is similar. This test again confirms the fact that although some of the components in the 1984 and 1986 ADM builds were different (these changes were made to improve the overall performance), it is the sole presence of stator O-ring that makes the engine perform per the thermodynamic code (engine performance without the stator O-ring repeats the earlier 1984 ADM test results).

Test 4 - Locked Displacer Test

This test was performed on 1 October 1986 using test data file TADMH7 with the displacer locked at about 7 mm from the midstroke position (toward the top dead center). Displacer was held in position by placing cylindrical annular rubber pieces in the load side and the heater side displacer gas spring cavities.



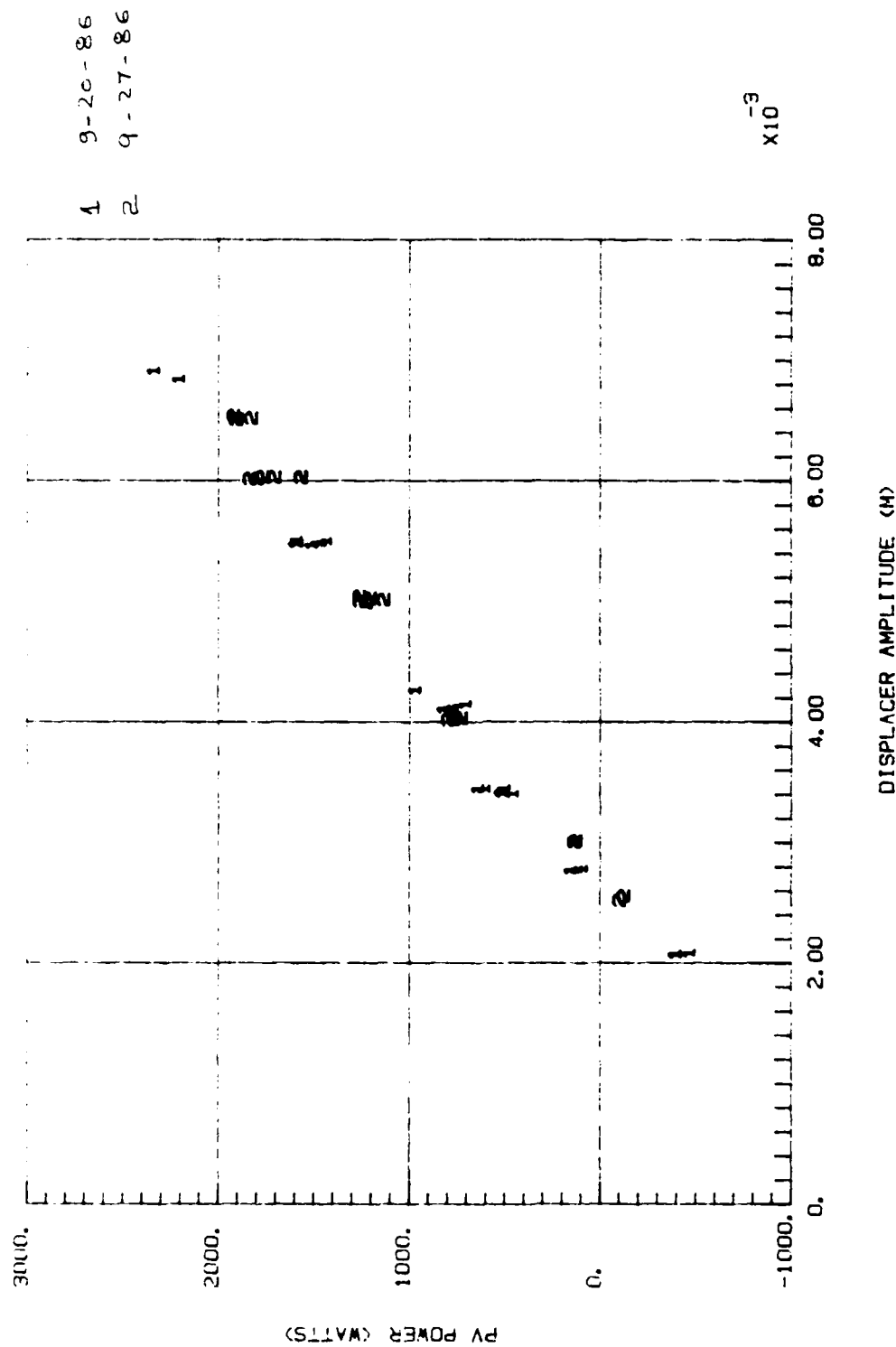


Fig. 21 PV Power Repeat Test with Stator O-Ring in;
Head Temperature = 660°C

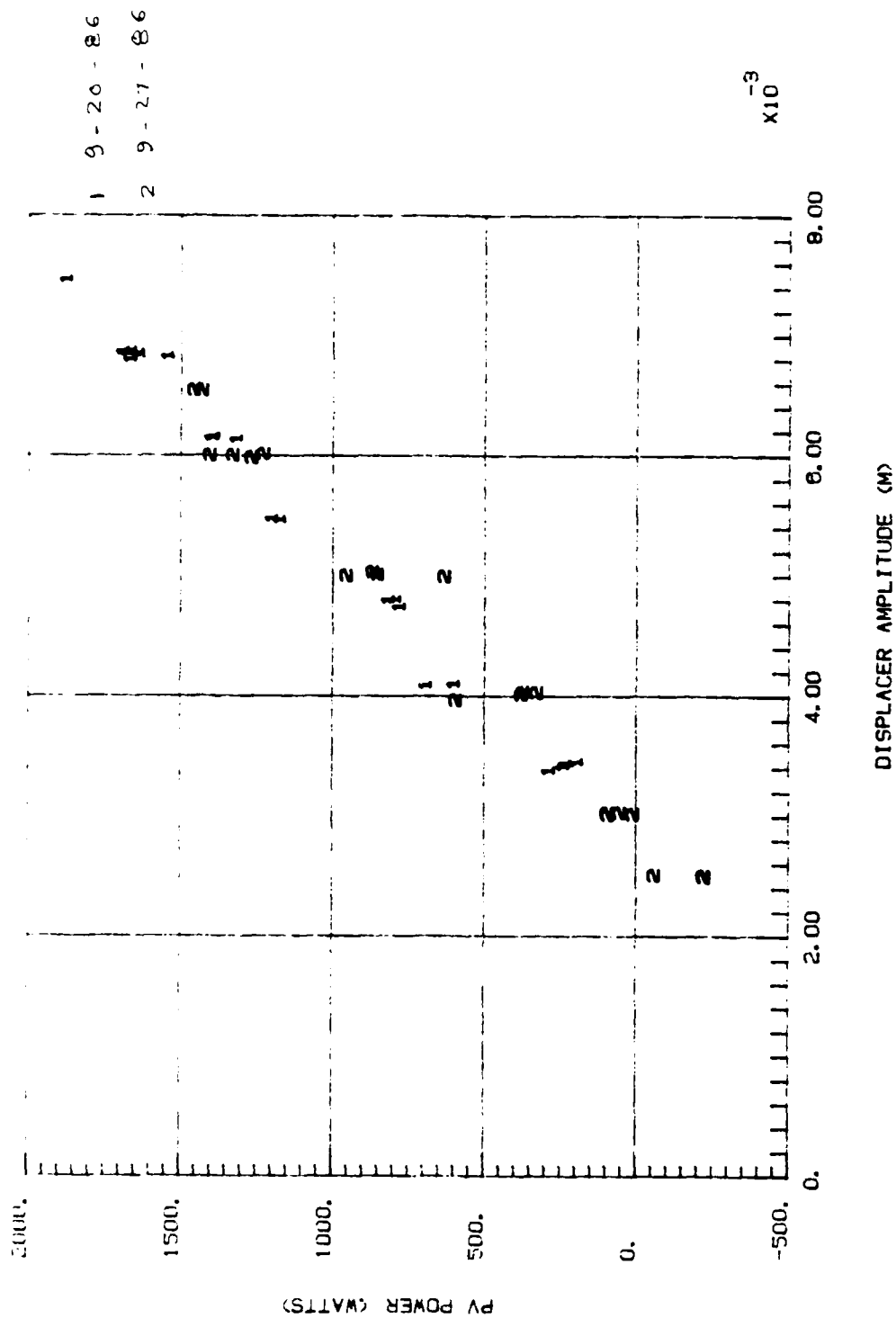


Fig. 22 PV Power, Repeat Test with Stator O-Ring In;
Head Temperature = 560°C

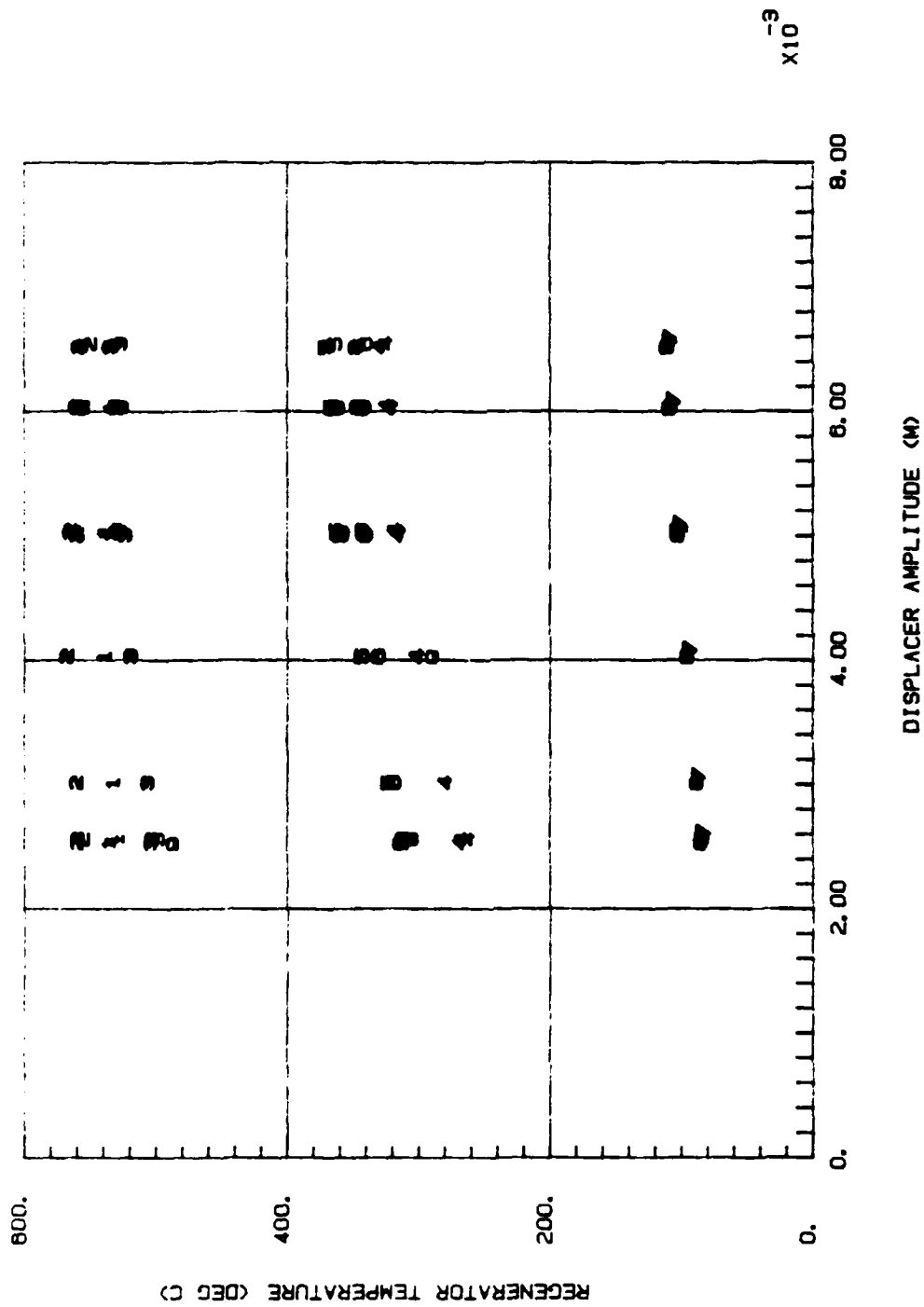


Fig. 23 Regenerator Temperatures; Repeat Test with Stator O-Ring In;
Head Temperature = 660°C

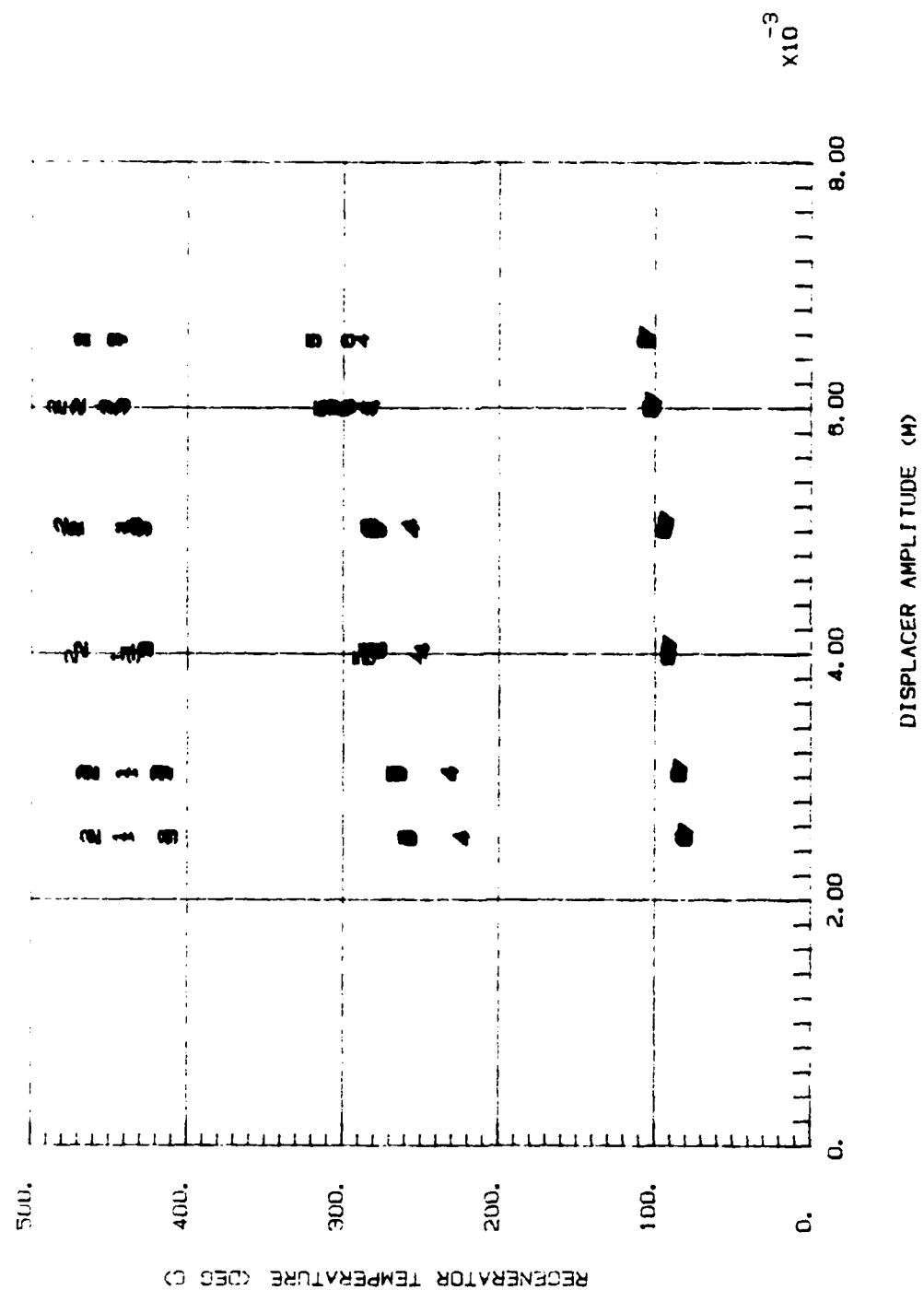


Fig. 24 Regenerator Temperatures; Repeat Test with Stator O-Ring In;
Head Temperature = 560°C

The purpose of this test was to evaluate the pressure-induced parasitic losses in the engine. The engine build was the same as the baseline configuration except that the combustor was not mounted on the engine. The Tests were performed at 60-, 50-, and 40-bar mean pressures. Power pistons were motored and the data were taken at piston amplitudes of 2 to 7 mm. Maximum piston amplitude was limited to 7 mm by the allowable current (28 A rms) in the alternator power supply (Algars).

Figures 25 and 26 show the measured- and code-predicted PV power levels. CFAST predicted the parasitic losses fairly well (as expected) and HFAST underpredicted the parasitic losses (HFAST also underpredicted the parasitic losses in the previous tests 1, 2, and 3 by about 300 W. It is believed that the reason for underprediction of the parasitic losses by HFAST was due to its inadequate modeling of the hysteresis losses. Figure 27 shows the comparison of the test data and corrected HFAST predictions (predicted loss increased by $4.4 \times \text{pressure amplitude}^2$ at each plotted point). With this correction, HFAST predictions have a better match with the test results at 60-bar mean pressure; however, a large discrepancy still exists at 50- and 40-bar mean pressures.

In summary, the parasitic losses in the engine are a strong function of piston amplitude square (Figure 28), which indicates that the dominant losses in the engine are hysteresis and leakage losses. The parasitic losses measured during the locked-displacer, cold-engine test are consistent with the parasitic losses measured during unlocked displacer hot engine tests.

Performance Prediction of ADM Monolithic Head at Larger Piston Amplitudes

The purpose for performing the above series of tests was to compare the thermodynamic performance of the present-build ADM configuration and the ADM build tested in 1984. Therefore, most of the testing was performed under the 1984 operating conditions with a piston amplitude of 7 mm. The design point piston amplitude of the ADM engine is 11 mm and the maximum possible piston amplitude is 14 mm.

As mentioned above, the ADM and the EM engines are thermodynamically similar and therefore should have similar power generation capability if run at simi-



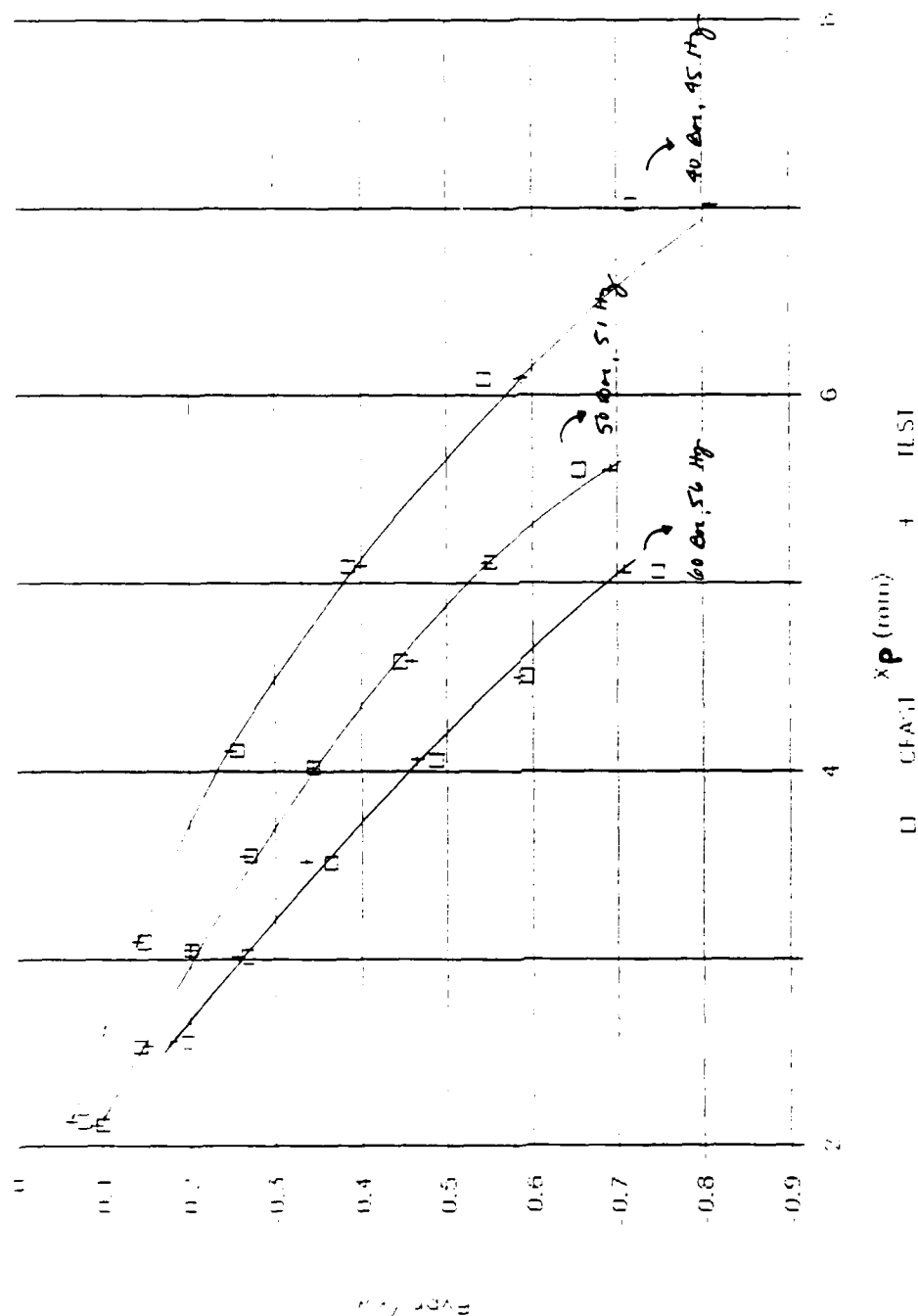


Fig. 25 Locked-Displacer Test; Comparison of CFAST Code Predictions and Measured Test Data

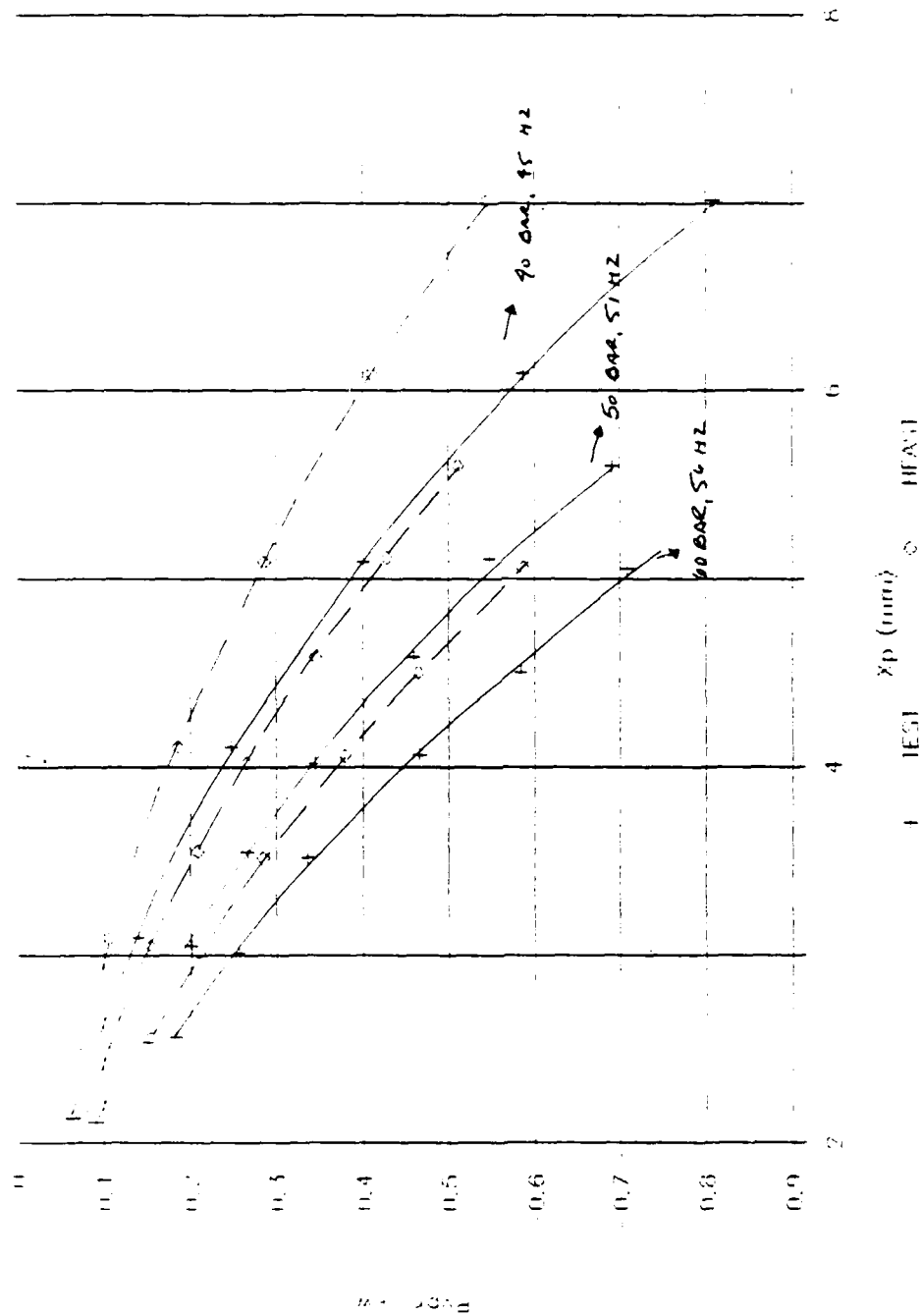


Fig. 26 Locked-Displacer Test; Comparison of HFAS1 Code Predictions and Measured Test Data

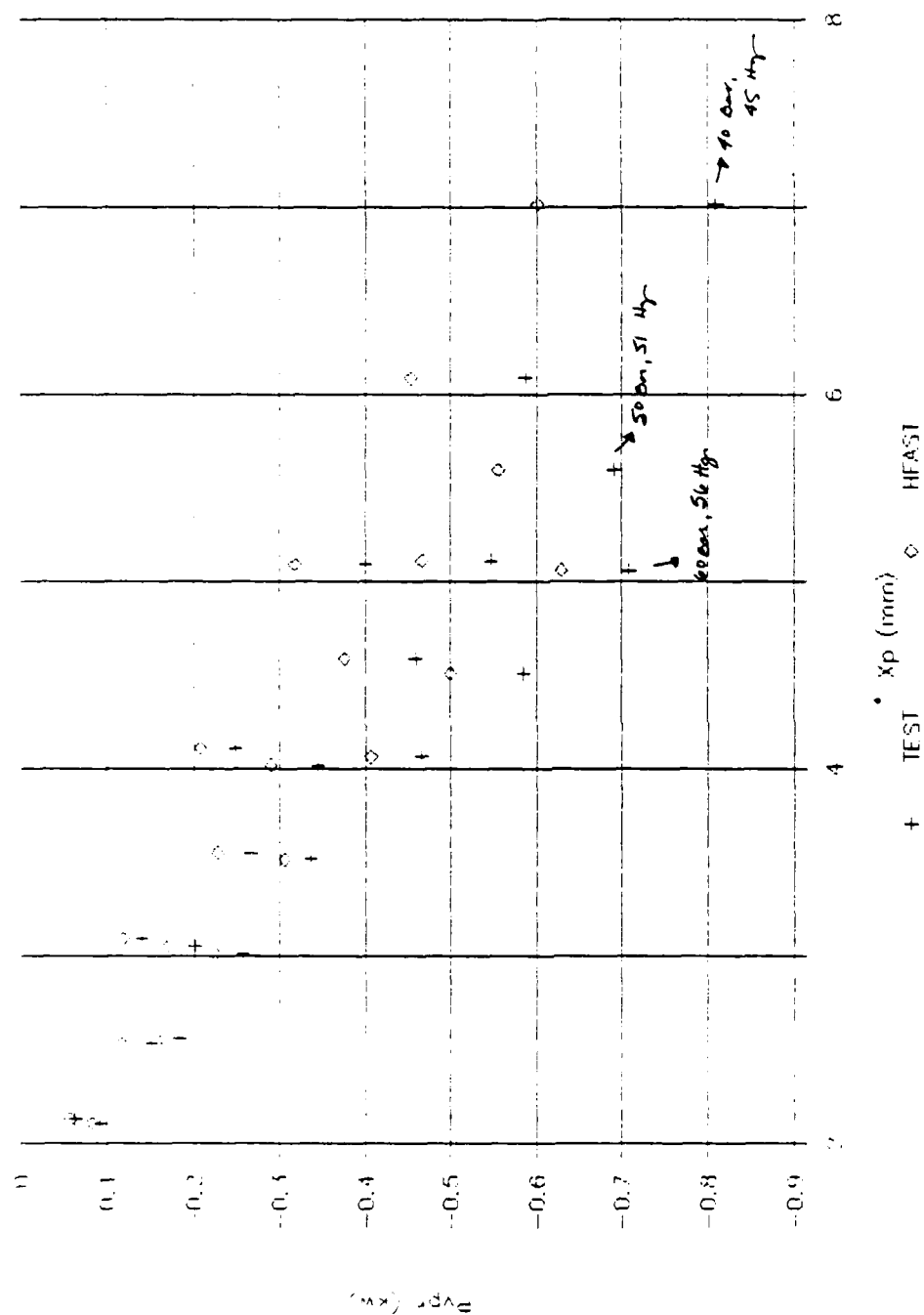


Fig. 27 Comparison of Test Data with Modified HFAS1 Code Predictions

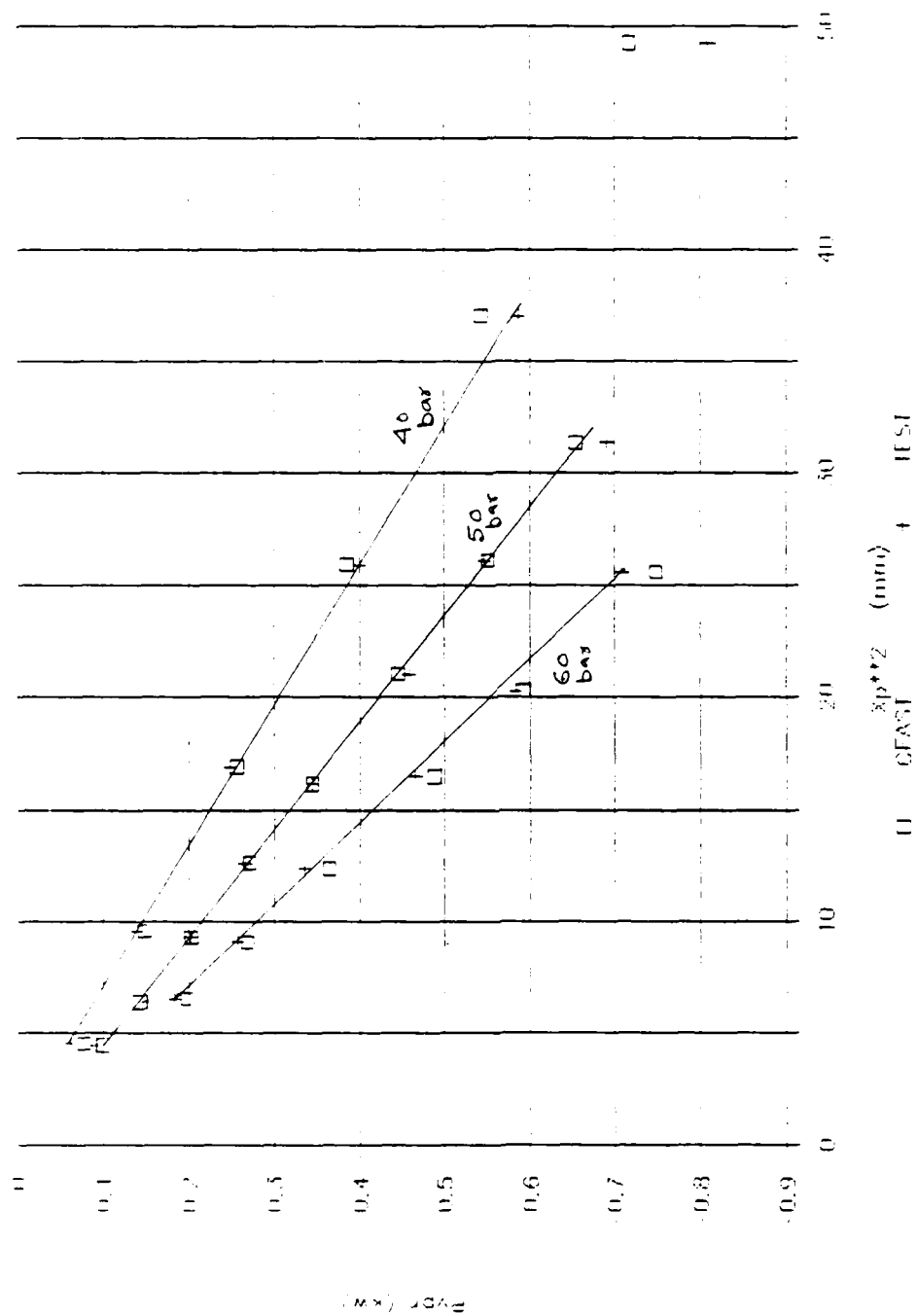


Fig. 28 Plot of Measured PV Power versus Piston Amplitude Square

lar operating conditions. Although the power generation capability of the two engines is similar, the ADM will have a lower PV power compared to the EM engine because of higher parasitic losses (more wetted surface area in the compression space and more number of clearance seals). The EM performance engine generated its maximum PV power (5 kW) at 10 bar compression space pressure amplitude. For the ADM engine, 10-bar pressure amplitude results at 9-mm piston amplitude.

Prediction of the ADM engine performance at 9 mm piston amplitude was made by running the HFAST code. The reasons for selecting HFAST was that it predicted the slope of the PV versus XD curve well, and the discrepancy in predicting the parasitic losses was consistent for the motoring as well as the engine run tests. At 10-bar pressure amplitude, HFAST underpredicts the parasitic losses by about 500 W. For a goal of 5-kW engine PV power, HFAST therefore should predict 5.5 kW. Figures 29 and 30 show the HFAST-predicted PV power plotted for various displacer amplitudes and displacer phase angles at heater head average temperatures of 760°C and 660°C, respectively. Figures 31 and 32 show the heater head heat input (Q_{in}) requirement for the above cases.

Achieving ADM PV power goal of 5 kW at 9 mm piston amplitude with the present build requires an average heater head temperature of 760°C, displacer amplitude of 10 mm, and displacer-to-piston phase angle of 75°.

The maximum possible displacer amplitude for the ADM engine is 12.5 mm. This assumes no offset in the displacer midstroke position. The maximum displacer amplitude that can be achieved in the present ADM configuration (because of displacer midstroke position drift) is about 9 mm. Figures 33 and 34 show the HFAST-predicted PV power plotted at 9 mm displacer amplitude for various power piston amplitudes and displacer phase angles at heater head average temperatures of 760°C and 660°C, respectively. Figures 35 and 36 show the heater head heat input (Q_{in}) requirement for the above cases. Increasing piston amplitude yields a small change in the engine PV power. This is because the parasitic losses in the engine (due to engine pressure wave) increase at higher rate than the thermodynamic power generation of the engine. Figure 37 shows the predicted leakage loss at various piston amplitudes and Figure 38 shows the corresponding pressure amplitude in the engine. The above results

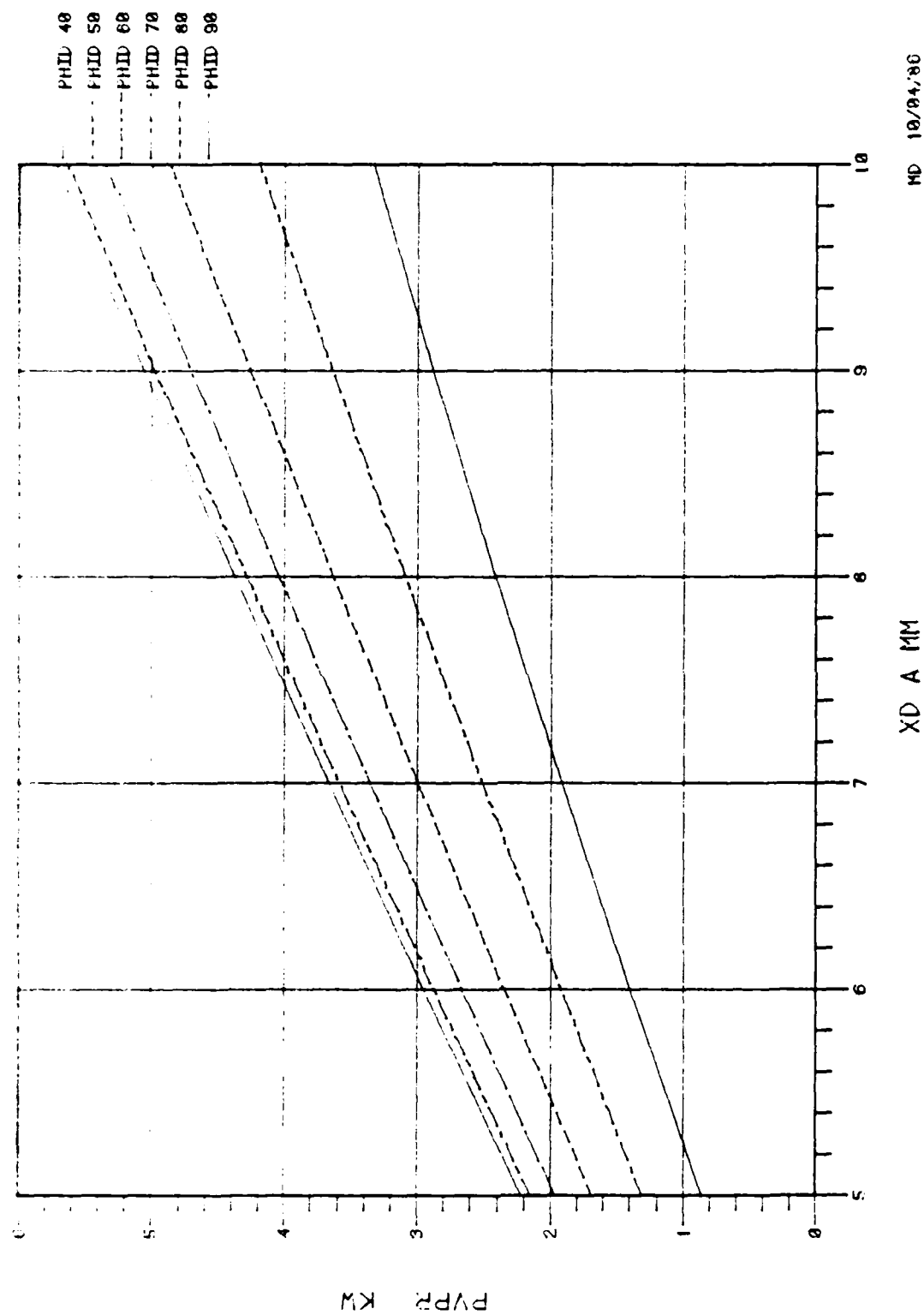


Fig. 29 HFAST-Predicted PV Power at 9-mm Piston Amplitude;
 Temperature Ratio = 760/50°C; Leakage Coefficient
 $= 1.343 \cdot 10^{-13} \text{ m}^3$

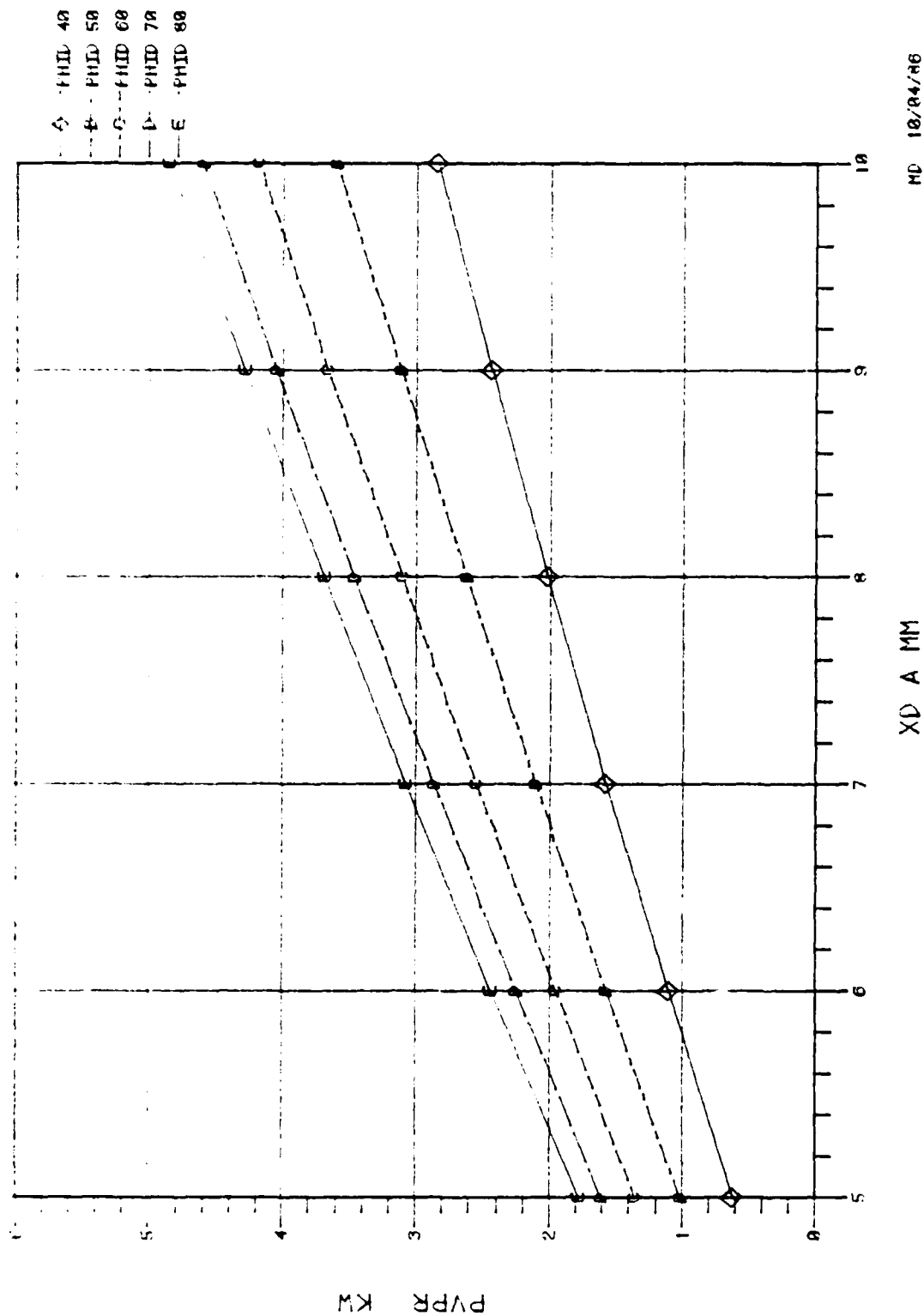


Fig. 30 HEAST-Predicted PV Power at 9-mm Piston Amplitude;
Temperature Ratio = 660/50°C; Leakage Coefficient
= $1.343 \times 10^{-13} \text{ m}^3$

MD 10/04/86

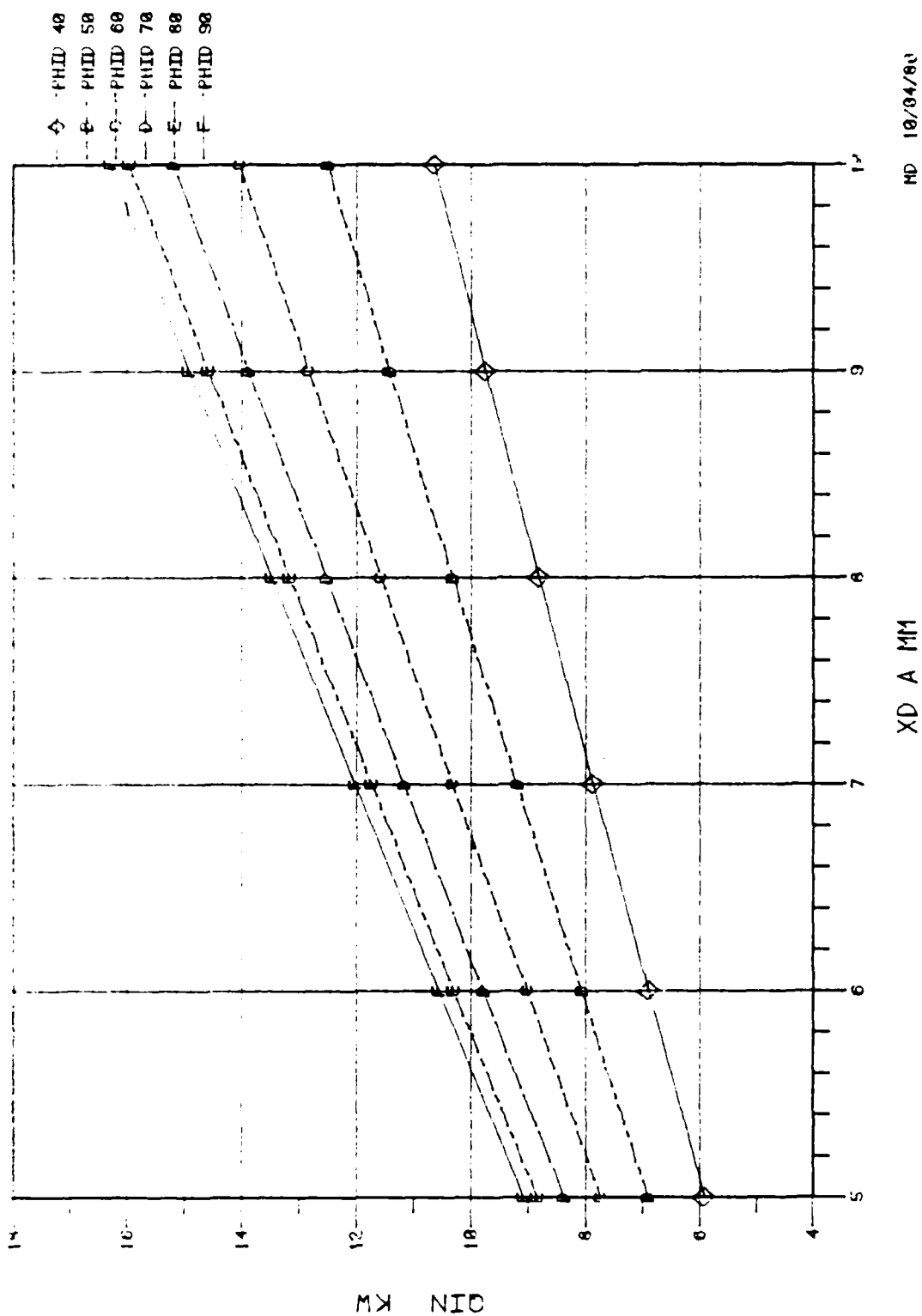
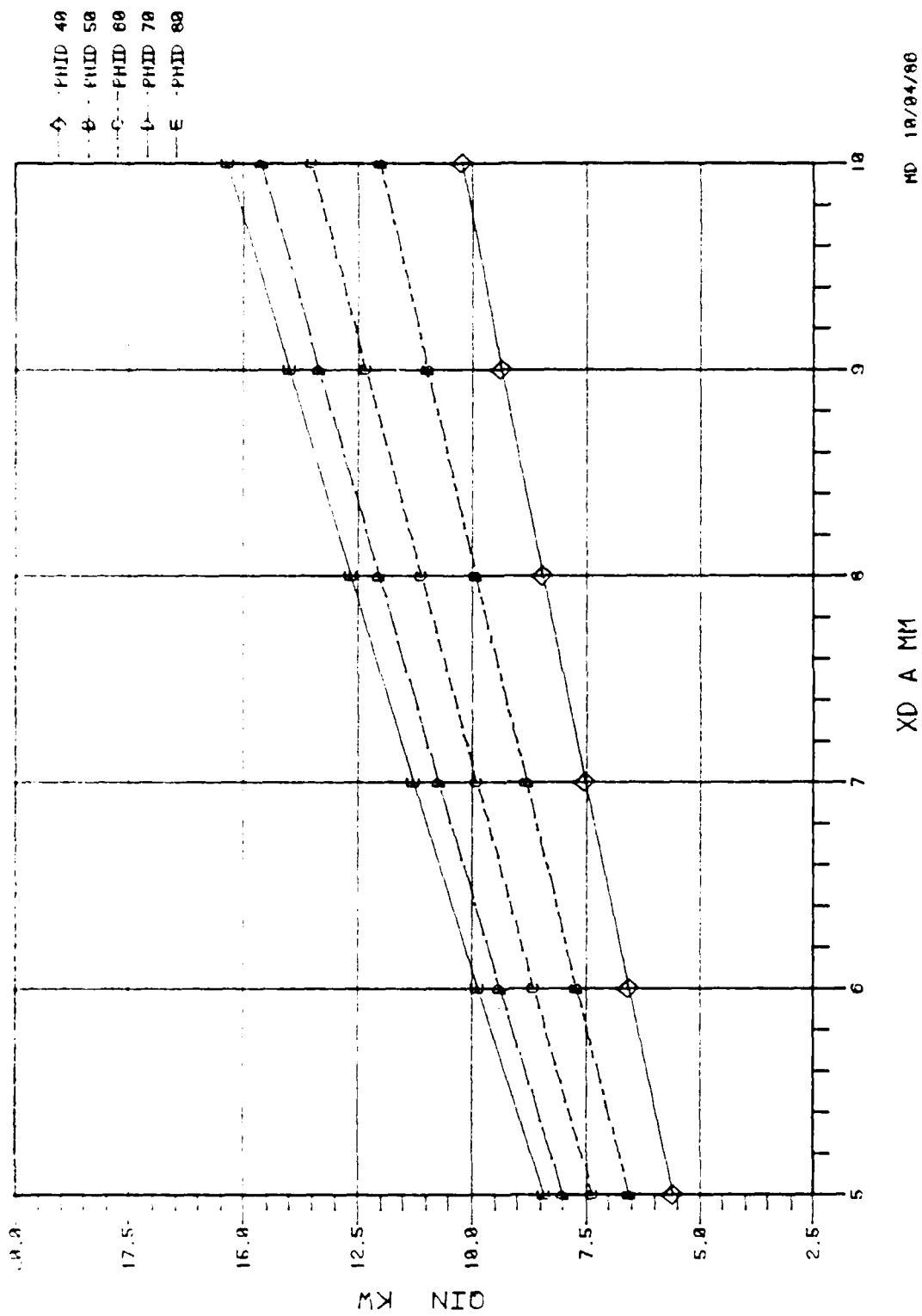


Fig. 31 HFAST-Predicted Heater Head Heat Input; 9-mm Piston Amplitude;
 Temperature Ratio = 760/50°C; Leakage Coefficient = $1.343 \cdot 10^{-3} \text{ m}^3$





MD 10/04/80

Fig. 32 HFAST-Predicted Heater Head Heat Input; 9-mm Piston Amplitude;
Temperature Ratio = 660/50°C, Leakage Coefficient 1.343 10^{-13} m^3

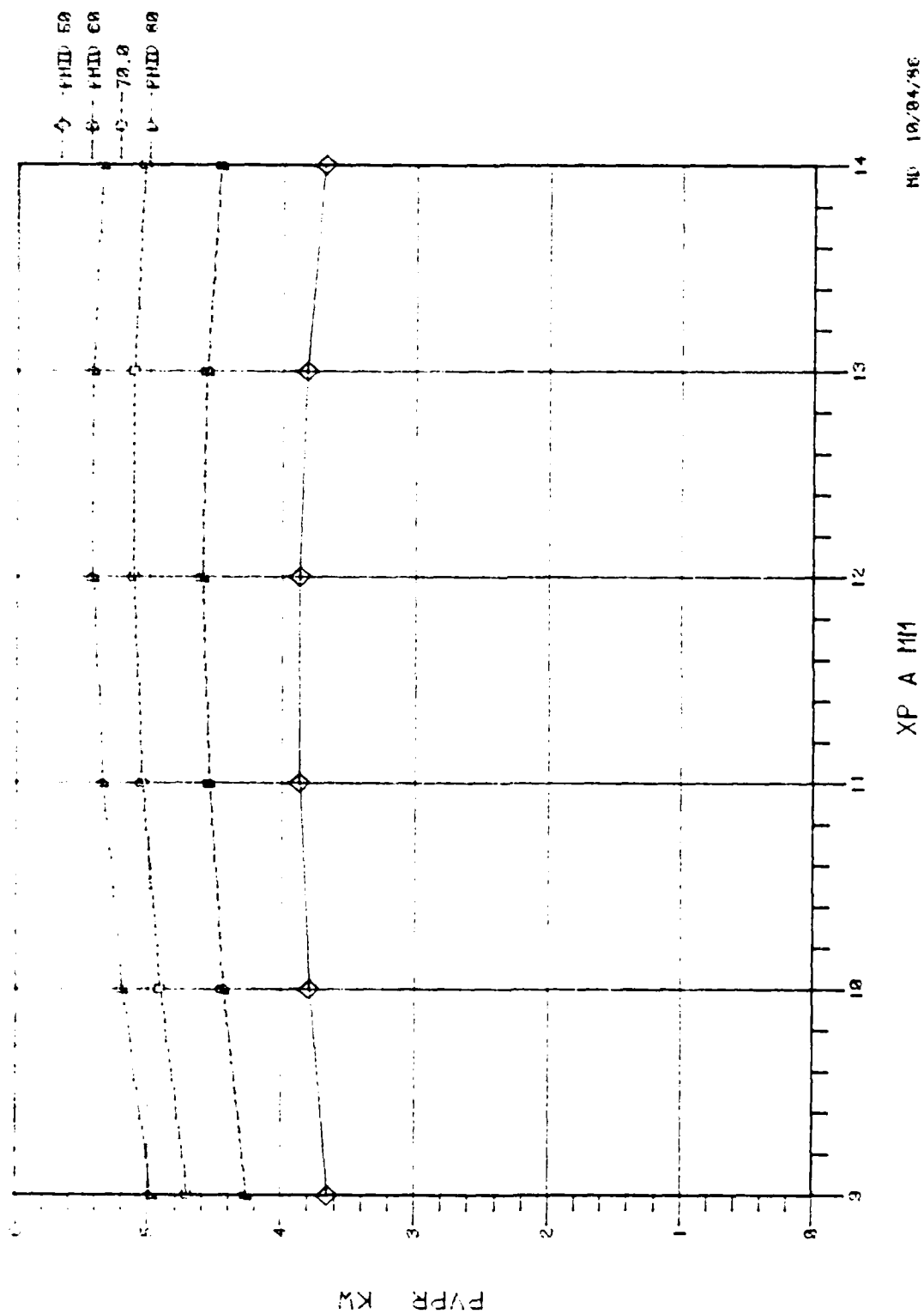


Fig. 33 HFAST-Predicted PV Power at 9-mm Displacer Amplitude;
 Temperature Ratio = 760/50°C, Leakage Coefficient
 = $1.343 \cdot 10^{-13} \text{ m}^3$

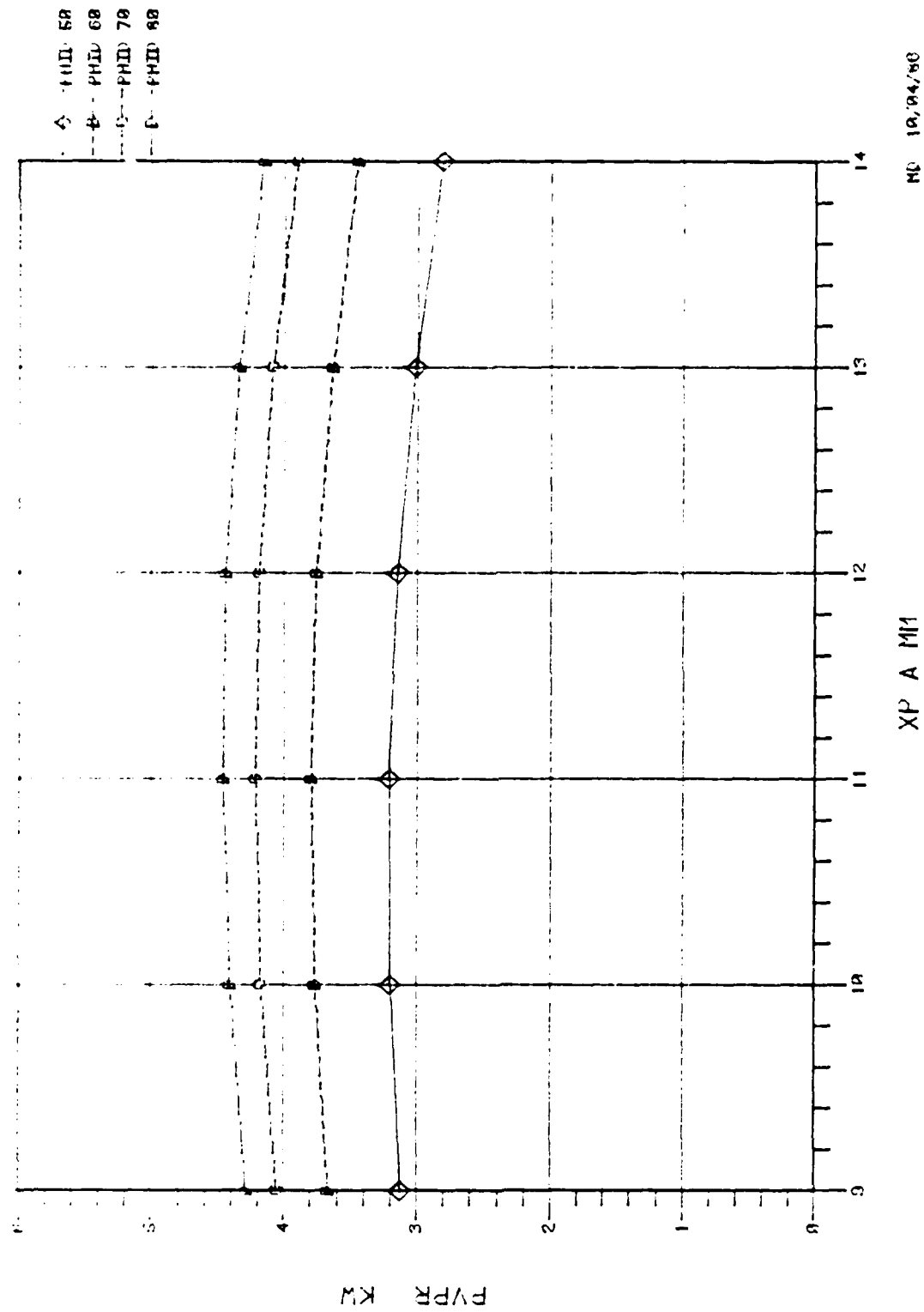
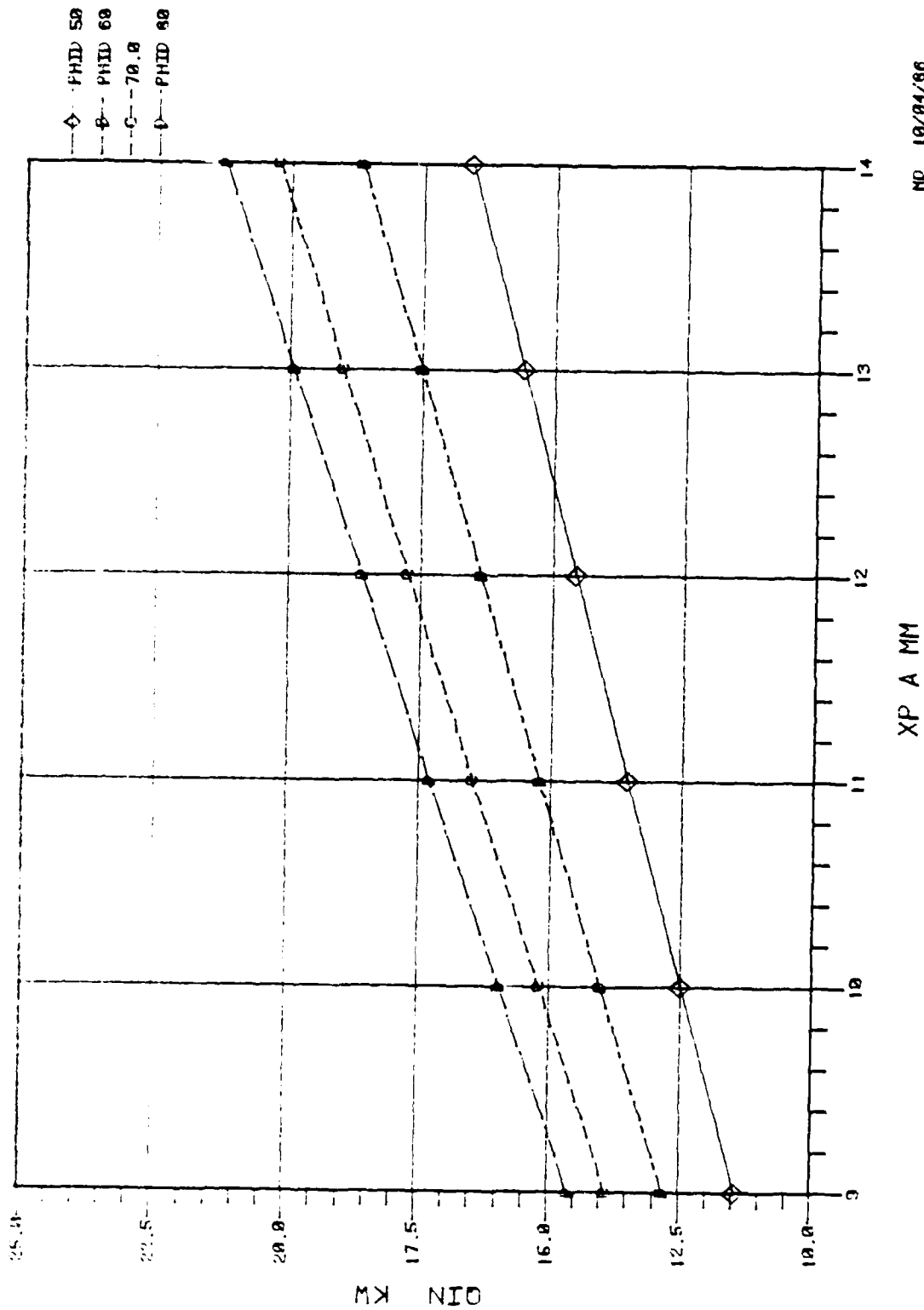


Fig. 34 HFAST-Predicted PV Power at 9-mm Displacer Amplitude;
 Temperature Ratio = 660/50°C; Leakage Coefficient
 $= 1.343 \cdot 10^{-13} \text{ m}^3$



ND 10/04/86

Fig. 35 HFAST-Predicted Heater Head Heat Input; Displacer Amplitude = 9-mm;
Temperature Ratio = 760/50°C; Leakage Coefficient = 1.343 10⁻¹³ m³

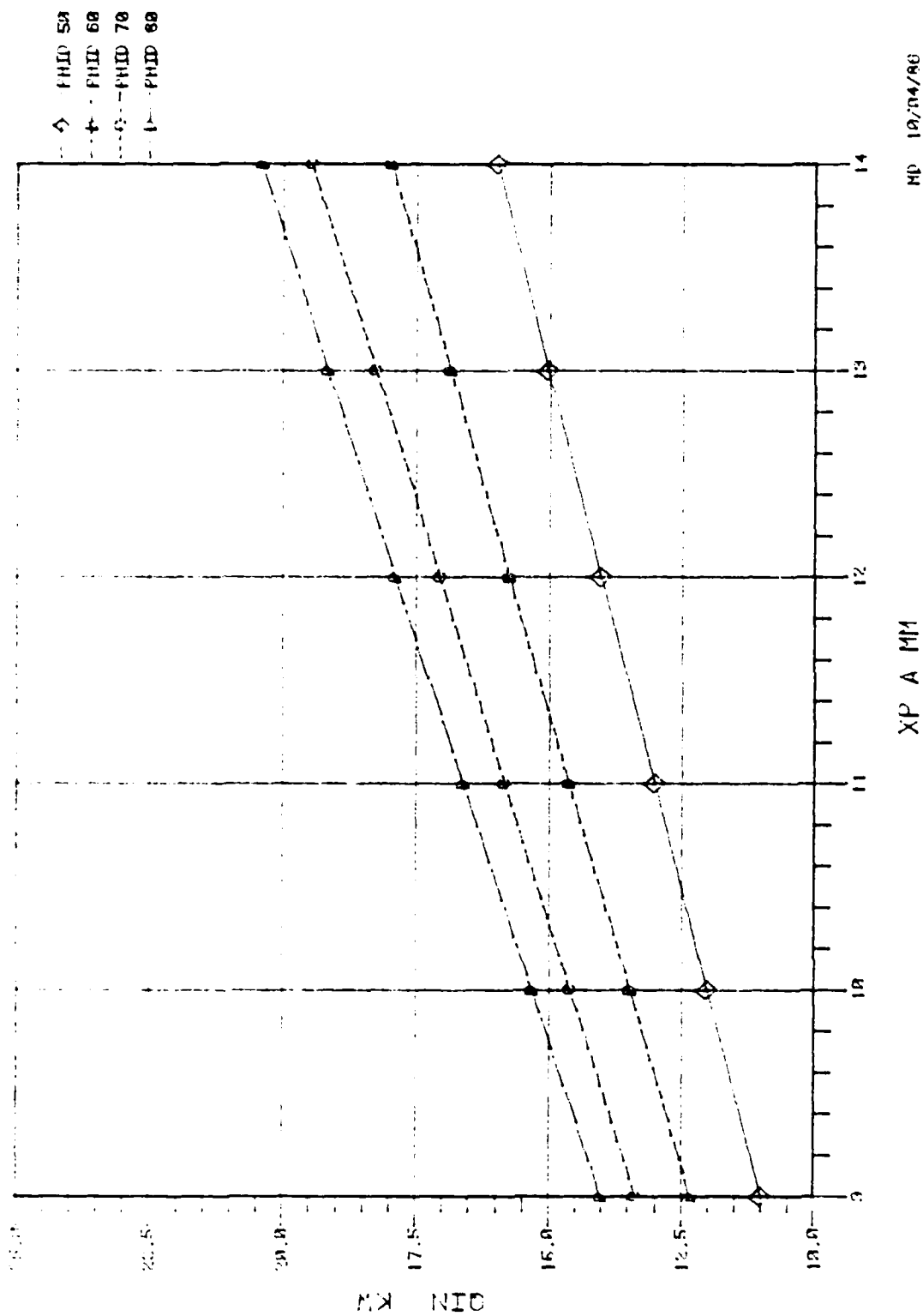


Fig. 36 HFAST-Predicted Heater Head Heat Input; Displacer Amplitude = 9-mm;
Temperature Ratio 660/50°C; Leakage Coefficient = 1.343 10⁻¹³ m³

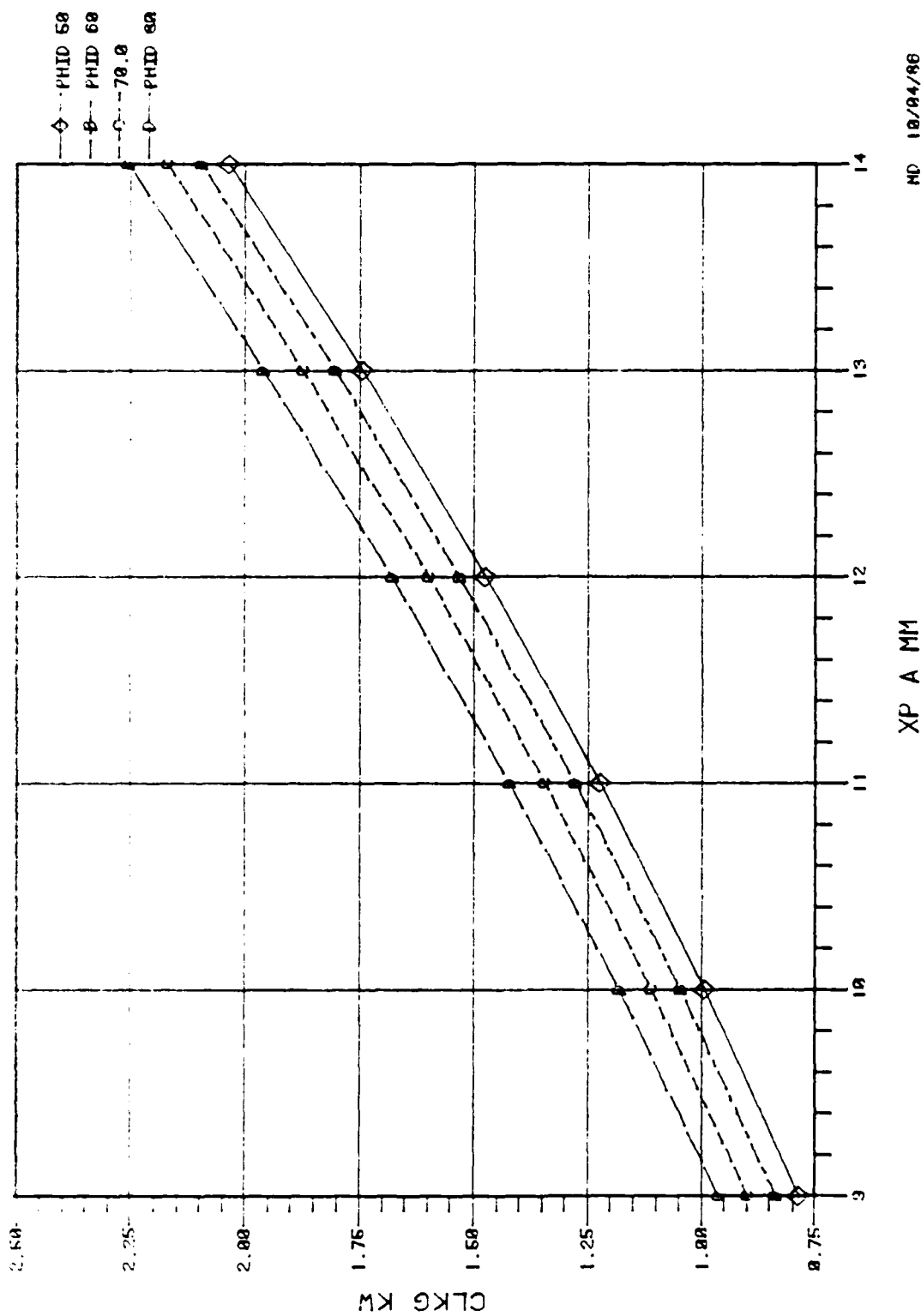


Fig. 37 Leakage Loss as a Function of Piston Amplitude; Displacer Amplitude = 9-mm;
Temperature Ratio = 760/50°C; Leakage Coefficient = 1.343 10⁻¹³ m³

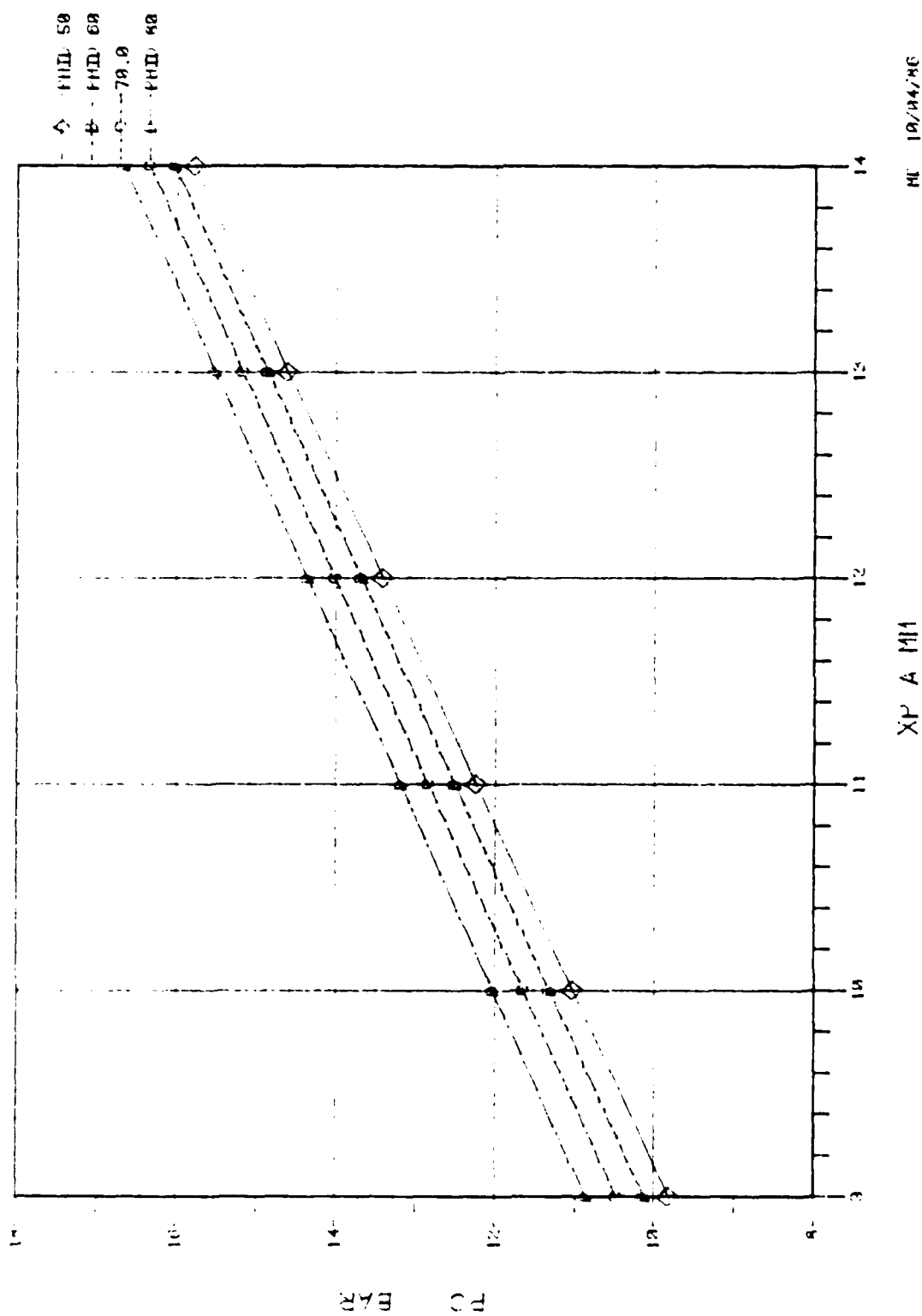


Fig. 38 Pressure Amplitude as a Function of Piston Amplitude;
Displacer Amplitude = 9 mm; Temperature Ratio = 760/50°C;
Leakage Coefficient = $1.343 \cdot 10^{-13} \text{ m}^3$

conclude that at 9 mm displacer amplitude, 5 kW of PV power cannot be achieved with the present-build ADM engine at any piston amplitude. In fact, the PV power of the engine will actually reduce at larger piston amplitudes primarily because of high predicted leakage losses.

The predicted leakage loss was calculated on the basis of the results obtained from the motoring tests and the measurement of pressure wave phase angles in various gas spring volumes. Detailed inspection of the ADM hardware showed that most of the seal clearances should be close to the design values. However, the results of the motoring tests indicate that these clearances may be opening up during the engine operation conditions. Therefore, the losses may not necessarily be due to opening up of the seal clearances, the leakage losses could be due to an unanticipated leakage path or some other unknown loss mechanism as well. Detailed inspection of the hardware did not identify other than known flow paths or loss mechanisms. A flow check of all working spaces and gas spring volumes is required.

Predictions were made with reduced leakage losses (by a factor of about 2; leakage losses corresponded to seal clearances at maximum design tolerance band). Figures 39 and 40 show the HFAST-predicted PV power plotted at 9-mm displacer amplitude for various power piston amplitudes and displacer phase angles at heater head average temperatures of 760°C and 660°C, respectively. Figures 41 and 42 show the heater head heat input (Q_{in}) requirement for the above cases. It is seen that a PV power of 5 kW is achievable at an average heater head temperature of 760°C, displacer amplitude of 9 mm, displacer phase angle of 75°, and at piston amplitudes of 10 mm and above. The modifications required in the present ADM hardware to achieve 5 kW of PV power are discussed in the following paragraph.

ADM Hardware Modification

The following lists the necessary modifications required to the ADM hardware for achieving 5 kW of PV power:

1. The ADM engine, under load-line operating conditions, runs at displacer to piston phase angle of 45°. In order to achieve a

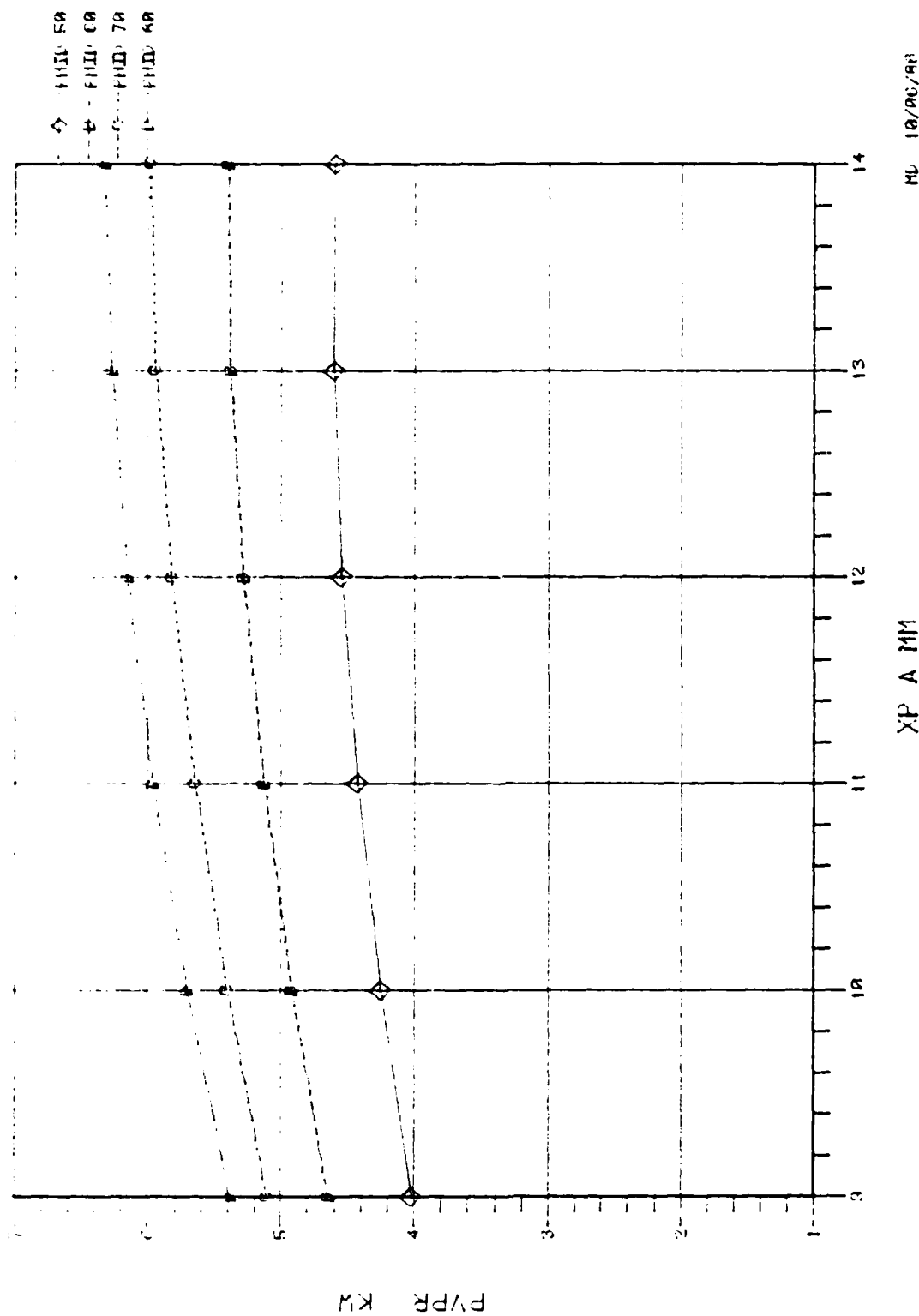


Fig. 39 PV Power as a Function of Piston Amplitude; Displacer Amplitude = 9 mm,
Temperature Ratio = 760/50°C; Leakage Coefficient = $7.7668 \cdot 10^{-14} \text{ m}^3$

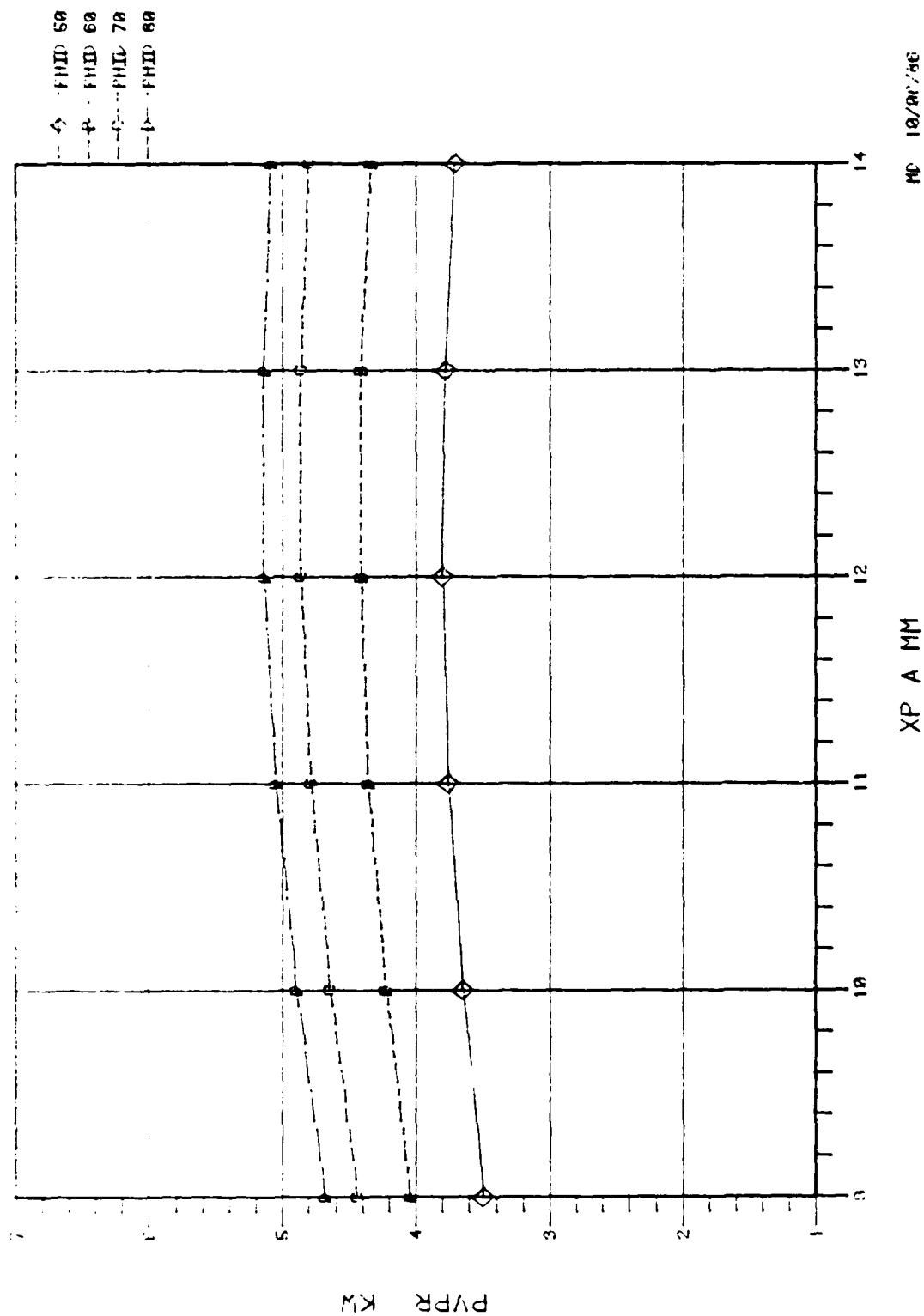


Fig. 40 PV Power as a Function of Piston Amplitude; Displacer Amplitude = 9 mm;
Temperature Ratio = 660/50°C; Leakage Coefficient = $7.7668 \cdot 10^{-14} \text{ m}^3$

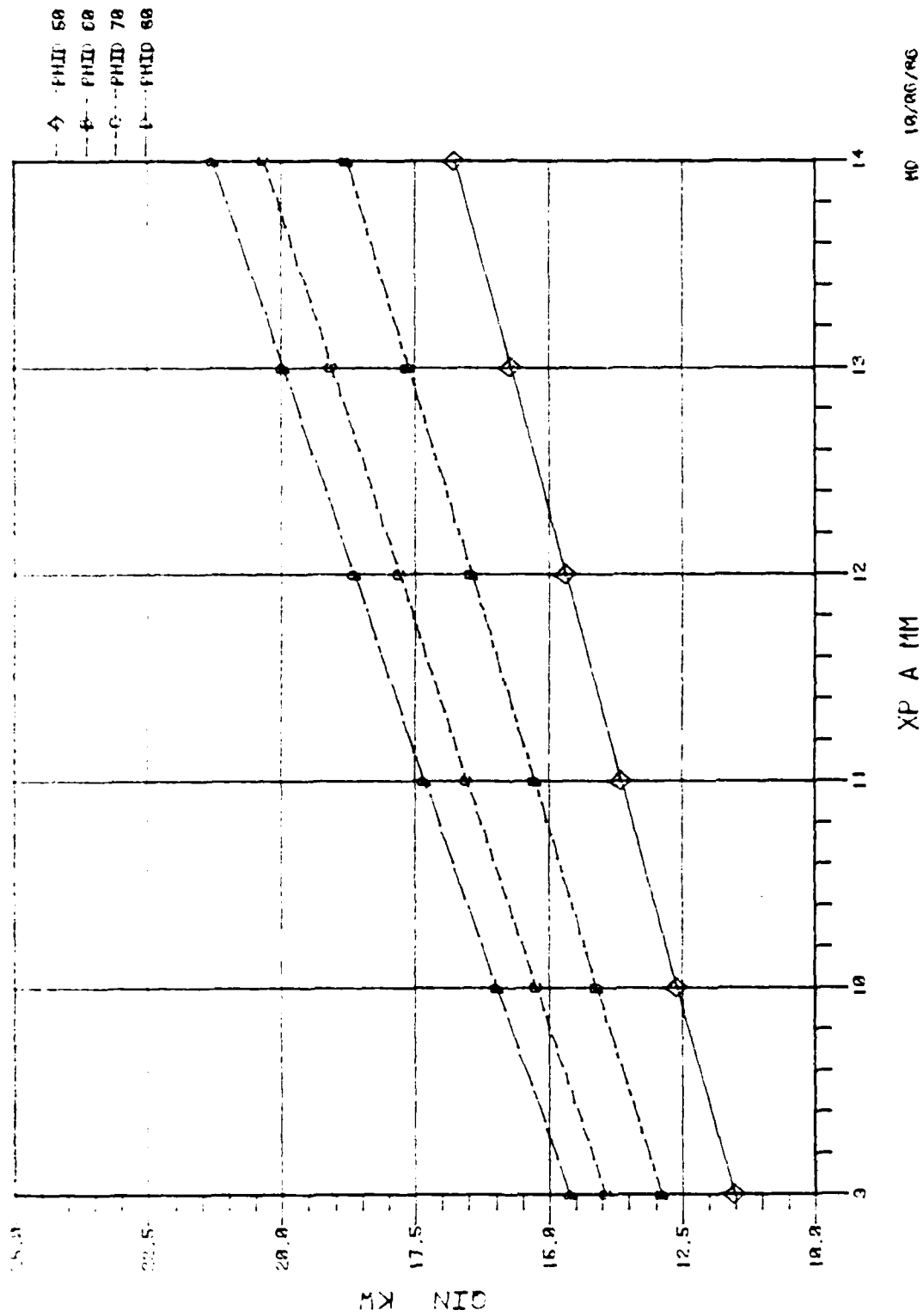


Fig. 41 Heater Head Input as a Function of Piston Amplitude;
 Displacer Amplitude = 9 mm; Temperature Ratio = 760/50°C;
 Leakage Coefficient = $7.7688 \cdot 10^{-14} \text{ m}^3$

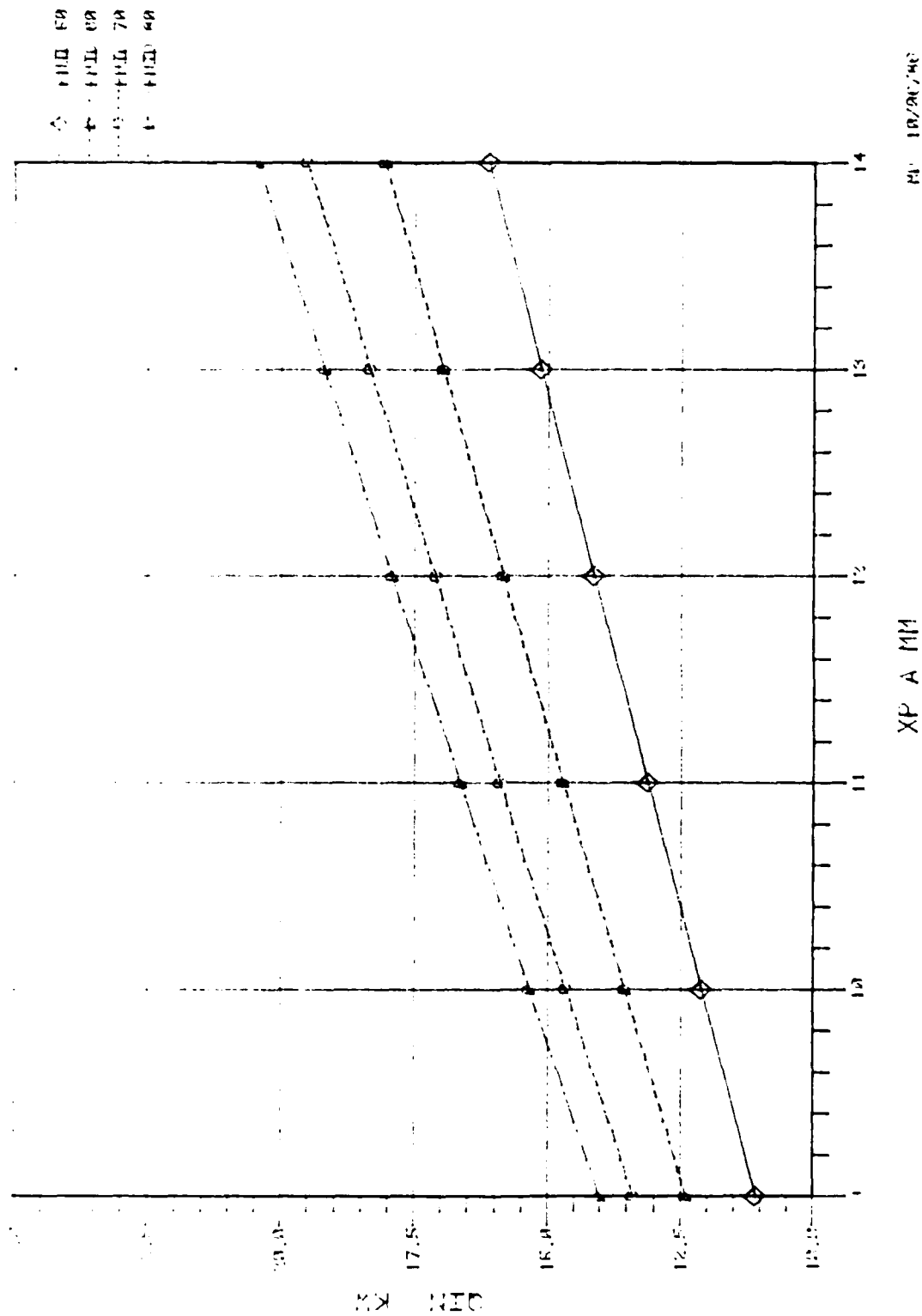


Fig. 42 Heater Head Heat Input as a Function of Piston Amplitude;
 Displacer Amplitude = 9 mm; Temperature Ratio = 660/50°C;
 Leakage Coefficient = 7.7688 10⁻¹⁴ m³

reasonably high PV power, this phase angle has to be increased to about 75° . The displacer phase angle can be increased by increasing the power piston mass and/ or by increasing the piston gas spring volume. The piston gas spring volume can be increased by removing the stuffer liner in the present gas spring volumes.

2. The displacer gas spring losses at present are high. The cause for this high loss needs to be identified by performing pressure leak checks. It may be necessary to reduce the seal leakage losses by incorporating piston rings or Xylan coating.
3. The displacer motor, displacer, and power pistons at present are not properly dynamically tuned to allow engine operation with high displacer phase angle and low motor reactive current. Proper tuning requires modification in the load side displacer gas spring volume.
4. With increasing displacer stroke, displacer midstroke offset increases. The cause for this behavior has to be understood; if necessary, the offset may have to be externally controlled by providing check valves.

Early ADM Tests

The ADM engine was first assembled in early February 1984. The engine was run under the following operating conditions:

- Mean pressure: 60 bar
- Operating frequency: 58 hz
- Mean head temperature: 680°C
- Piston stroke: 22 mm
- Stroke ratio: 0.9
- Displacer-to-piston phase angle: 65°

The measured piston PV power for the above test was 2.8 kW, which was substantially less than the code prediction. The following observations were made after engine disassembly:

- Level of discoloration of the regenerator screens and the displacer dome indicated regenerator and expansion space temperatures were much lower than previously experienced with the EM engine at similar mean head temperatures
- Expansion space stuffer liner was cracked.

The loss mechanisms postulated for the power shortfall were:

- Low expansion space temperature due to poor stuffer-fin interface with the ADM head
- Excessive compression space leakage and/or hysteresis loss
- Excessive hysteresis loss in the ADM cooler
- Maldistribution of flow
- Excessive loss in cold-connecting duct
- Large volume in compression space caused some unknown loss
- Gas resonance resulting in high viscous losses
- Cooler plenum too tight.

The following paragraphs give the results of the tests performed to evaluate the influences of the above on power shortfall.

Low Expansion Space Temperature Due to Poor Stuffer-Fin Interface. A back-to-back test of the ADM engine with ADM and EM heater heads showed similar performance. Therefore, the ADM heater head could not be the cause of the power shortfall. Next, the ADM engine was tested with a modified EM heater head that incorporated an expansion space thermocouple. At a heater head wall mean temperature of 680°C , the measured expansion space temperature was 574°C . The code predicted both the expansion and compression space temperatures within $\pm 15^{\circ}\text{C}$. Although the calculated temperature difference between the expansion space and the heater head mean temperature agreed with only a small deviation to the measured temperature difference, the code heater head heat input (Q_{in}) was higher than the measured Q_{in} . Test and predicted cooler heat rejection were similar. Correction of gas temperature for the Q_{in} difference resulted in relatively small change in predicted piston PV power. Therefore, heater head stuffer fin interface was not the cause for the power shortfall.

Compression Space Leakage and Hysteresis. A static flow check of the power piston seals indicated that the seal clearances were 0.7 mil and 0.816 mil, respectively. Per design, the seal clearance is 0.5 mil.

To evaluate the compression space leakage and hysteresis losses, the lower end was tested separately by bolting a plate on the engine flange. A motoring test of the lower end indicated that leakage and hysteresis losses, when projected to the design stroke, would be approximately 1800 W, which is about 800 W higher than design. Analytical evaluation showed reasonable agreement with these test data when measured clearances and hysteresis factor of 2 were applied. Running the code with these modifications had a small impact on power shortfall. The conclusion was that the compression space leakage and hysteresis were not the major cause of power shortfall.

ADM Cooler. ADM cooler internal fin gap is twice that of the EM cooler. Tests were performed again with the bolted flange lower end with both ADM and EM coolers to evaluate cooler hysteresis losses. Results indicated that while the ADM cooler did add some additional hysteresis loss, this loss was small.

Flow Maldistribution. Flow deflectors were installed in the compression space aligned with the slot in the hub, to reduce any maldistribution of flow velocity in the cold duct. This test was repeated by installing the deflectors to increase maldistribution. Comparison of test results indicated no appreciable performance change.

Compression space surface temperature profile was measured by incorporating thermal strips (100-170°F range; resolution 10°F). Eight strips were located circumferentially around the displacer gas spring cylinder, four strips on the compression space hub, and one strip on the piston face. Strips were also located in both displacer gas springs and on the motor stator just beneath the regenerator. The engine was tested at a mean head temperature of 660°C with a displacer stroke of 18 mm. All the temperature strips on the compression space surface indicated a temperature of 140°F. Temperatures at the top of the displacer motor liner and at the top of the head side displacer gas spring were in excess of 170°F, which was expected.

Cold-Connecting Duct. Pressure measurements at the two extreme positions of the cold connecting duct did not indicate any major loss.

Compression Space Volume. The top end of the EM was assembled on the bottom end of the ADM engine with an additional compression space volume of 500 ccs. The test results could not be explained in terms of a direct dead volume effect. It was decided to repeat this test again.

Gas Resonance. Eigenvalues and eigenfunctions of the fluid motion in the ADM engine were calculated. The results indicated that gas resonance was not the cause for power shortfall.

Tight Cooler Plenum. ADM cooler cold-side entrance was machined back 0.2 in. to provide an entrance plenum. A close-mesh screen was installed at the cold side of the regenerator. The addition of the close-mesh screen was detrimental to engine performance. In subsequent tests, this screen was removed. Test results indicated that incorporation of cooler plenum did not result in any significant performance change.

FY84 ADM/EM Diagnostic Testing

Since the above investigation did not yield any clues for the power shortfall, it was decided to lay out a logical test plan that compared the performance of the thermodynamically similar EM and ADM engines.

The differences between the ADM and the EM engine components are:

- Lower end - two power pistons versus one power piston; larger surface area and dead volume in the ADM compression space; and different cold connecting ducts
- Cooler - more open internal fins in the ADM; different water side fins
- Displacer - the ADM has different displacer drive than the EM.

The logic for using the EM engine to evaluate the reasons for the ADM power shortfall was:

- If the ADM power shortfall was due to the displacer drive and/or cooler, testing the EM engine on the ADM engine bottom end should result in higher performance than ADM top on ADM bottom.
- If the problem is in the lower end, testing the EM on the ADM should give the same performance as ADM on ADM.
- Since earlier EM test data matched code predictions, EM on EM performance should be better than ADM on ADM performance if the ADM engine is run under EM thermodynamic conditions (same pressure amplitude, displacer amplitude, and phase between the two).

Based on the above, the following series of tests were performed with the ADM, the EM, and the combination of the two engines at EM thermodynamic conditions:

- ADM top (ADMT) on ADM bottom (ADMB)
- EM top (EMT) on EM bottom (EMB)

- EM top on ADM bottom
- ADM top on EM bottom.

These tests were performed in a slope/intercept format that allowed separation of locked displacer parasitic losses from moving displacer parasitic losses and power generation. The EM system Cell 5 engine was used for the above tests.

Figures A-1 through A-4 show the results that indicated that there was essentially no performance difference between EMT on EMB, ADMT on ADMB, and EMT on ADMB builds (very small difference between the EM system engine and the ADM engine performance). ADMT on EMB was tested latter in 1985 and this test also showed similar results. In addition, the EMT on EMB test data differed from the code predictions in the same manner as the ADMT on ADMB test data differed from the code predictions. The performance of the EM system engine was well below the previously measured (1982 and March 1984) EM performance Cell 3 engine data.

It was a surprise that the EM system engine behaved similar to the ADM engine. The question that arose was that if a good (good refers to EM engine which has performance similar to EM performance engine) EMT is tested on ADMB, will the performance be similar to the EM engine; looking at all the available facts, the answer was yes. The focus, therefore, shifted to the understanding of why the EM system engine performed poorly as compared to the EM performance engine. Understanding this difference was the first goal of FY85 IR&D program, which was a necessary step in identifying the reason for the ADM power shortfall (see Figure A-5). The other goals of IR&D FY85 program were:

- Validate slope/intercept performance evaluation technique
- Build a good EM engine for testing on the ADM bottom end
- Investigate influence of compression space volume on engine performance.



PV Power (kW)

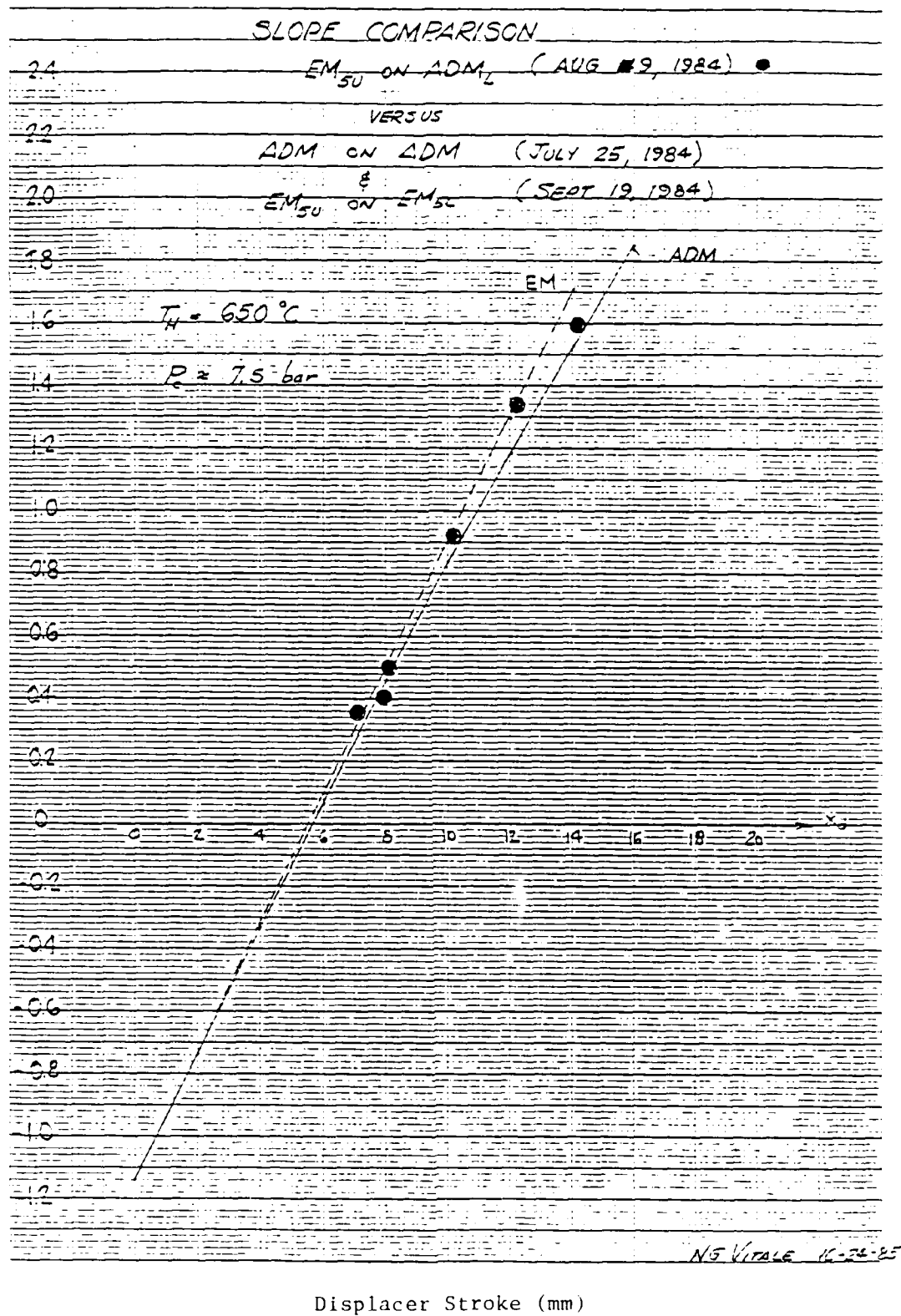


Fig. A-1 PV Power Slope Comparison of ADM and EM Engines;
Head Temperature = 650°C



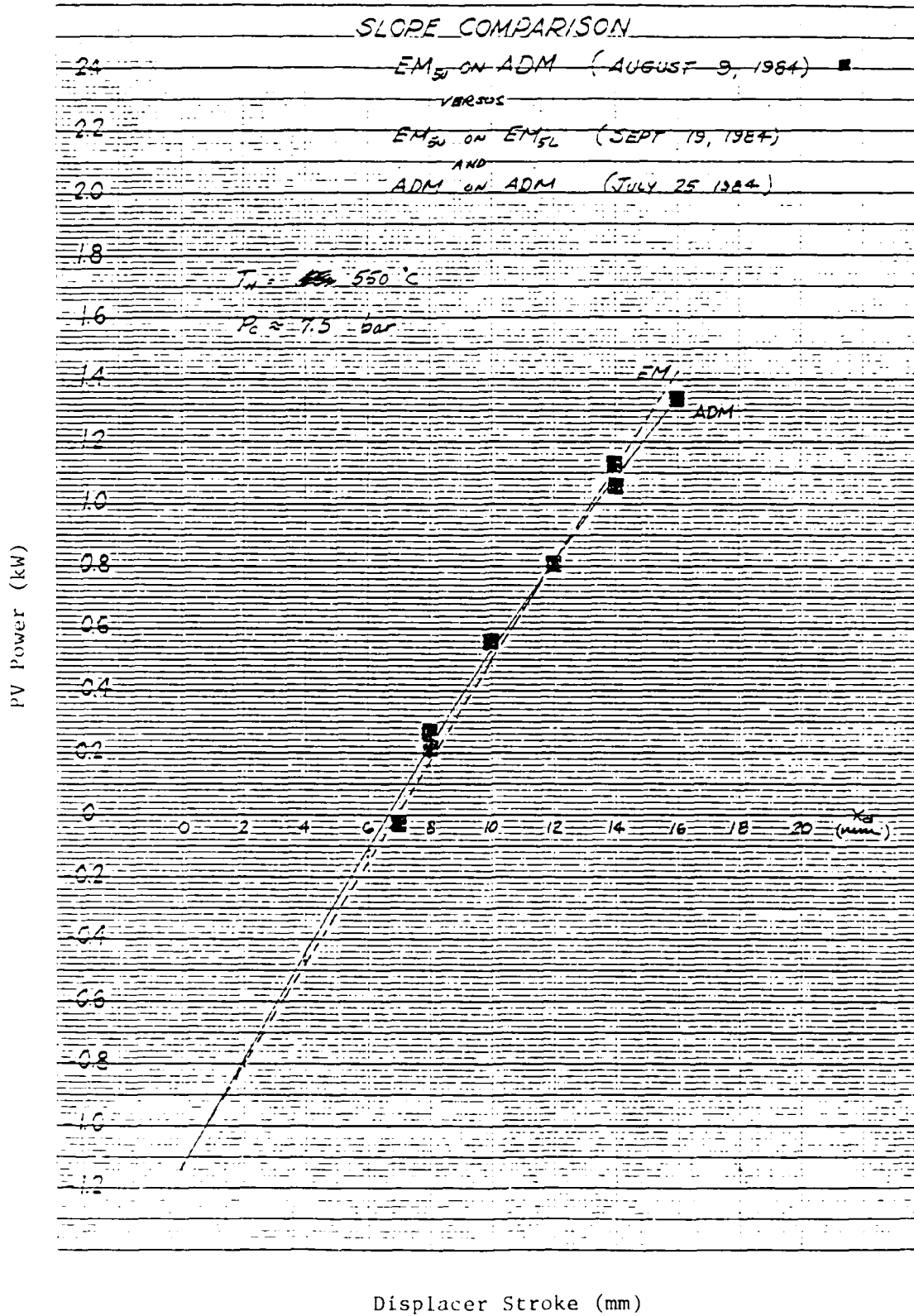


Fig. A-2 PV Power Slope Comparison of ADM and EM Engines;
 Head Temperature = 550°C

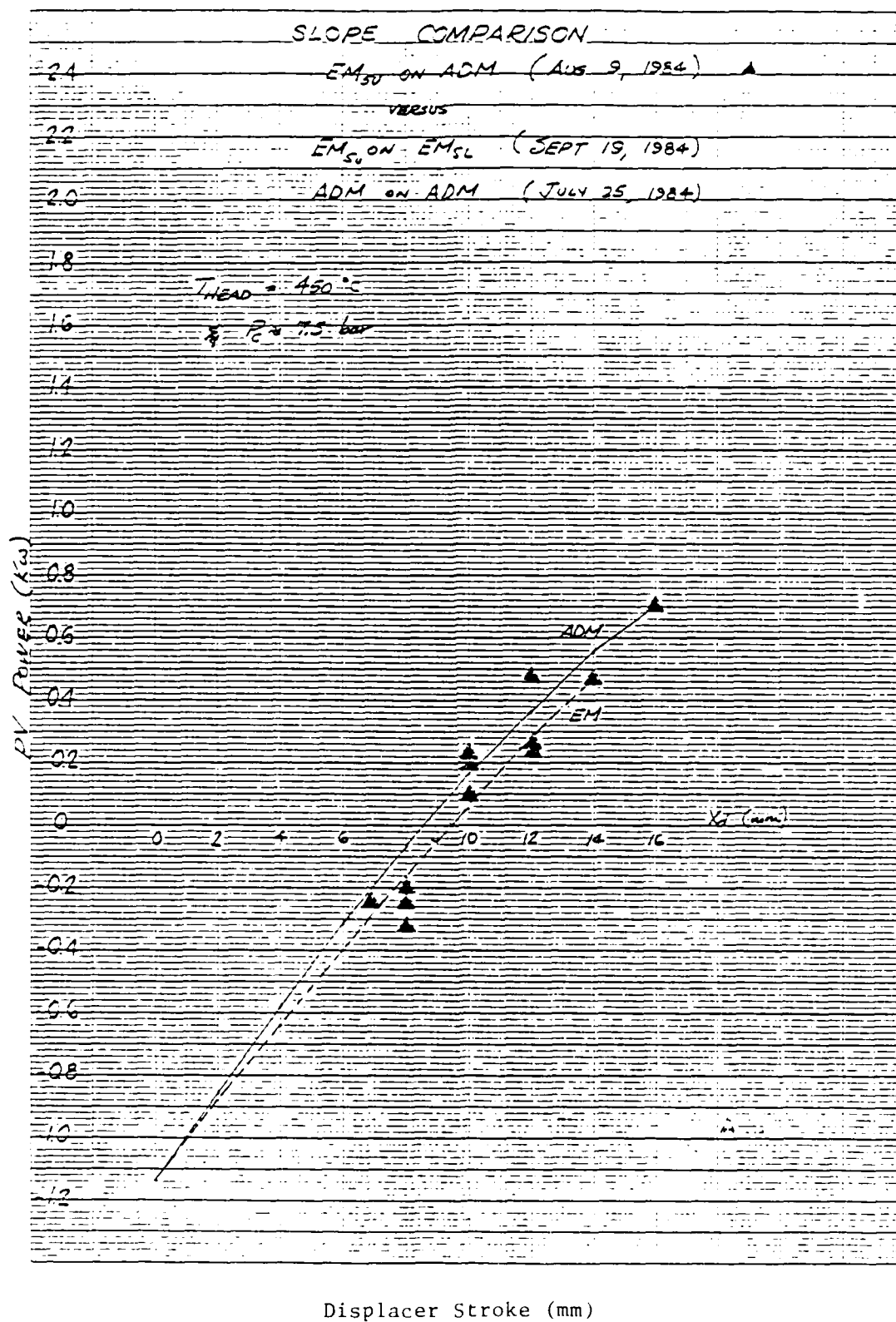


Fig. A-3 PV Power Slope Comparison of ADM and EM Engines;
Head Temperature = 450°C

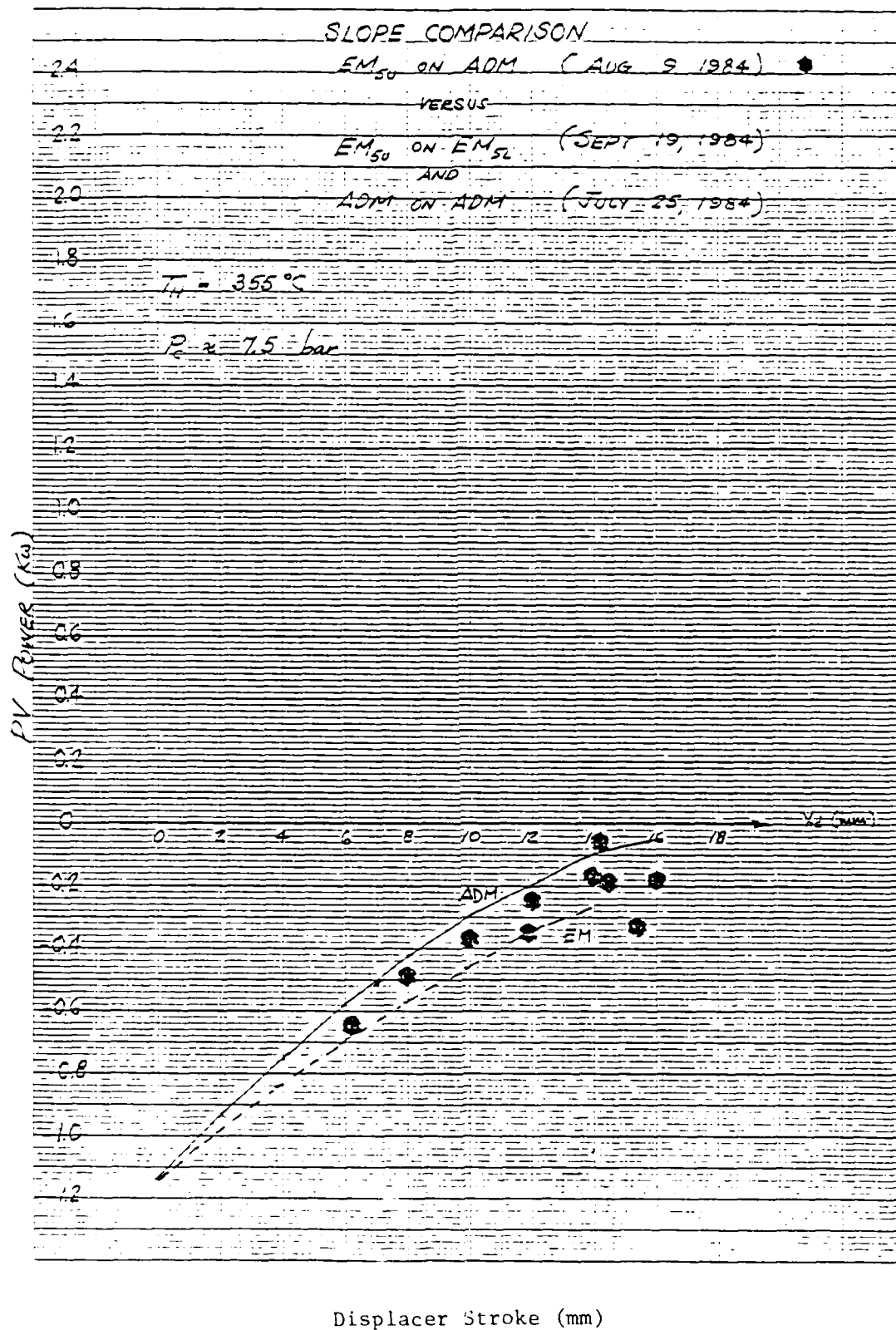


Fig. A-4 PV Power Slope Comparison of ADM and EM Engines;
Head Temperature = 355°C

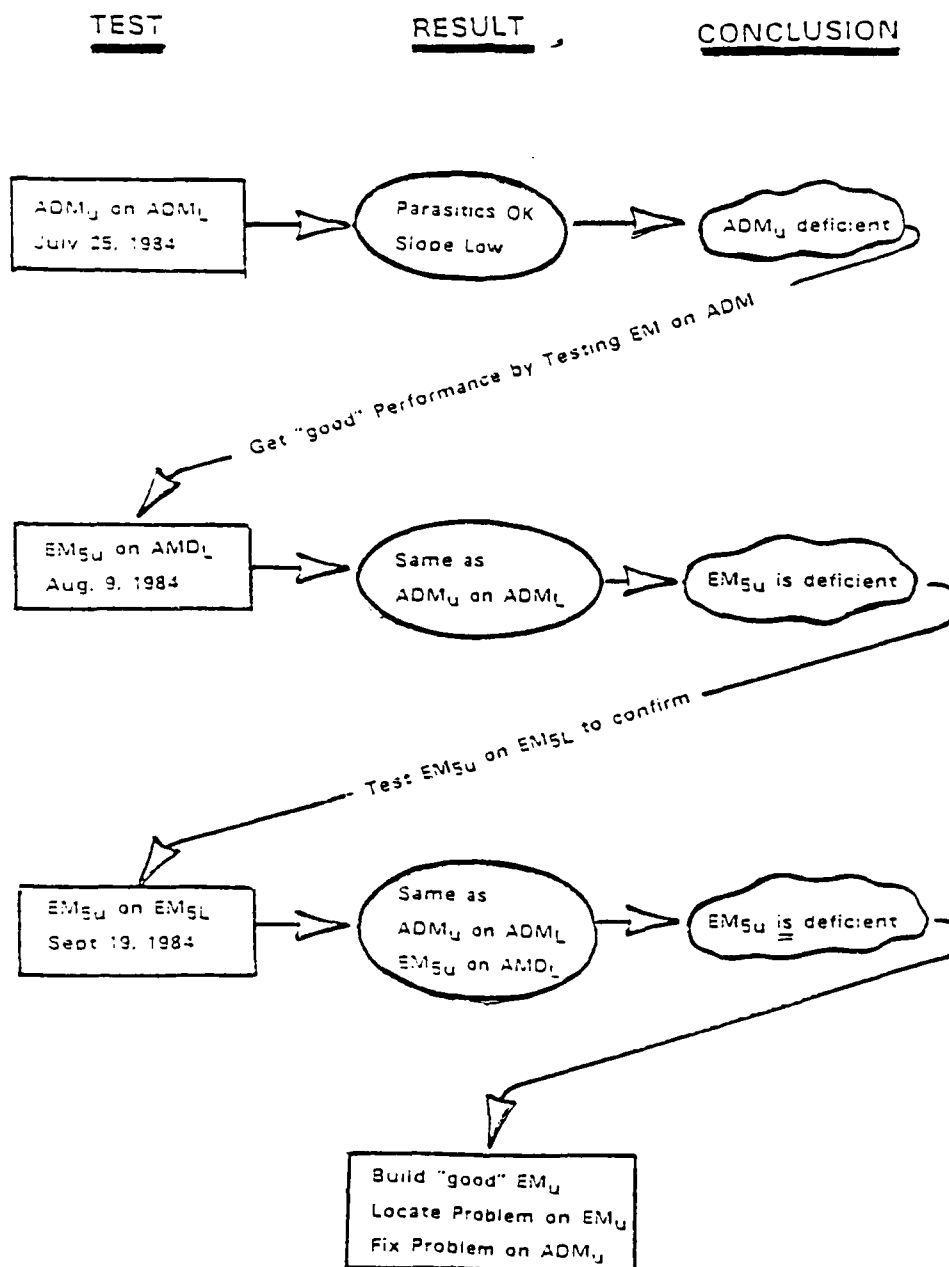


Fig. A-5 Three Key ADM Diagnostic Tests

FY85 IR&D Program Results

The conclusions drawn from the above work were:

- The stator O-ring is necessary in order to maintain a high performance level of the EM system engine. Incorporation of the O-ring improves cycle efficiency by 6 points and PV power by 10 to 15%. Absence of the O-ring results in a significant axial and circumferential regenerator temperature maldistribution. With the O-ring in, the axial temperature profile is linear and circumferential temperature profile is uniform.
- A performance engine with a generation 1 cooler is thermodynamically stronger than the system engine. A performance engine with a generation 2 cooler is thermodynamically similar to the system engine.
- A system engine with a generation 1 cooler and stator O-ring is thermodynamically similar to the performance engine.

From all of the above, we can summarize the following facts:

1. The difference between the EM performance engine and system engine is in their build configuration. EM performance engine was assembled with stator O-ring in (only in FY85; earlier tests showed good performance with builds without stator O-ring) from which we can conclude that the O-ring is necessary only if the hardware has degraded with use), and with generation 1 cooler. The EM system engine was tested without stator O-ring, and with generation 2 cooler.
2. EM performance engine (built with generation 1 cooler) is thermodynamically much stronger than the EM system engine (built with generation 2 cooler).
3. EM system engine when tested with stator O-ring in and with generation 1 cooler performs similar to EM performance engine.



4. ADM engine and EM system engine with generation 2 cooler have similar thermodynamic performance.
5. Water side manifold in the ADM cooler is similar to the generation 2 cooler.
6. All ADM testing was performed without stator O-ring

Based on the above results the possible causes for the ADM power shortfall were narrowed to:

1. Cooler configuration
2. Inadequate clearance seal between the displacer liner and motor stator in absence of the stator O-ring.
3. Large compression space dead volume causing some unknown loss.

Early FY86 Program Test Results

The EM performance engine was tested with and without increased dead volume in the compression space. No performance degradation was seen with increase in dead volume (17 cubic inches were added to the EM compression space to make the dead volume similar to that in the ADM engine).

From the above test results, we would expect that the ADM engine performance would significantly improve if the engine was tested with EM generation 1 cooler and with stator O-ring in.

From these test data, the influence of stator O-ring on performance was understandable. Without the O-ring, the effective temperature ratio across the regenerator is reduced and a large temperature variation exists in the circumferential direction which would obviously reduce the power generation capability of the engine.



The influence of generation 2 cooler on engine performance was not clear. The following gives the results of generation 1 and generation 2 tests on EM engine (engine was tested with stator O-ring), performed in FY86.

- At 5.9-bar pressure amplitude, the slope of PV power versus displacer amplitude was similar between the two builds and the code prediction.
- At 7.5-bar pressure amplitude, the generation 2 cooler build had lower slope than the generation 1 cooler build and the code predictions
- At 9.1-bar pressure amplitude, the slope difference between the generation 2 cooler build and the code predictions increased
- Compression space temperature for generation 1 and generation 2 cooler builds were similar for both 5.1- and 7.5-bar pressure amplitude tests
- Regenerator temperature profile between the generation 1 and generation 2 cooler builds were similar for both 5.9- and 7.5-bar pressure amplitude tests
- Temperature profile on the external surface of the generation 2 cooler build was measured by a hand-held thermocouple. No significant temperature variations were found on housing the surface
- Analysis did not indicate any significant performance penalty for generation 2 cooler (1.5% slope difference)
- Load-line test results did not indicate any significant performance difference between the generation 1 and generation 2 cooler builds.

The only logical conclusion that can be drawn from the above is that the performance degradation in the generation 2 cooler build is not because of inadequate heat transfer capability of generation 2 cooler. However, the performance degradation with the generation 2 cooler was repeatable. We have not been able to understand the reason for this degradation in performance



that exists in some tests and not in others (may be due to build to build differences).

The conclusion reached after the early FY86 IR&D testing was that most probably the ADM engine will perform well if the engine is assembled with the stator O-ring in. This assumed that the external heat transfer in the generation 2 EM cooler was not the reason for the poor performance of the EM system engine. The next planned test in FY86 IR&D program was to test the ADM engine with generation 3 EM cooler and with stator O-ring in.

Summary

A tubed-head ADM engine was tested in both the load-line and the slope/intercept format. These tests showed large temperature differential between the back and the front row of the heater tubes (back row tubes had about 150 to 200°C lower temperature than the front row tubes). In addition, the heater tubes had large axial temperature variation. This was because of the nonuniform gap between the tubes in the axial direction. Since the regenerator is connected to the back row tubes, the regenerator top temperature was about 250 to 300°C lower than the front row tube temperatures. Under these temperature conditions, the maximum PV power of 2.6 kW was achieved at approximately 18-mm of the displacer and the piston strokes. Any substantial improvement in the engine PV power would require a better heater head temperature distribution, which would involve a major modification to the heater head tubes. The available funds and time were not sufficient to perform the necessary hardware corrections.

The only other major difference between the tubed head and monolithic head builds was in the regenerator screens. Wire thickness of tubed head regenerator was 3.5 mil, whereas the monolithic head regenerator matrix was made of 2.5-mil thick wire.

The only purpose of this appendix is to document the results obtained for future reference.

Load-Line Test

Figures B-1* through B-8 show engine operating parameters plotted against piston amplitude. Figures B-9 and B-10 compare the measured- and code-predicted (CFAST) PV and thermodynamic power, respectively. Comparisons for pressure amplitude, pressure wave phase angle, regenerator top and bottom temperatures are shown in Figures B-11 through B-14.

*Figures for this appendix begin on page B-5.



Slope/Intercept Test

This test was performed at 600°C average front row tube temperature, 80° displacer phase angle, and 7.6-bar compression space pressure amplitude (60-bar mean pressure). Displacer stroke was varied from 4 to 12 mm. Test results and code predictions are plotted on Figures B-15 through B-22.

Both the load-line and slope/intercept tests were performed on 23 August 1986 using test data file DADM1.



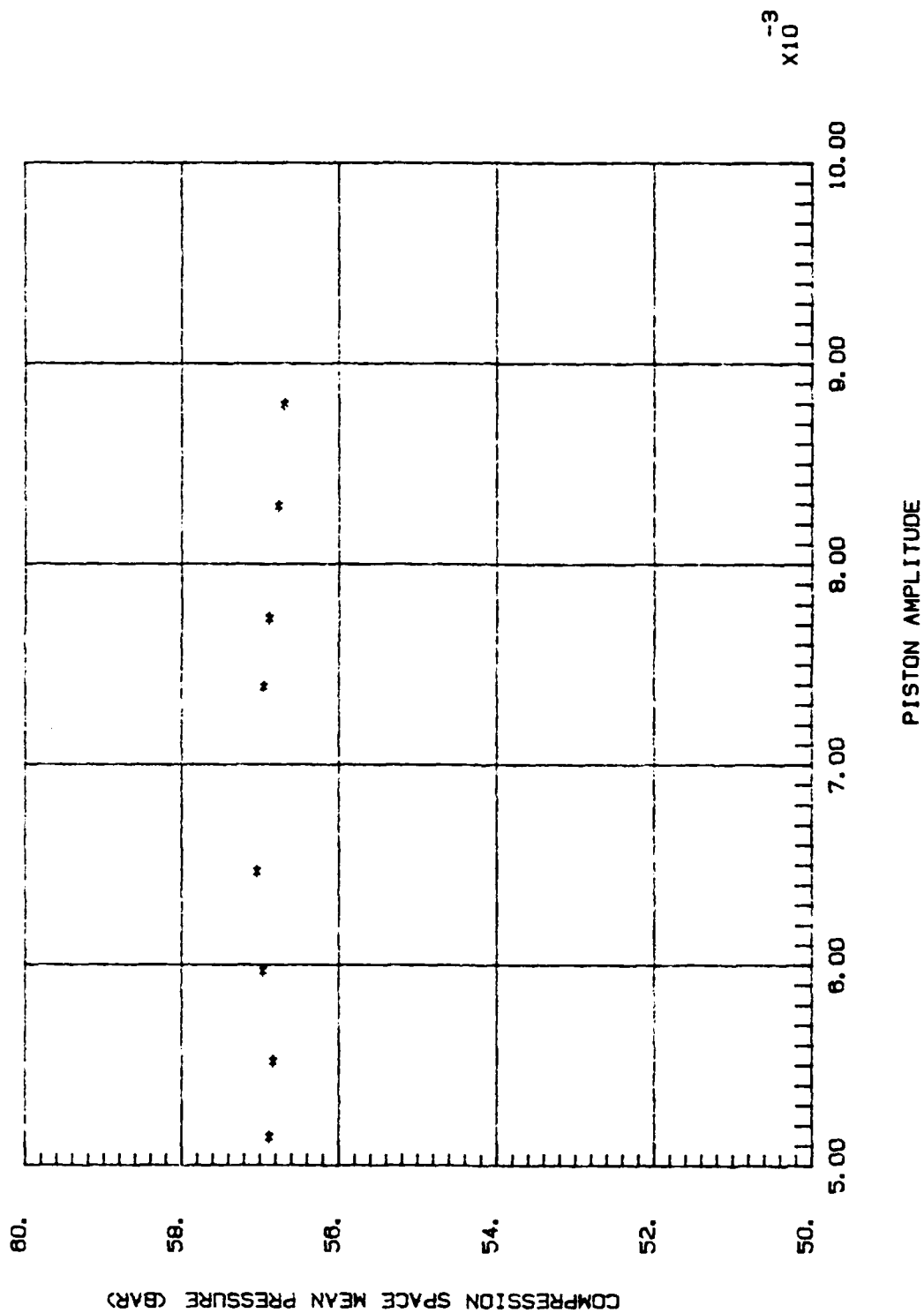


Fig. B-1 Tubed Head; Compression Space Mean Pressure; Load-Line Test

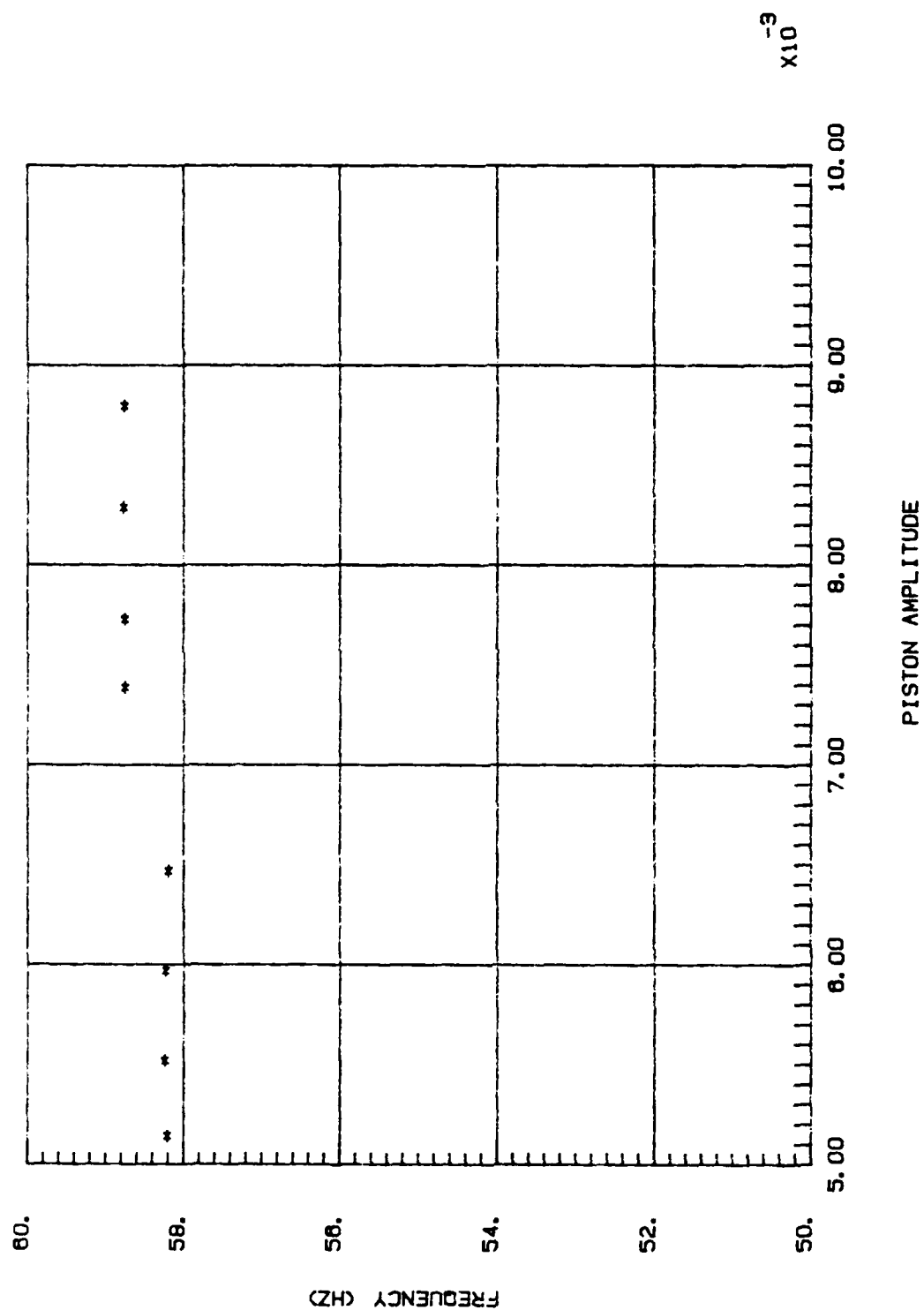


Fig. B-2 Tubed head; Operating Frequency; Load-Line Test

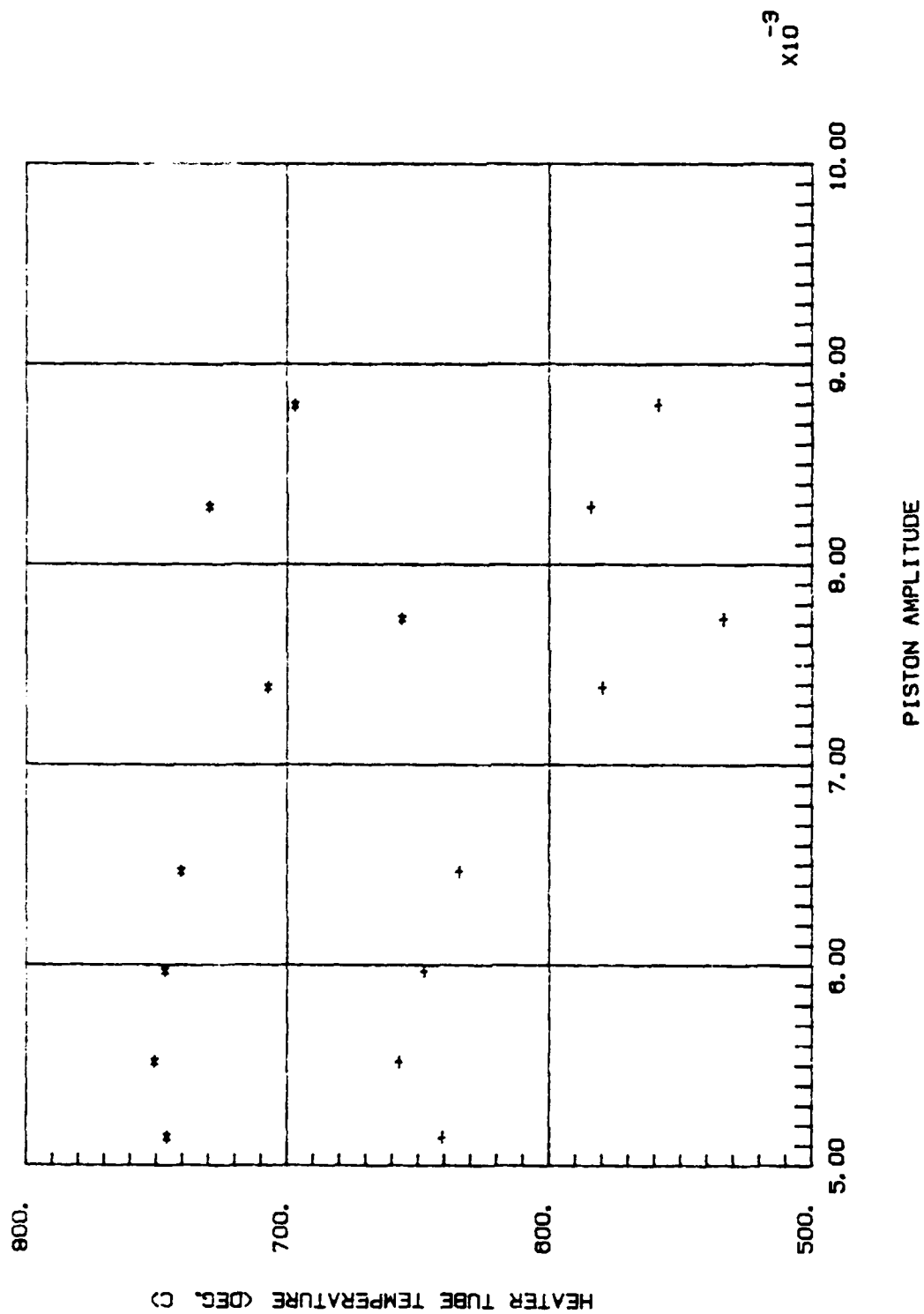


Fig. B-3 Tubed Head; Front and Back Row Average Temperatures; Load-Line Test

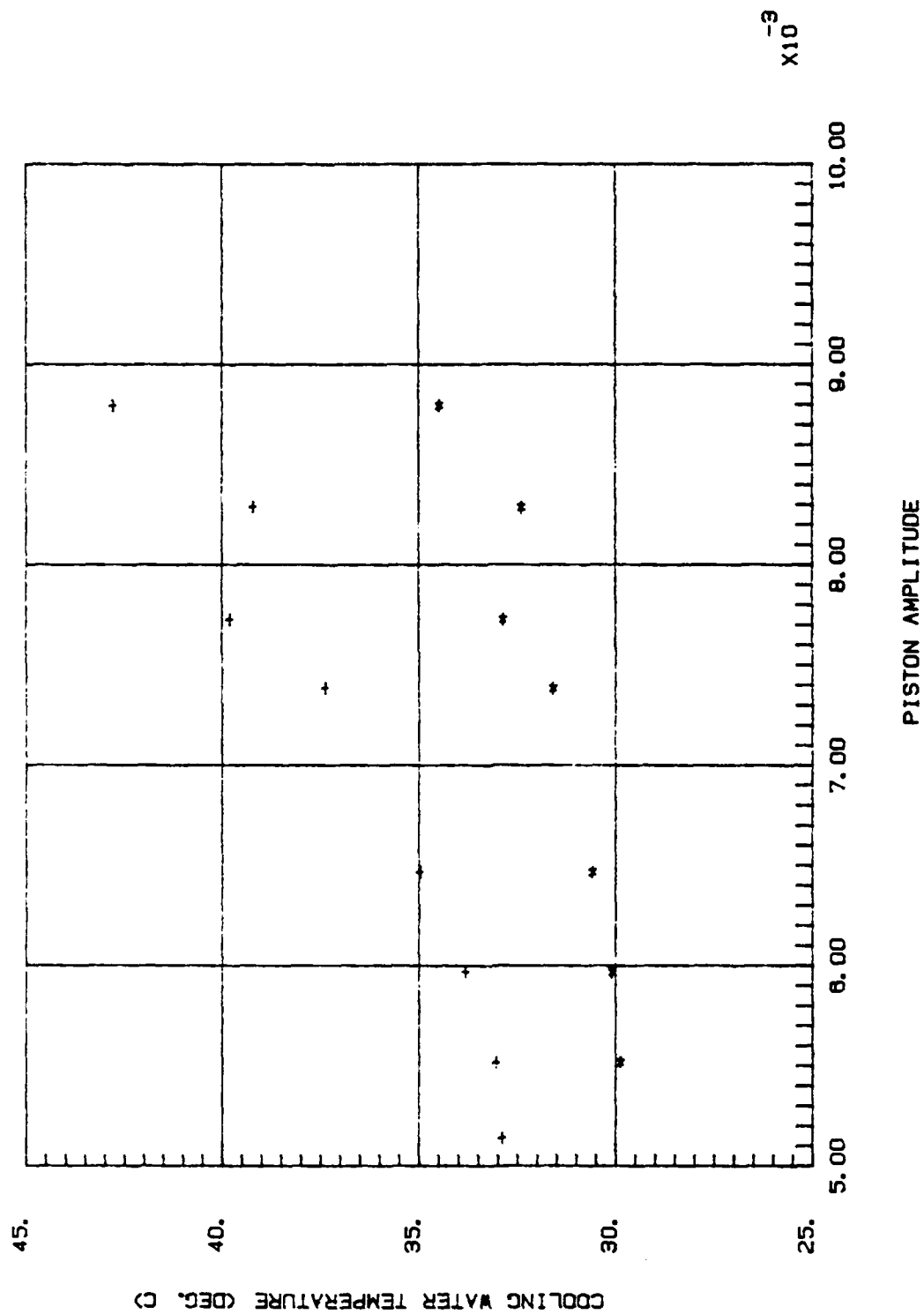


Fig. B-4 Tubed Head; Cooling Water Inlet Temperature; Load Line Test

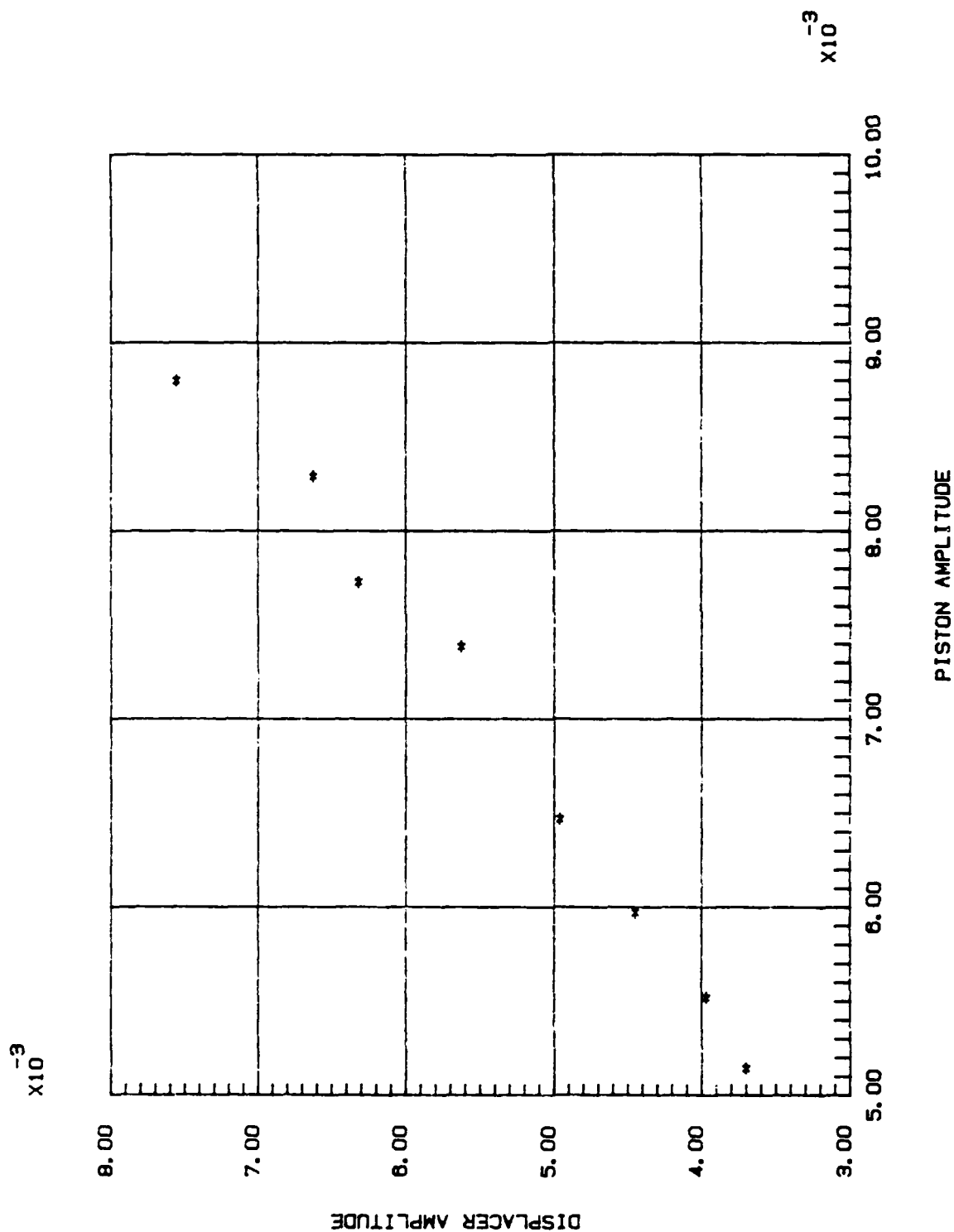


Fig. B-5 Tubed Head; Displacer Amplitude; Load-Line Test

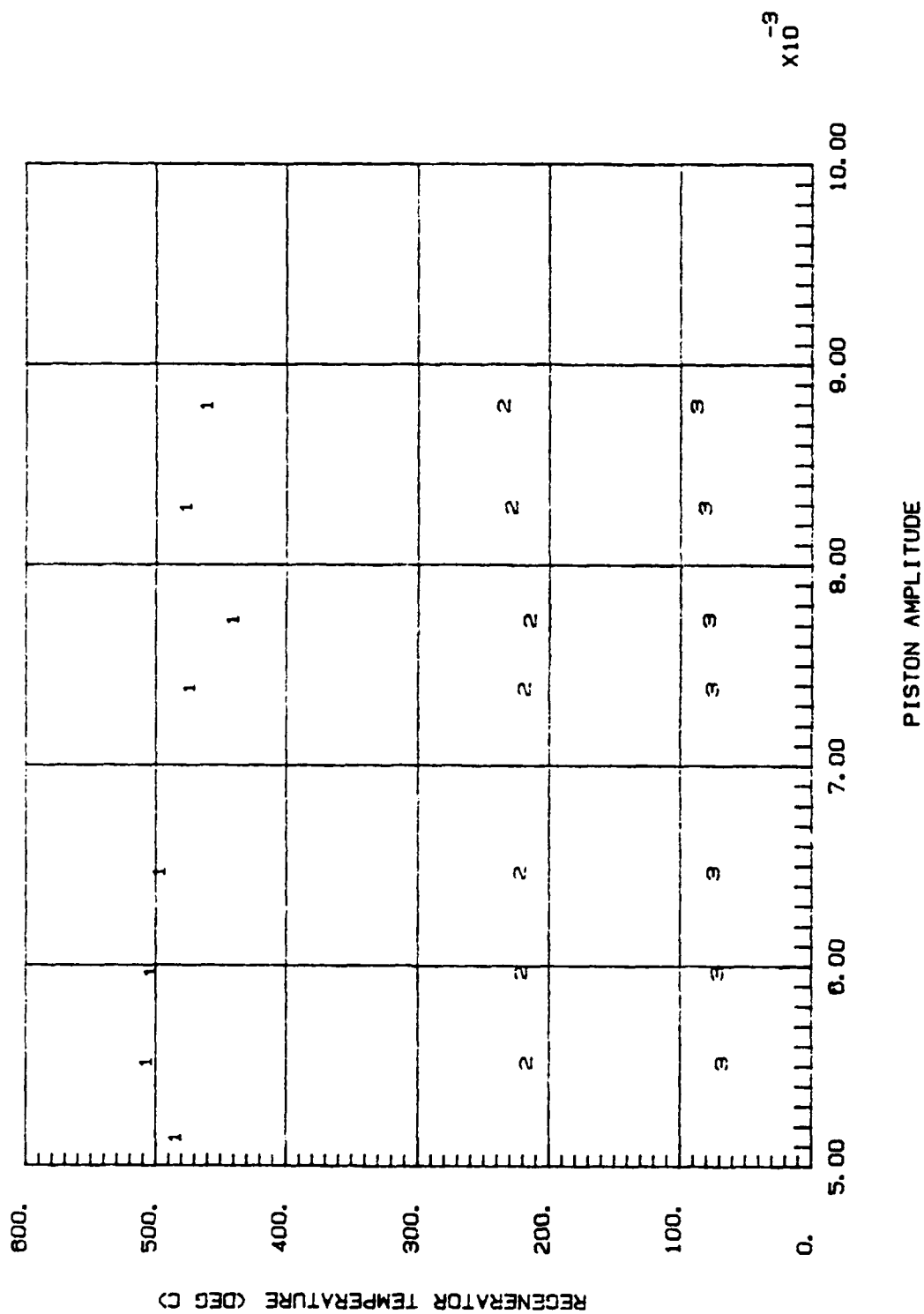


Fig. B-6 Tubed Head; Regenerator Temperatures; Load-Line Test

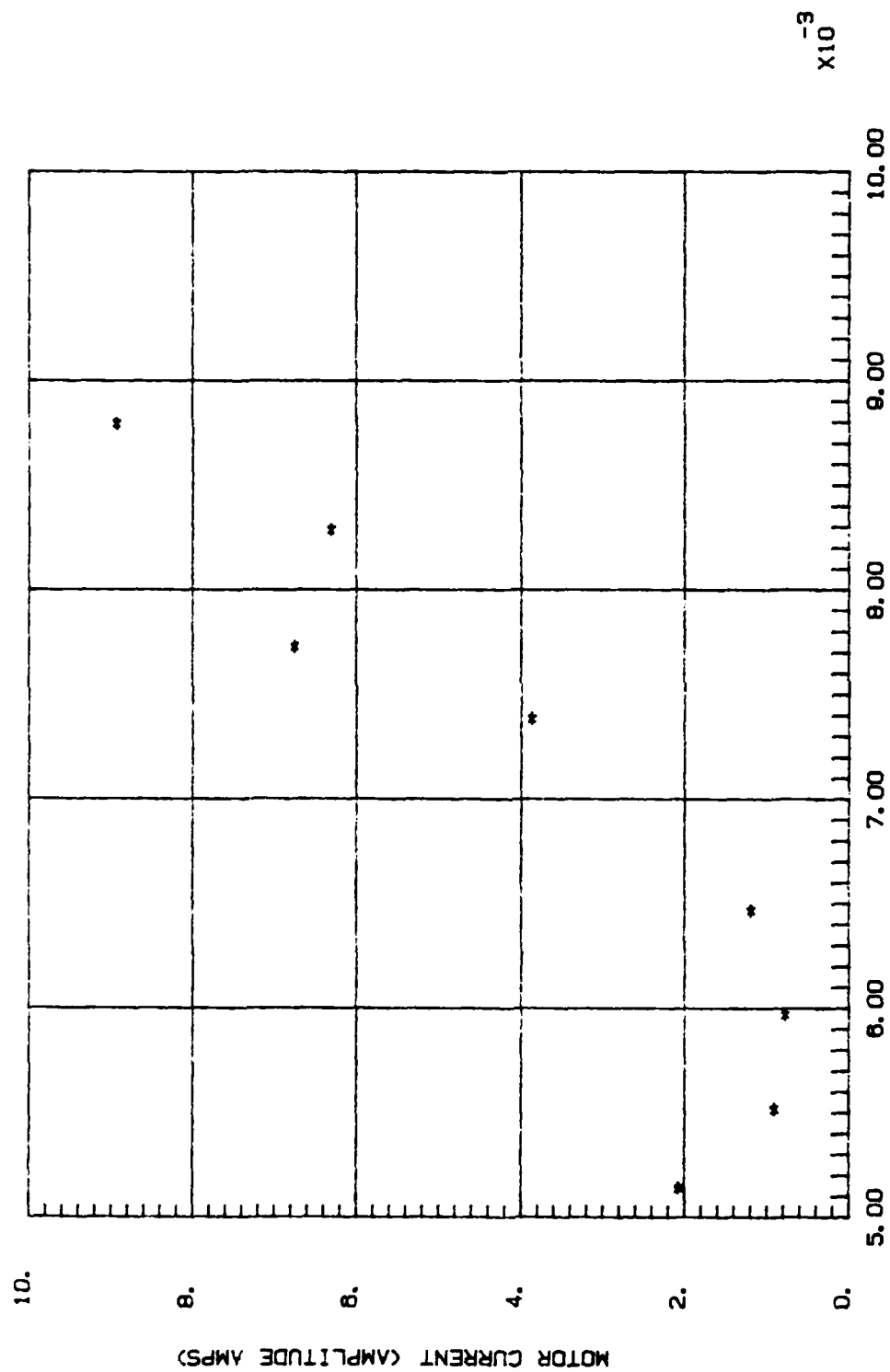


Fig. B-7 Tubed Head; Motor Current; Load-Line Test

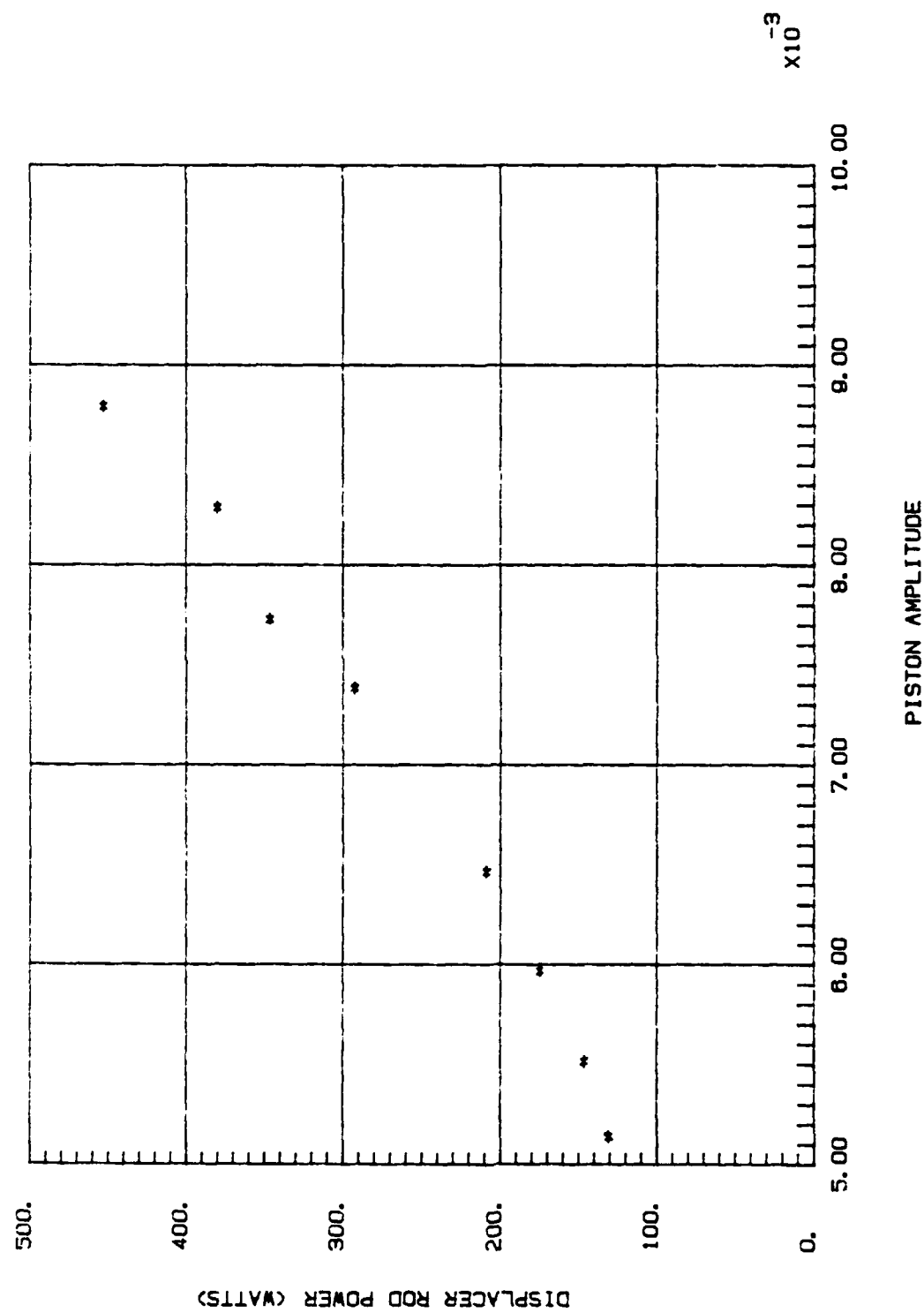
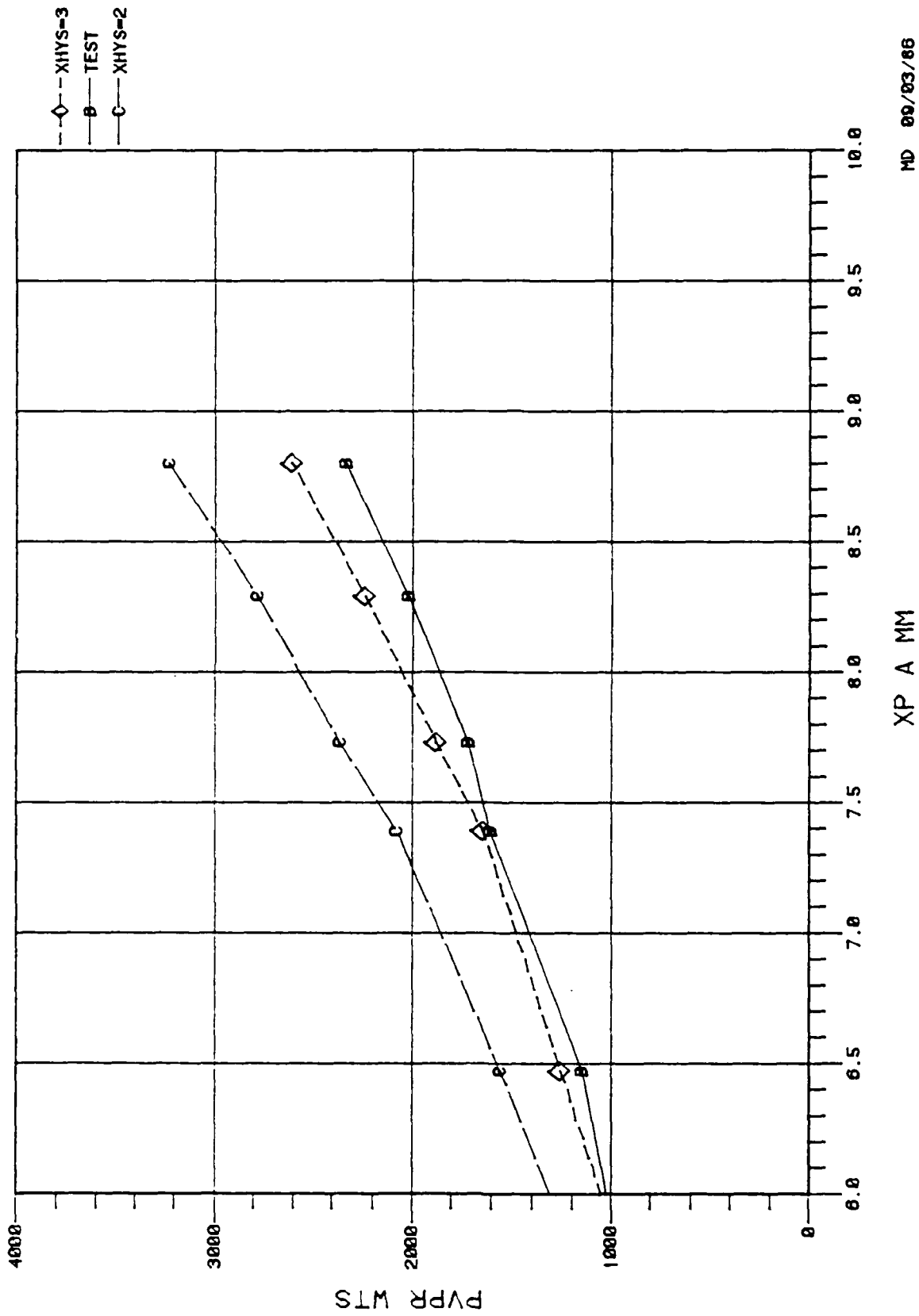


Fig. B-8 Tubed Head; Power to Displacer from the Compression Space; Load-Line Test

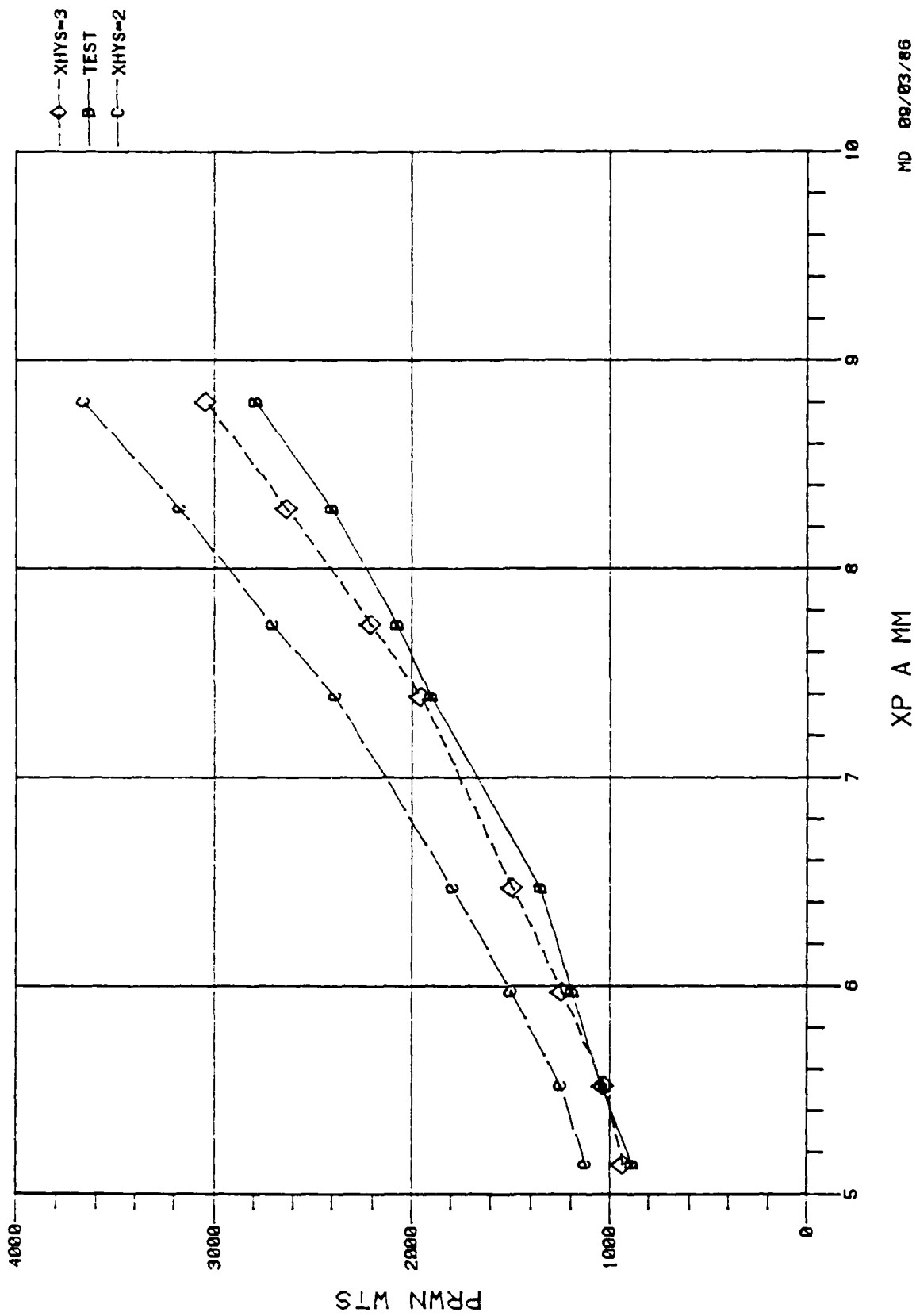


MD 00/03/86

XP A MM

Fig. B-9 Tubed Head; Piston PV Power; Load-Line Test





MD 08/03/86

Fig. B-10 Tubed Head; Net Thermodynamic Power; Load-Line Test

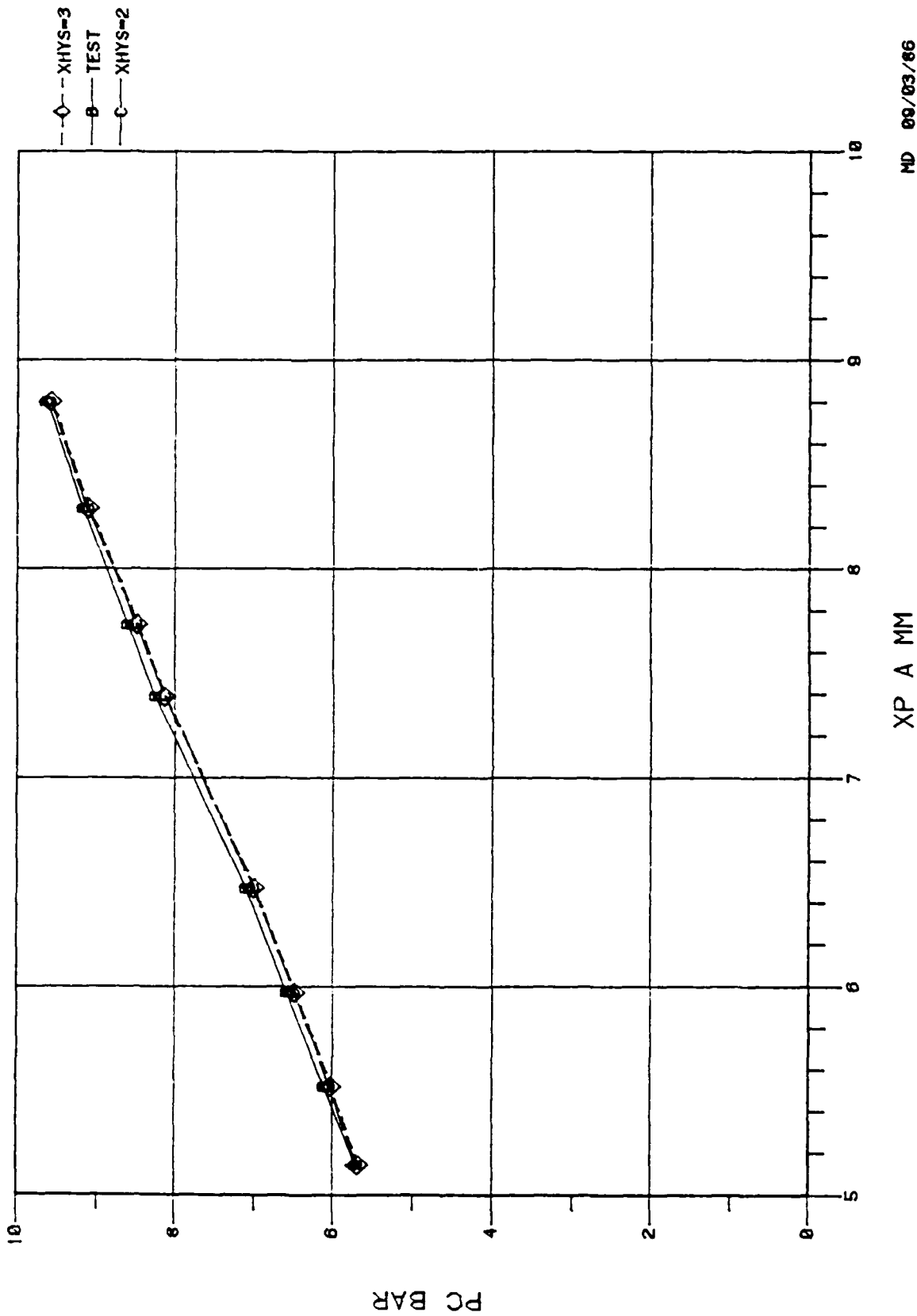
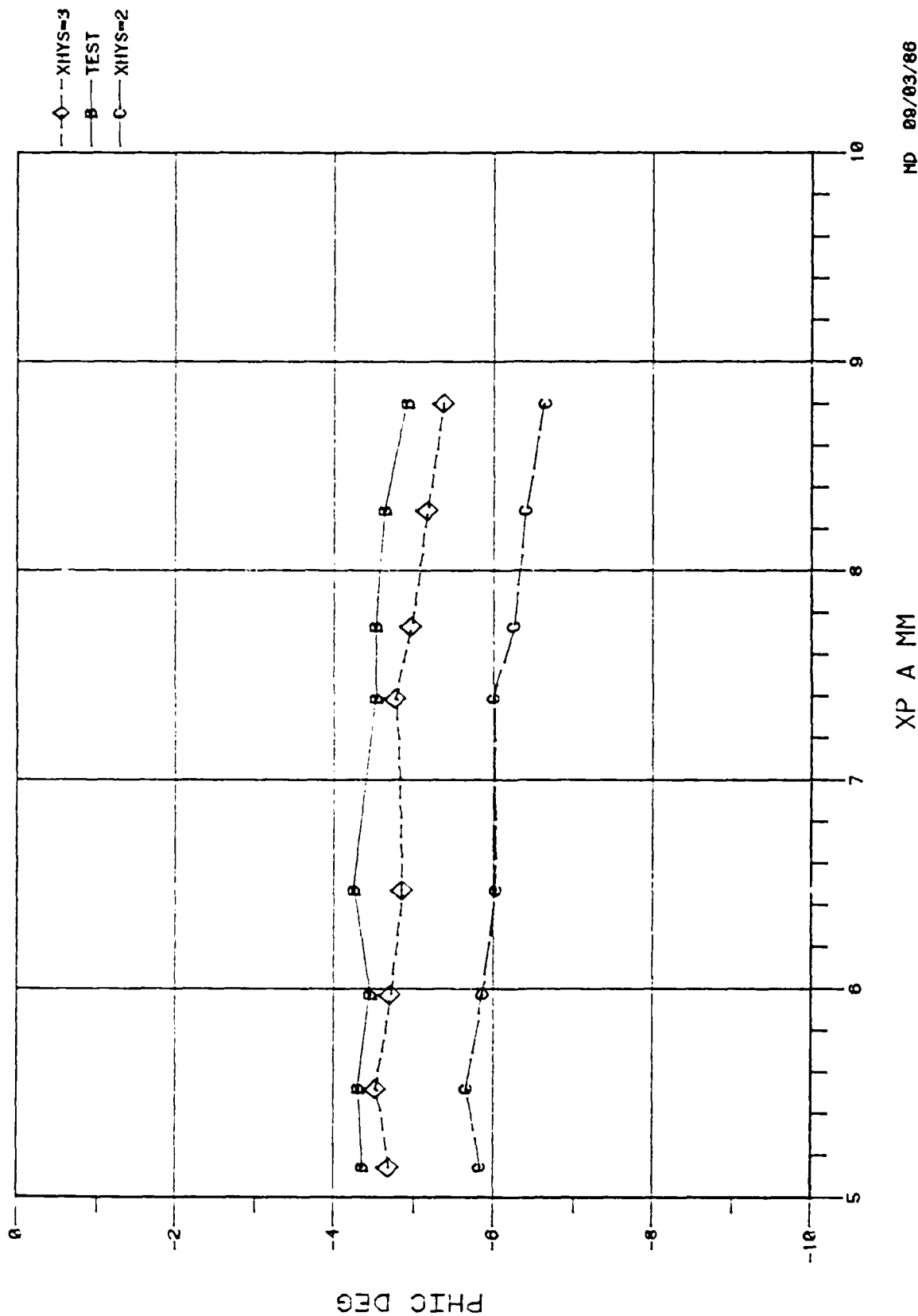


Fig. B-11 Tubed Head; Compression Space Pressure Amplitude; Load-Line Test

MD 00/03/86

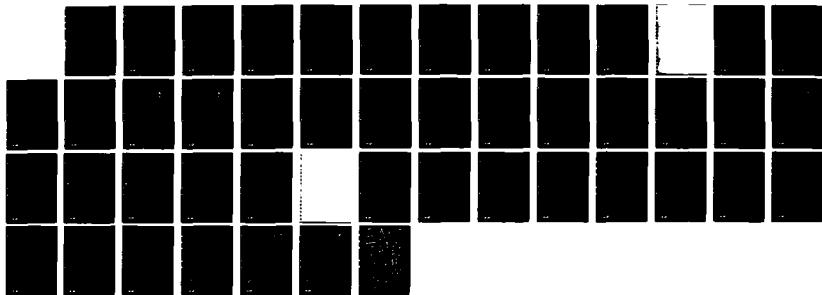


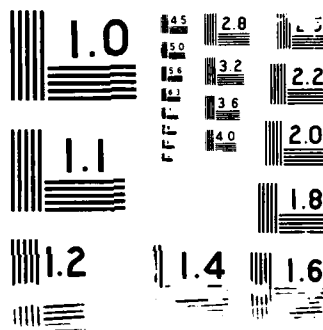
MD 09/03/86

Fig. B-12 Tubed Head; Compression Space Pressure Wave Phase Angle
with Respect to the Piston; Load-Line Test

AD-A194 789

FISCAL YEAR 1986 PROGRAM 26802 - TASK 20 ADM TEST
RESULTS(U) MECHANICAL TECHNOLOGY INC LATHAM NY STIRLING
ENGINE SYSTEMS DIV M DHAR FEB 87 MTI-87SESD37
DAAK70-82-C-0255 F/G 21/7





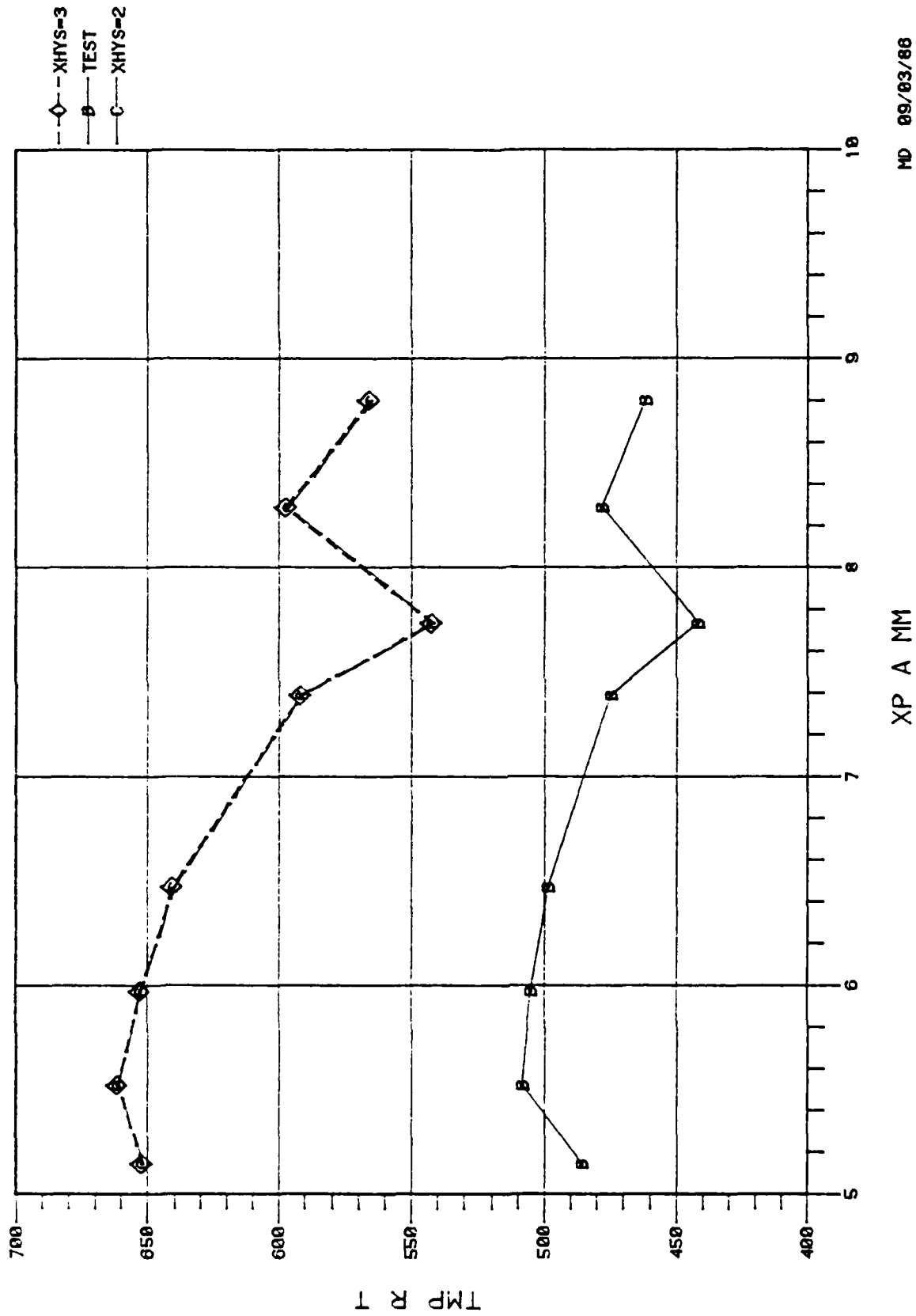


Fig. B-13 Tubed Head; Regenerator Top Temperature Compared to the Code Predictions; Load-Line Test

MD 09/03/88

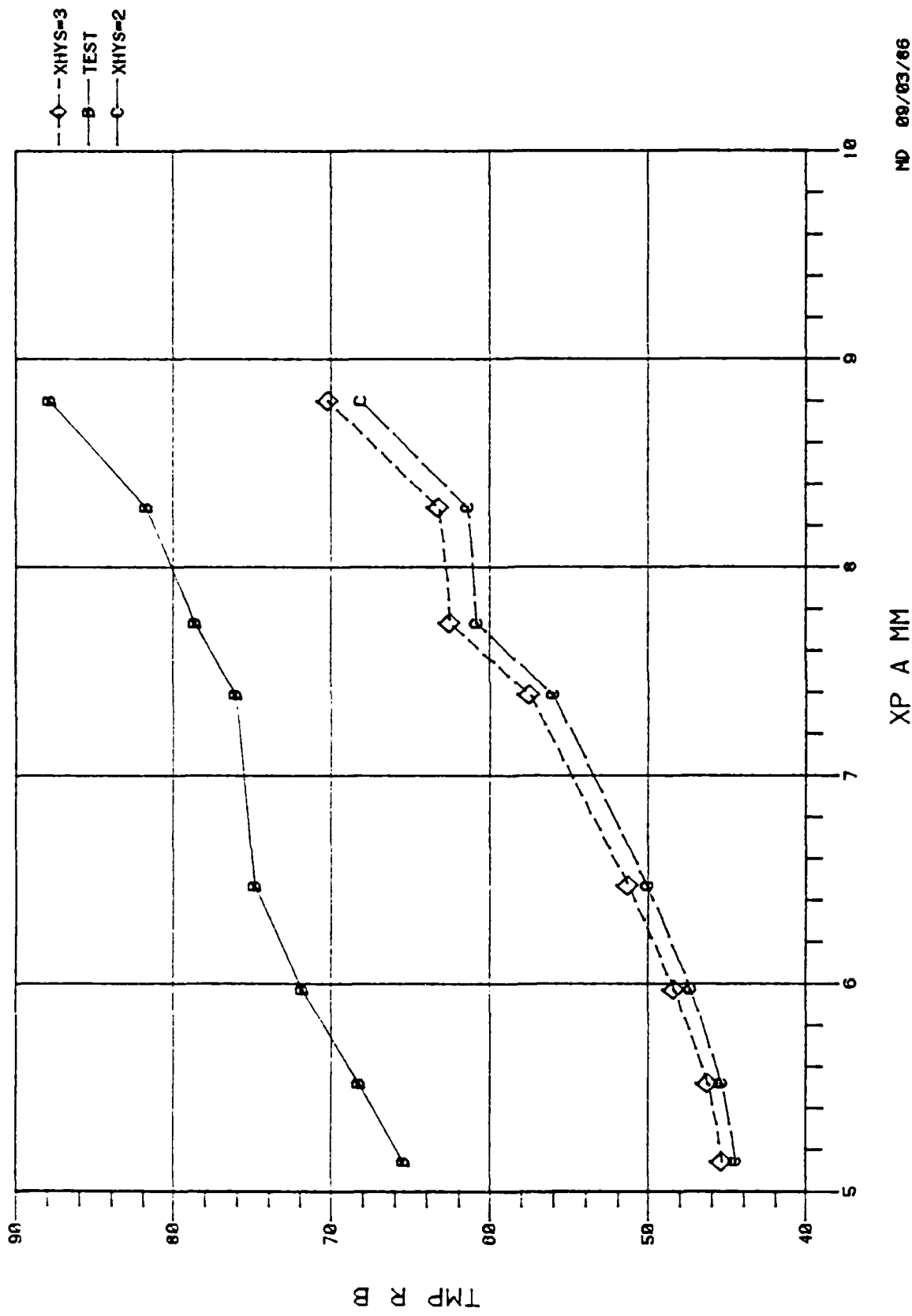


Fig. B-14 Tubed Head; Regenerator Bottom Temperature Compared to the Code Predictions, Load-Line Test

MD 00/03/86

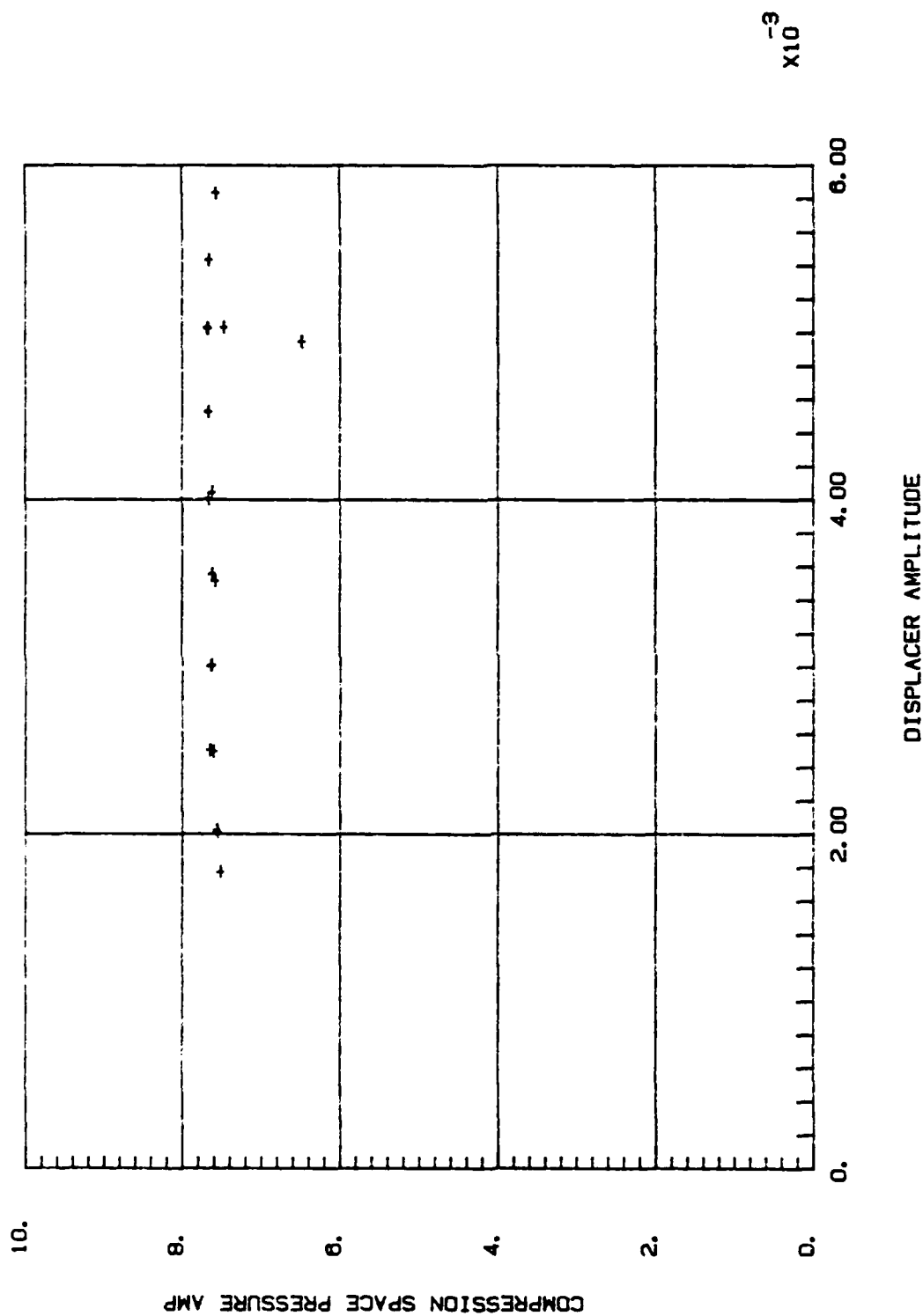


Fig. B-15 Tubed Head; Compression Space Pressure Amplitude; Slope/Intercept Test

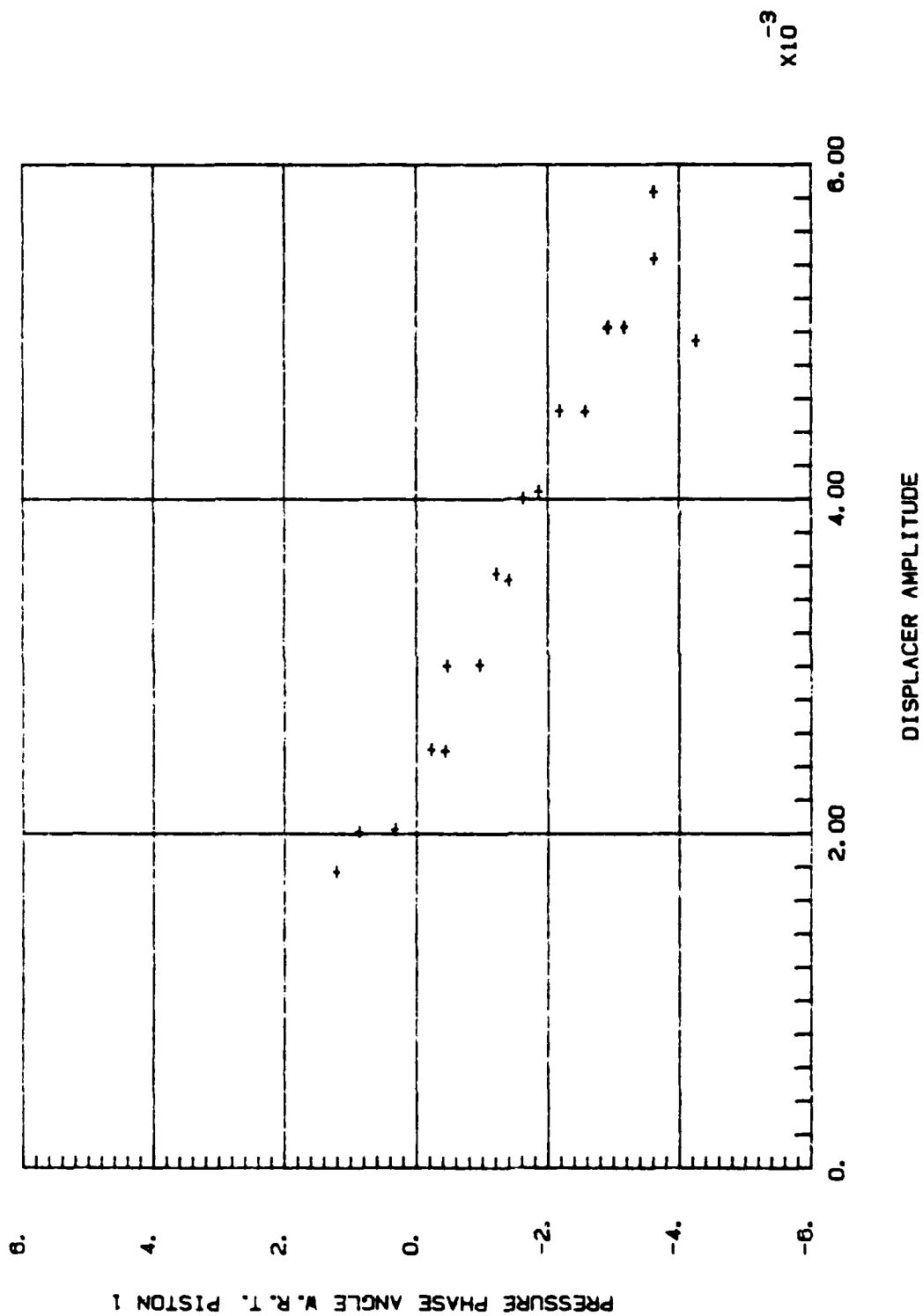


Fig. B-16 Tubed Head; Compression Space Pressure Wave Phase Angle with Respect to Power Piston; Slope/Intercept Test

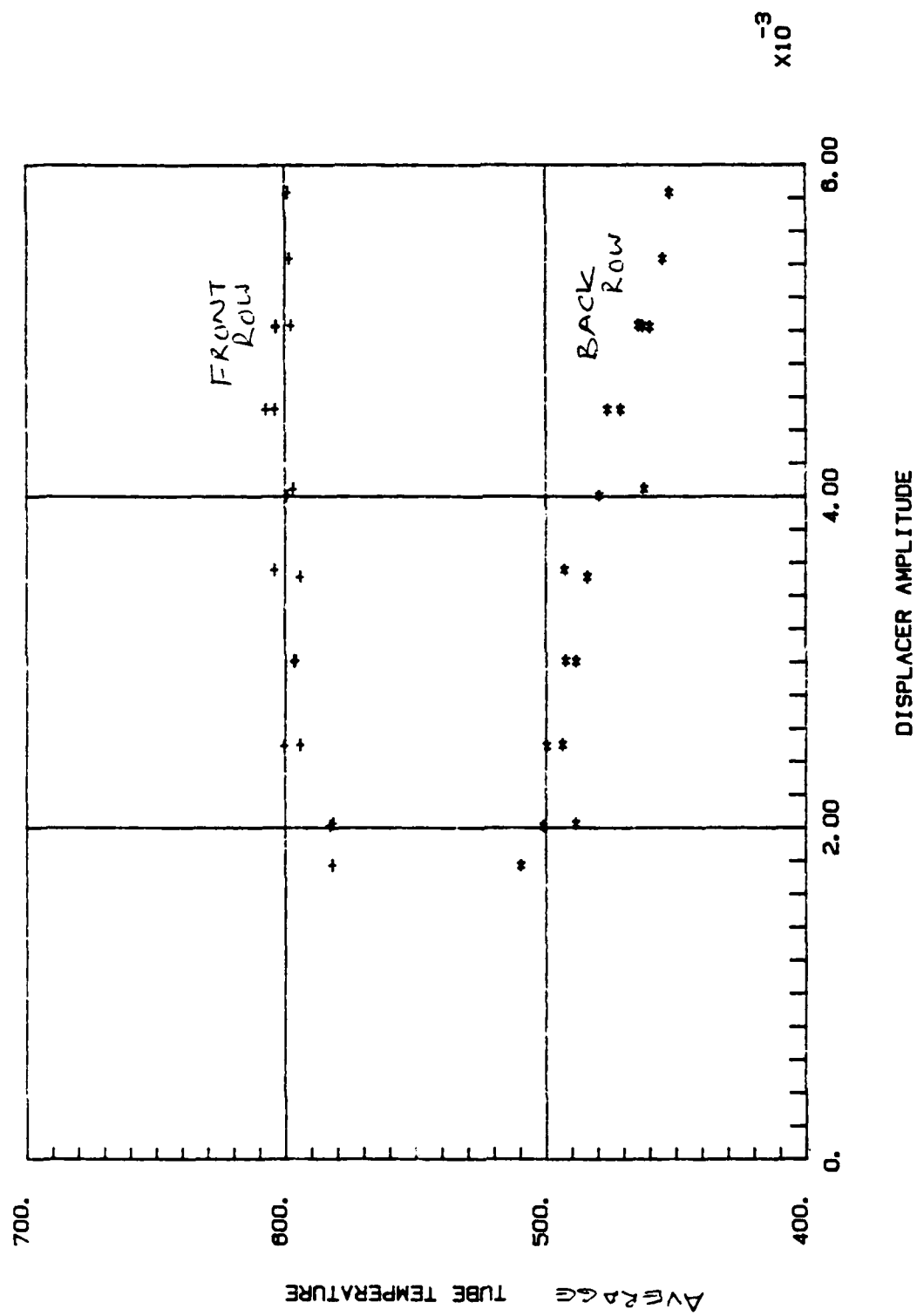


Fig. B-18 Tubed Head; Front and Back Row Tube Temperatures;
Slope/Intercept Test

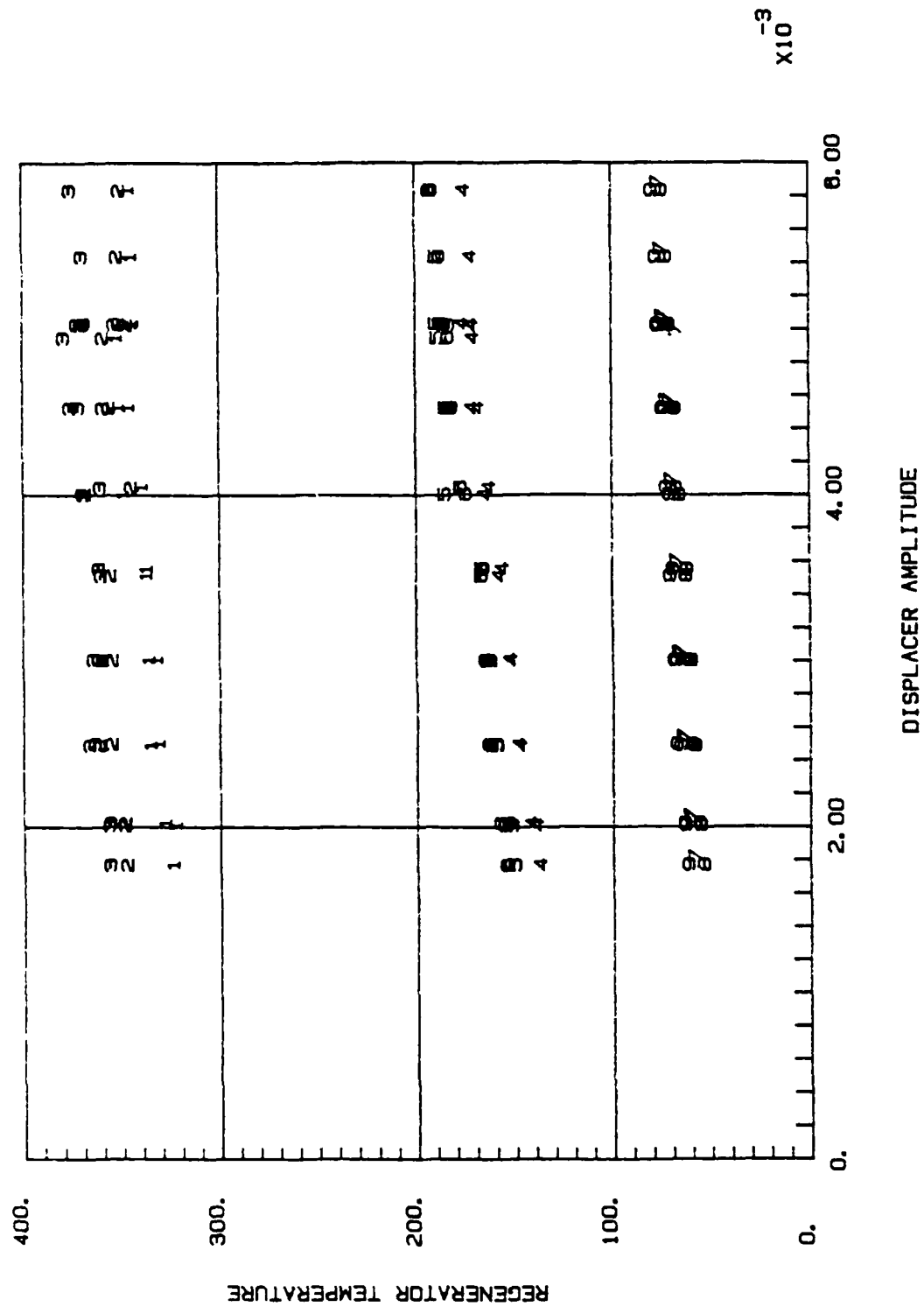


Fig. B-19 Tubed Head; Regenerator Temperatures;
Slope/Intercept Tests

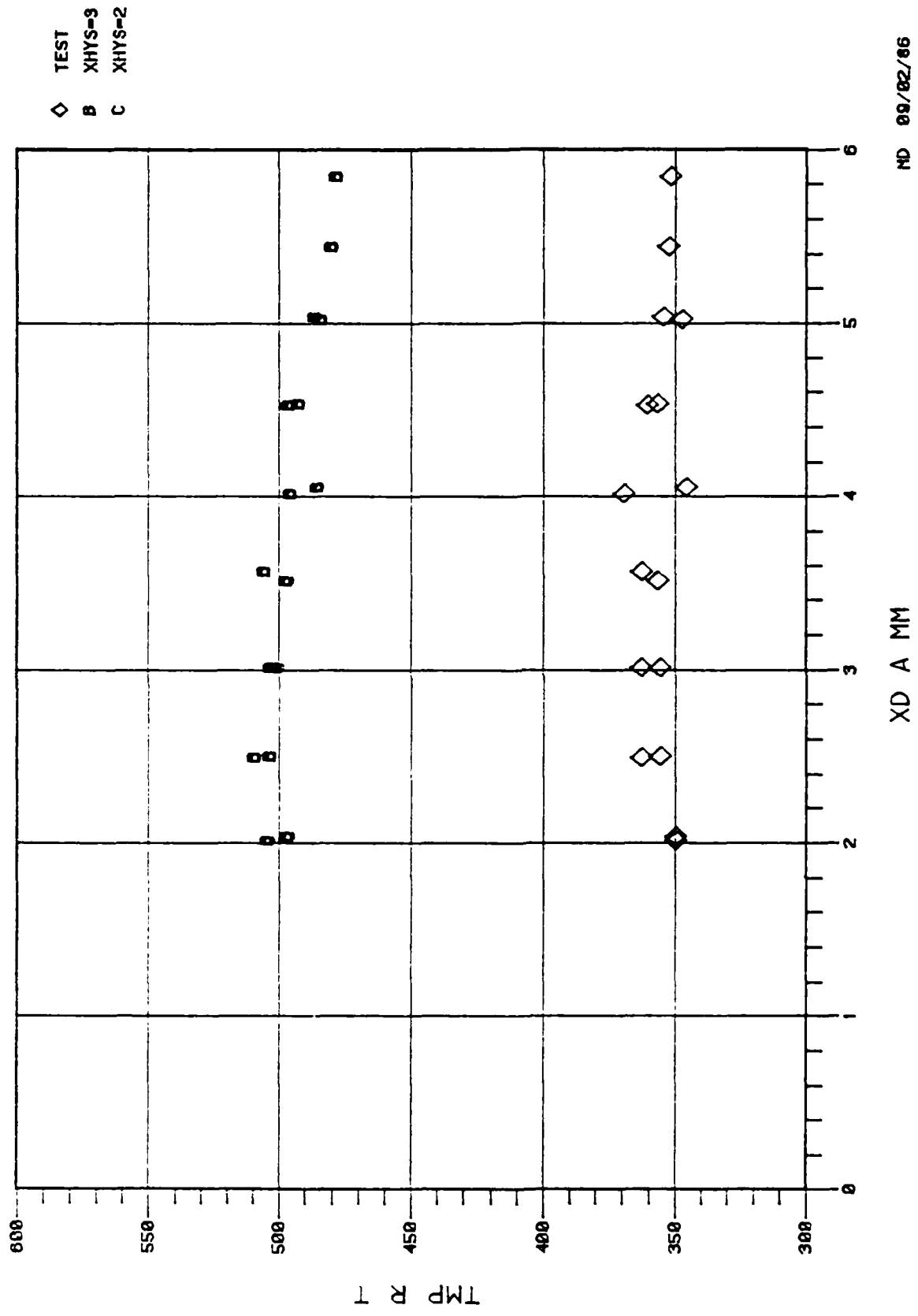


Fig. B-20 Tubed Head; Comparison of Measured and Predicted Regenerator Top Temperature; Slope/Intercept Test

ND 09/02/86

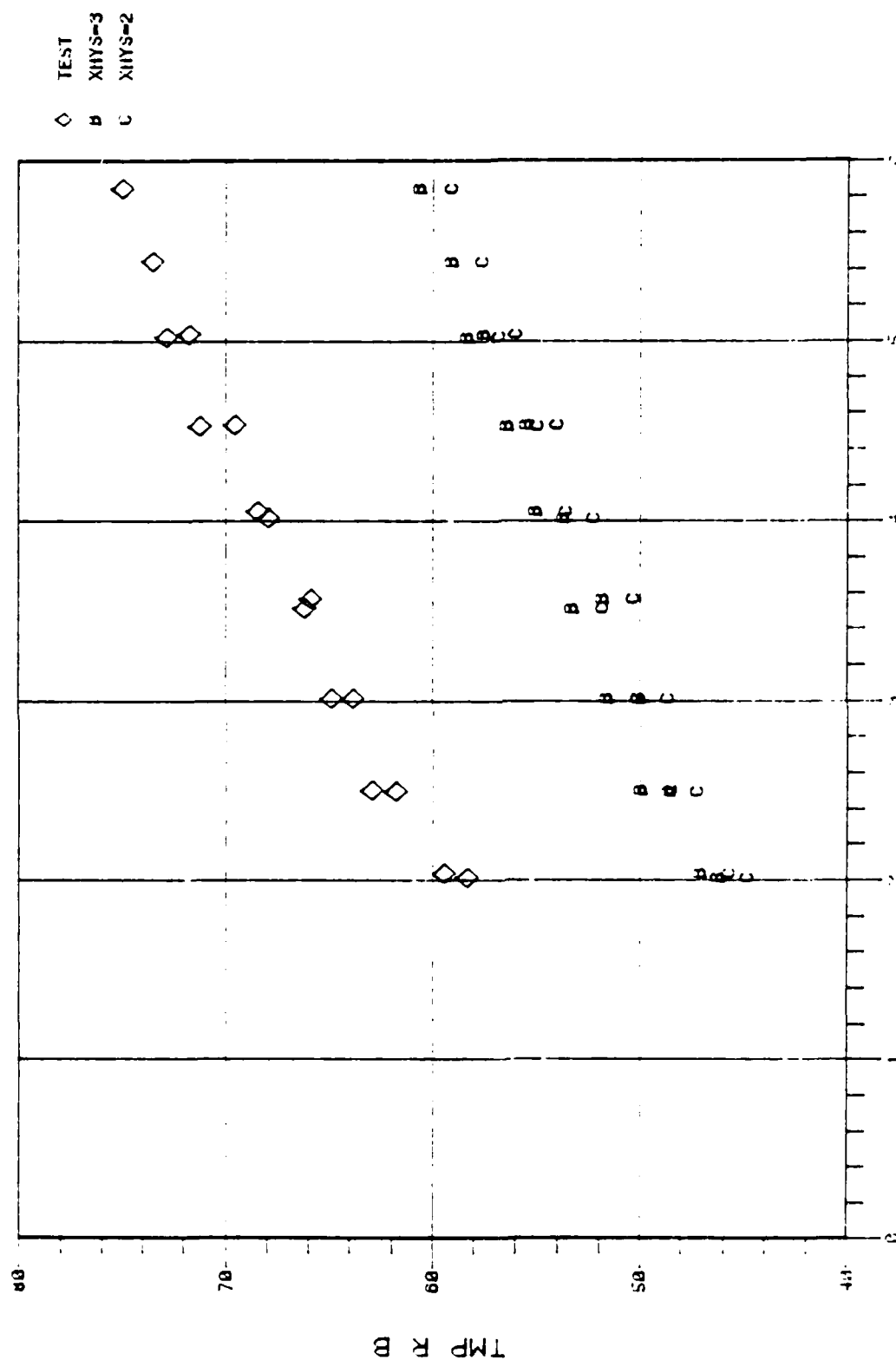


Fig. B-21 Tubed Head; Comparison of Measured and Predicted Regenerator Bottom Temperatures; Slope/Intercept Test

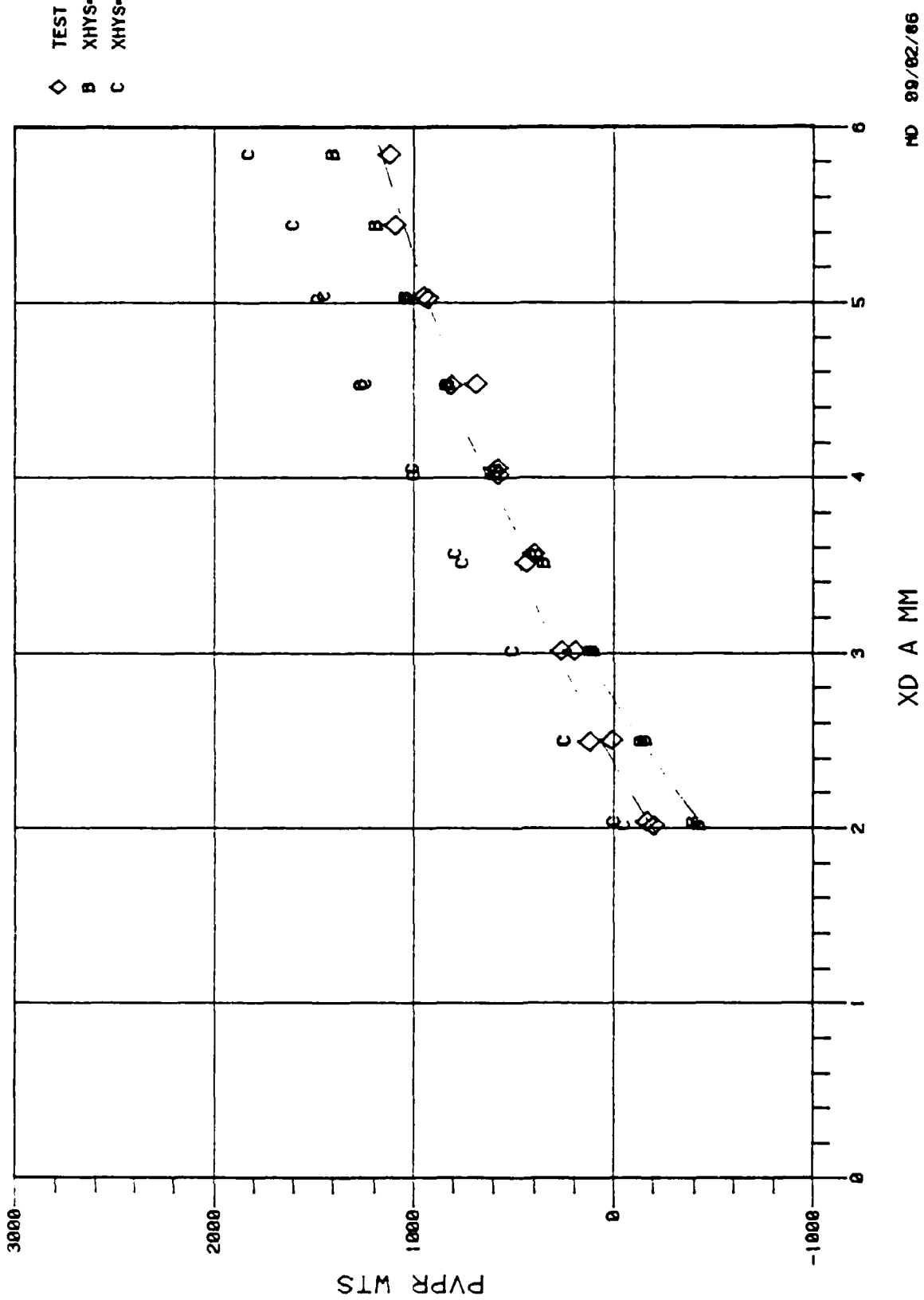


Fig. B-22 Tubed Head PV Power; Slope/Intercept Test

ADM Clearance Summary*

Gas Spring: Seal Between Gas Spring and Compression Space

	<u>Piston</u>	<u>Cylinder</u>	<u>Radial Clearance</u>
Print Diameter	2.9541	2.9555	0.0006 (min)
	2.9539	2.9553	0.0008 (max)
Measured Diameter	2.95364	2.9538	0.0001 (avg)

Power Piston: Seal Between Gas Spring and Compression Space

	<u>Piston</u>	<u>Cylinder</u>	<u>Radial Clearance</u>
Print Diameter	4.200 (nom)	4.201	0.00045 (min)
	Match	Match	0.00055 (max)
	Machined	Machined	
Measured Diameter	4.20067	4.2023	0.0008 (avg)

Displacer Motor

	<u>Displacer</u>	<u>Sleeve in Motor</u>	<u>Radial Clearance</u>
Print Diameter	3.680	3.6840	0.0017 (min)
	3.679	3.6835	0.0025 (max)
Measured Diameter	3.67924	3.6878	0.0043 (avg)

Post and Flange

	<u>Rod</u>	<u>Post</u>	<u>Radial Clearance</u>
Print Diameter	1.6001	1.6011	0.0004 (min)
	1.5999	1.6009	0.0006 (max)
Measured Diameter	1.59942	1.60089	0.0007 (avg)

Displacer: Seal Between P_{mean} and Compression Space

	<u>Displacer</u>	<u>Post</u>	<u>Radial Clearance</u>
Print Diameter	3.0715	3.0701	0.0006 (min)
	3.0713	3.0699	0.0008 (max)
Measured Diameter	3.07290	3.06964	0.0016 (avg)

*All dimensions in inches



Power Piston/Cylinder Tolerance Study*

Serial Number	Piston	Cylinder	Port Band	
1	4.20068 High: 4.20090 Low: 0.0001 Avg.: 0.0006	(No. 1 L) High: 4.2012 Low: 4.2009 Avg.: 0.0004	4.2040 4.2010 4.2043	4.2031
2	4.20060 High: 4.20110 Low: 0.0001 Avg.: 0.0004	(No. 2 R) High: 4.2018 Low: 4.2016 Avg.: 0.0001	4.2017 4.2019 4.2022	4.2019
3	4.20086 High: 4.20100 Low: 0.0001 Avg.: 0.0005	Defective - Not Inspected		
4	4.19997 High: 4.20040 Low: 0.0001 Avg.: 0.0001	(No. 4 L) High: 4.2017 Low: 4.2016 Avg.: 0.0002	4.2020 4.2018 4.2040	4.2026

*All dimensions in inches

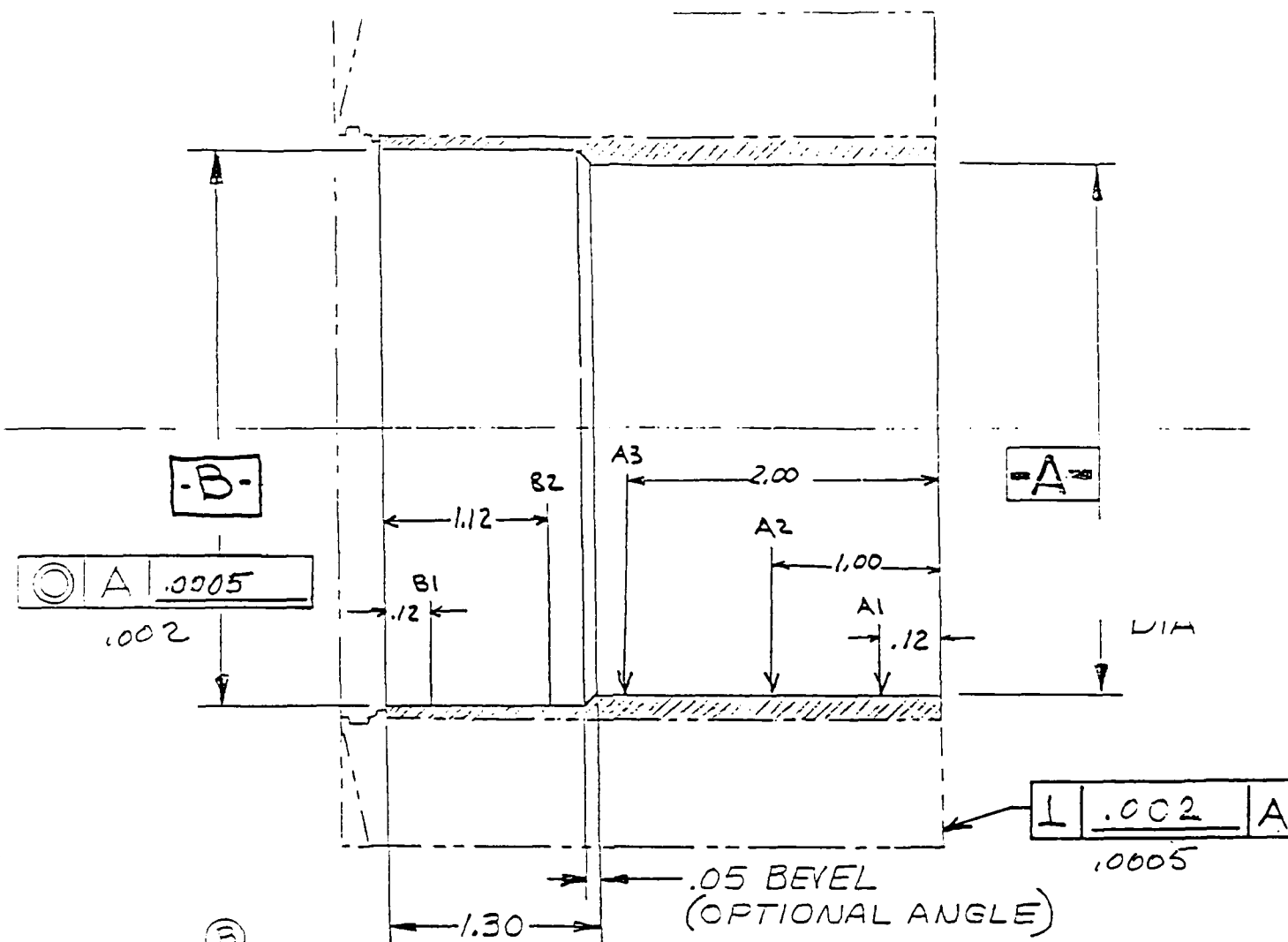


Possible Combinations*

Cylinder	Piston				
	No. 1	No. 2	No. 3	No. 4	
1L	Bore:	4.2012	4.2012	4.2012	4.2012
	Shaft:	4.20068	4.20060	4.2086	4.19997
	Rad. Clearance:	0.08026	0.0003	0.00017	0.00062
2R	Bore:	4.2018	4.2018	4.2018	4.2018
	Shaft:	4.20068	4.20060	4.2086	4.19997
	Rad. Clearance:	0.00056	0.00060	0.00047	0.00092
	Band Radial:	0.0006			
4L	Bore:	4.2017	4.2017	4.2017	4.2017
	Shaft:	4.20068	4.20060	4.2086	4.19997
	Rad. Clearance:	0.00051	0.00055	0.00042	0.00087
	Band Radial:		0.001		

*All dimensions in inches





③

DETAIL OF INNER SLEEVE (ITEM 6) FINAL MACHINING
(EXAGGERATED SCALE)

STA NO.	DIA-A* (MEASURED 3 PLCS, 120° APART)		
A1	<u>3.6876</u>	<u>3.6862</u>	<u>3.6860</u>
A2	<u>3.6893</u>	<u>3.6881</u>	<u>3.6890</u>
A3	<u>3.6880</u>	<u>3.6878</u>	<u>3.6882</u>

STA NO.	DIA-B* (MEASURED 3 PLCS, 120° APART)		
B1	<u>3.6906</u>	<u>3.6913</u>	<u>3.6905</u>
B2	<u>3.6915</u>	<u>3.6916</u>	<u>3.6914</u>

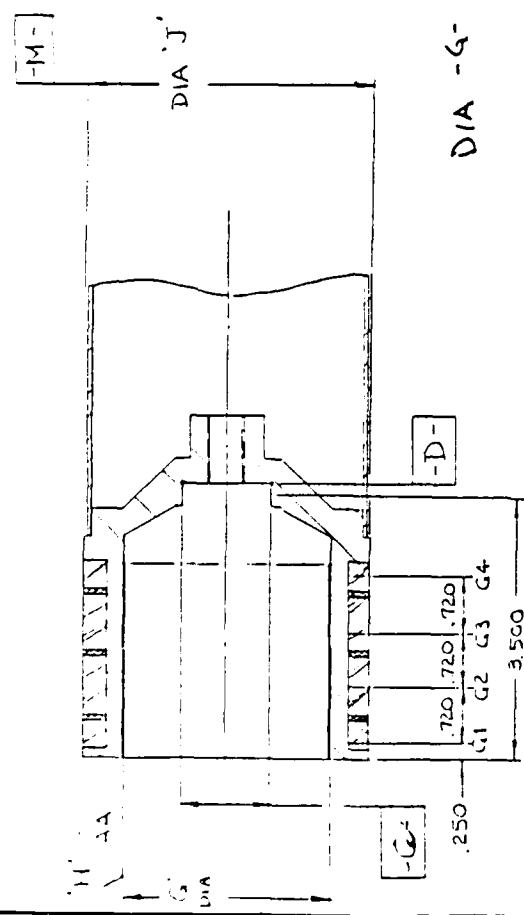
DIA-A-
3.6840
3.6835
DIA-B-
3.704
3.702
* MEASURED TO 4 PLACE
ACCURACY

MOTOR STATOR P/N 1010003-0047





REV. B		1018B14-0038		REV. B	
REVISIONS		SIZE		DATE	
SYM	DESCRIPTION	ISSUED		APPROVAL	
A				11/16/86	
B	CHANGED INSPECTED DIA FROM 'J' TO 'C'			10/12/86	



PART NO 1010003-0175
 SERIAL NO 001
 REQUESTED BY
 INSPECTED BY L. L. L. L. L.
 DATE 6/18/86
 ROOM TEMP 70 °F
 HUMIDITY 53 %
 WEIGHT 1868.5 LBS
 GMS

3.0715
 DIA -G- 3.0713
 1.6001
 DIA -C- 1.5999

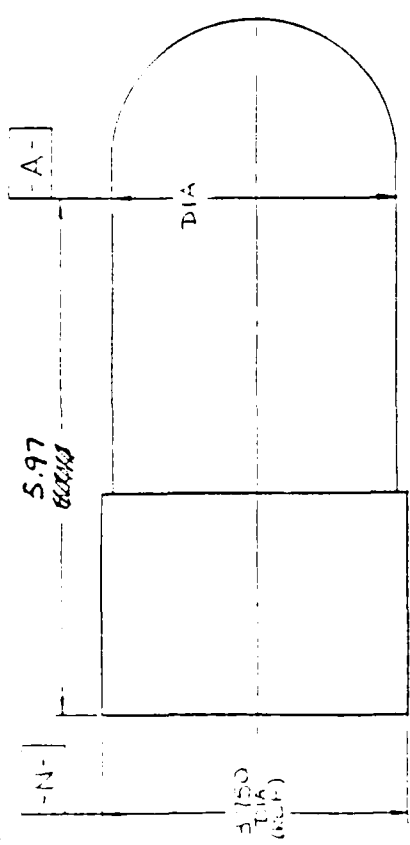
STA NO	DIA 'G' & 'C' (THREE PERCENT TOLERANCE TO 5 DECIMAL PL)	VISIBLE FLAWS SURFAC -G- DESCRIBE
G1	3.07255	3.07255
G2	3.07275	3.07250
G3	3.07255	3.07222
G4	3.07238	3.07154
ØC1	1.6001	1.6000

TOTAL RUNOUT
 DIA 'G' WRT DATUM -M- .0017 FIM (3 DECIMAL PL)
 SURFACE -D- WRT DATUM -M- .0002 FIM (3 DECIMAL PL)
 DIA 'C' WRT DATUM -D- .0001 FIM (3 DECIMAL PL)
 SURFACE FINISH (DIN H) 1.6 IN AA

DRAWN P. D. E. 11/16/86		Mechanical Technology Inc. Leham, New York	
CHECK	DESIGN	TITLE DISPLACER ASS'Y	
ANALYTICAL	MATERIALS	FINAL MACHINING INSPECTION	
MFG. ENGR.	PROJ. ENGR.	CODE IDENT NO. 26741	SIZE B
QUALITY CONTROL	REVISIONS 11-18-86	ISSUED	SCALE
UNLESS OTHERWISE SPECIFIED DIMENSIONS ARE IN INCHES		ACT. WT. CALC.	
TOLERANCES ON: DECIMALS FRACTIONS ANGLES			
XXX ± ± ±			
XX ± ± ±			
X ± ± ±			
BREAK SHARP CORNERS AND REMOVE BURRS			
MATERIAL			
TREATMENT			



REV		A	
SIZE		B	
REVISIONS		1018B14-0038	
SYM	DESCRIPTION	DATE	APPROVAL
A	ISSUED	7 DEC 1954	MLO



PART NO 1010003-0175
 SERIAL NO 001

REQUESTED BY
 INSPECTED BY
 DATE 6/1/56
 ROOM TEMP 70°F
 HUMIDITY 53%
 WEIGHT 185 LBS
 1868.5 GMS

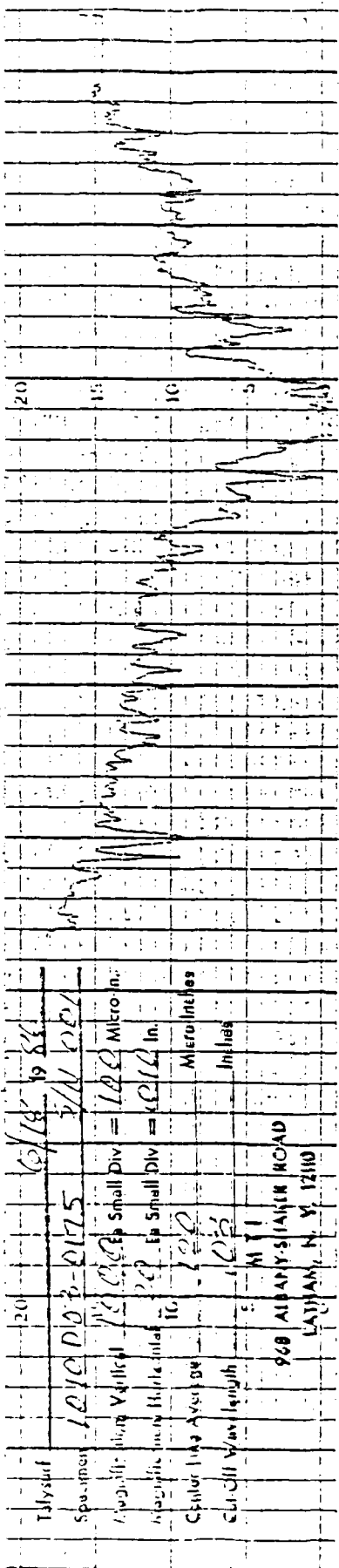
RUNOUT Δ
 DATUM - A - V.R.T. DATUM - N
 .001 FIM (3 DECIMAL PL.)
 PRESSURE TEST
 WELDS BUBBLE TIGHT AT 100 PSIG
 AIR PRESSURE
 Y N

Δ RUNOUT APPLIES AFTER WELDING -
 NO MACHINING PERMITTED

DRAWN BY De Franco 11/16/54		MTI Mechanical Technology Inc. Latham, New York	
CHECKED K. K. K. 20 Nov 54	TITLE		
DESIGNED K. K. K. 10 Nov 54	DISPLACER ASSY		
APPROVAL	WELD INSPECTION		
MATERIALS	CODE IDENT NO. 26741		
MFG ENGR	SIZE B		
PROD ENGR	SH 1005		
QUALITY CONTROL	1018B14-0038		
TREATMENT		ISSUED	MT CALC



PRINTED IN U.S.A.

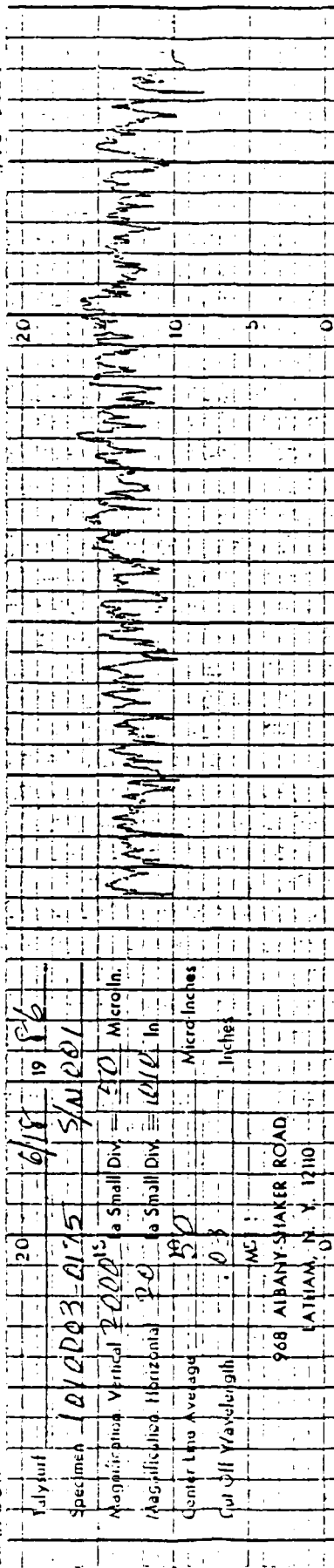


RTI

C-8

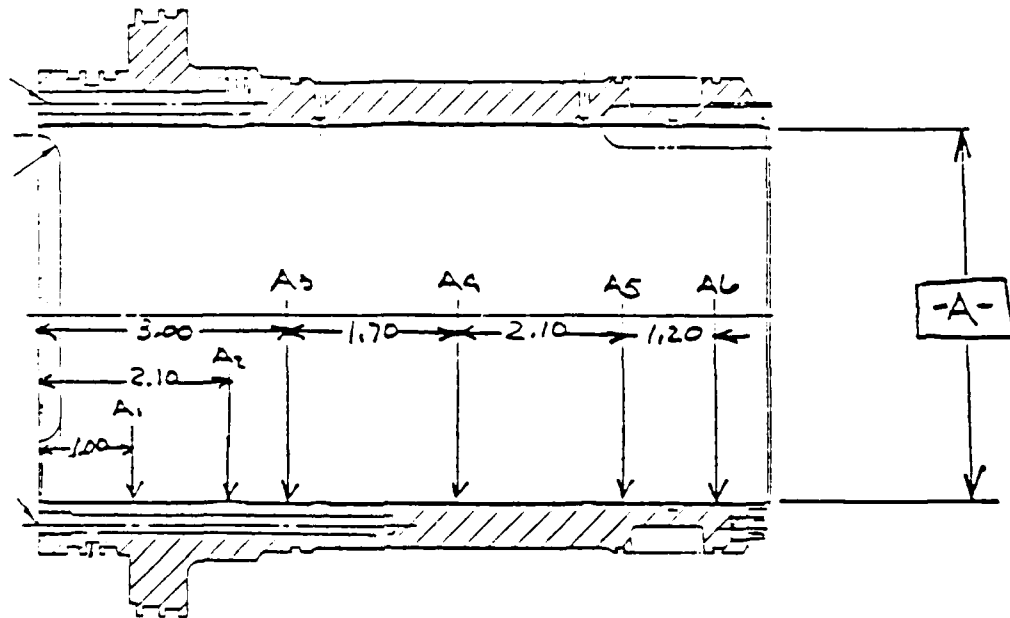
PRINTED IN U.S.A.

#79-2004



CYLINDER PIN 101DE06-0012

S/N LEFT = 1



4.202
4.200

DIAMETRAL
CLEARANCE

.0009
.0011

STA NO	DIA-A- (MEASURED 3 PLCS. 120° APART) W/ 4 PLACE ACCURACY		
A1	4.2015	4.2013	4.2016 OUT
A2	4.2040	4.2010	4.2043
A3	4.2009	4.2011	4.2013
A4	4.2012	4.2011	4.2011
A5	4.2012	4.2011	4.2012
A6	4.2012	4.2010 (OUT)	4.2015

PORT

STRAIGHTNESS OF DIA-A- BETWEEN STA 1 & STA 6

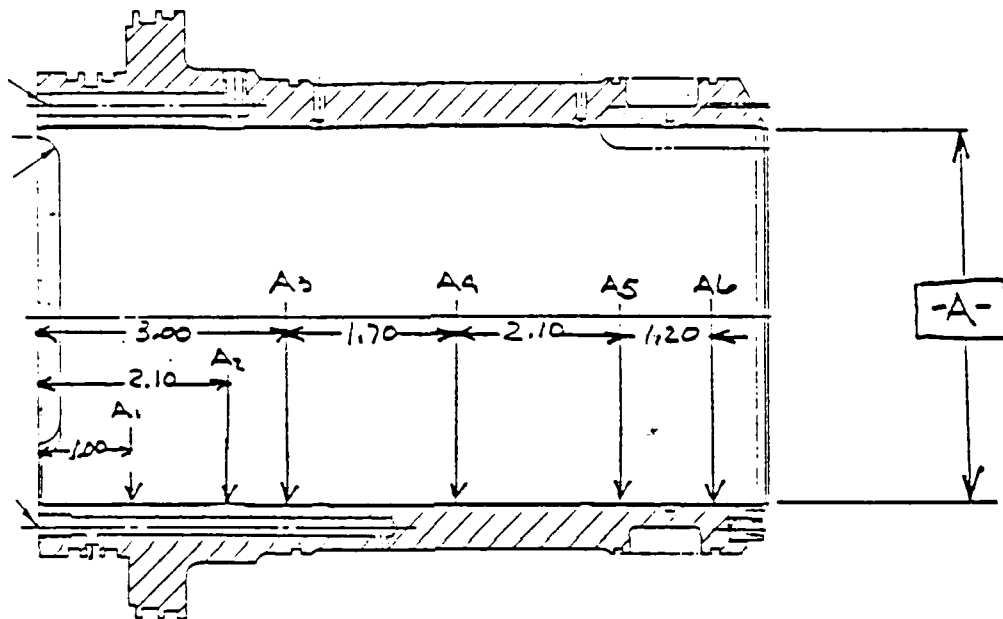
.0004 F.I.M (4 DECIMAL PLACE ACCURACY)

.0002 ECC.



CYLINDER P/N 1010E06-0012

S/N RIGHT 2

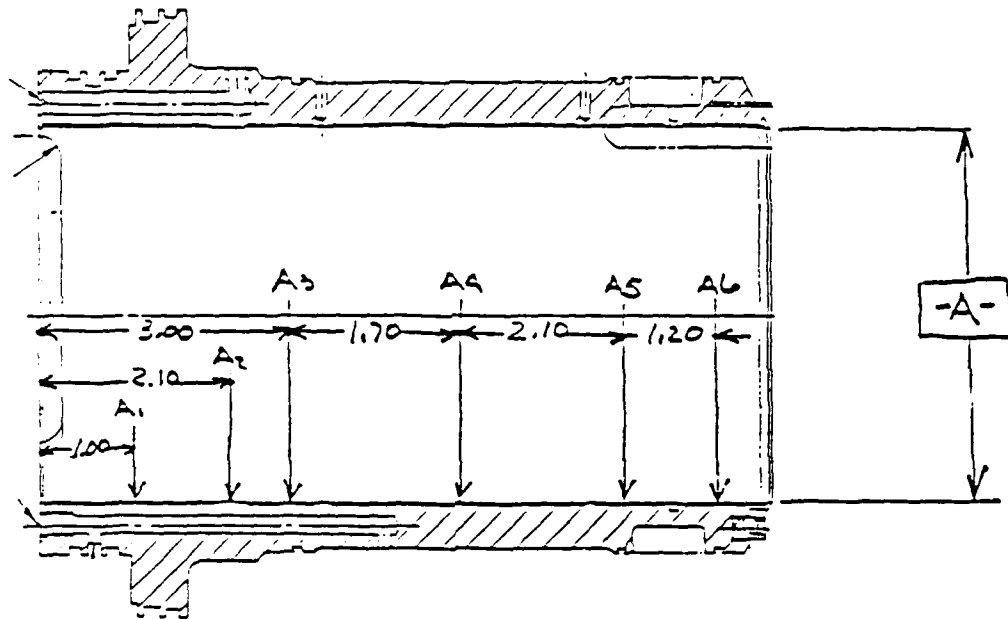


STA NO	DIA-A- (MEASURED 3 PLCS. 120° APART) w/ 4 PLACE ACCURACY		
A1	4.2017	4.2018	4.2018
A2	4.2017	4.2019	4.2022
A3	4.2017	4.2018	4.2018
A4	4.2017	4.2018	4.2017
A5	4.2016 out	4.2018	4.2017
A6	4.2018	4.2019	4.2019 out

STRAIGHTNESS OF DIA-A- BETWEEN STA 1 & STA 6
.00010 F.I.M (4 DECIMAL PLACE ACCURACY)
.00005 ECC.

CYLINDER PIN 101DE06-0012

S/N LEFT SIDE 4

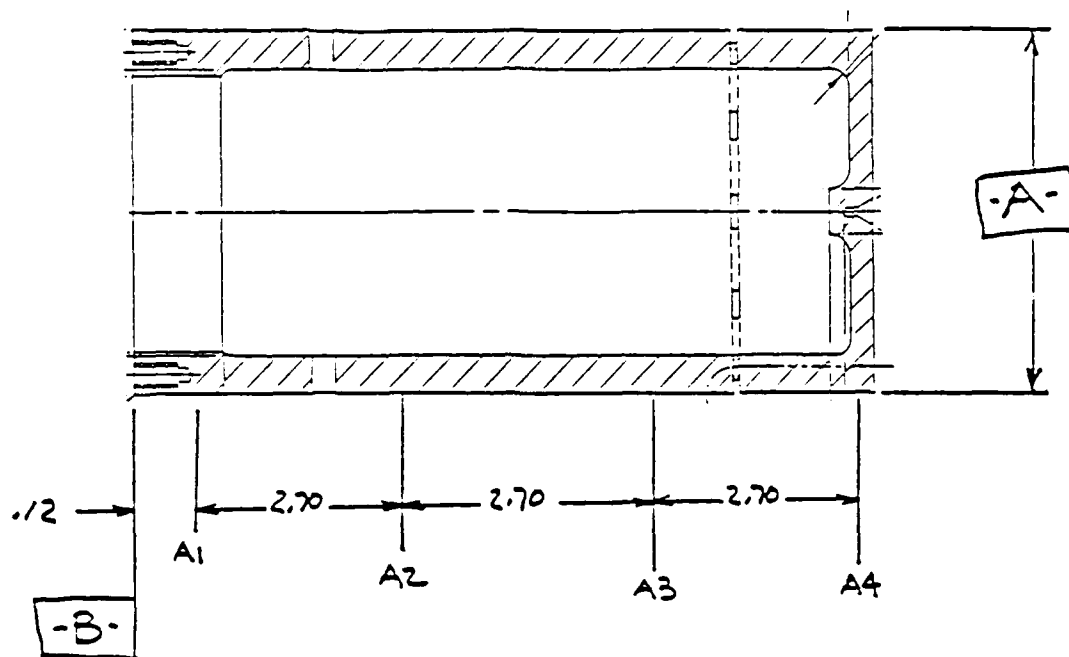


STA NO	DIA-A- (MEASURED 3 PLS. 120° APART) WI 4 PLACE ACCURACY		
A1	4.2017	4.2016	4.2018 OUT
A2	4.2020	4.2018	4.2040
A3	4.2017	4.2017	4.2017
A4	4.2017	4.2017	4.2016 ON
A5	4.2017	4.2016	4.2016
A6	4.2017	4.2017	4.2017

POAT

STRAIGHTNESS OF DIA-A- BETWEEN STA 1 & STA 6
.0002 F.I.M (4 DECIMAL PLACE ACCURACY)
 .0001 ECC.

PISTON P/N 101DD06-0010 S/N 1



4.201
4.199
DIAMETRAL
CLEARANCE
.0009
.0011

STA NO	DIA-A- (MEASURED 3 PLCS .120" APART W/ 4 DECIMAL PLACE ACCURACY)		
A1	<u>4.20085</u>	<u>4.20070</u>	<u>4.20090</u> ^{out}
A2	<u>4.20075</u>	<u>4.20075</u>	<u>4.20040</u> ^{out}
A3	<u>4.20065</u>	<u>4.20045</u>	<u>4.20065</u>
A4	<u>4.20065</u>	<u>4.20065</u>	<u>4.20065</u>

STRAIGHTNESS OF DIA-A- BETWEEN STA 1 & STA 4

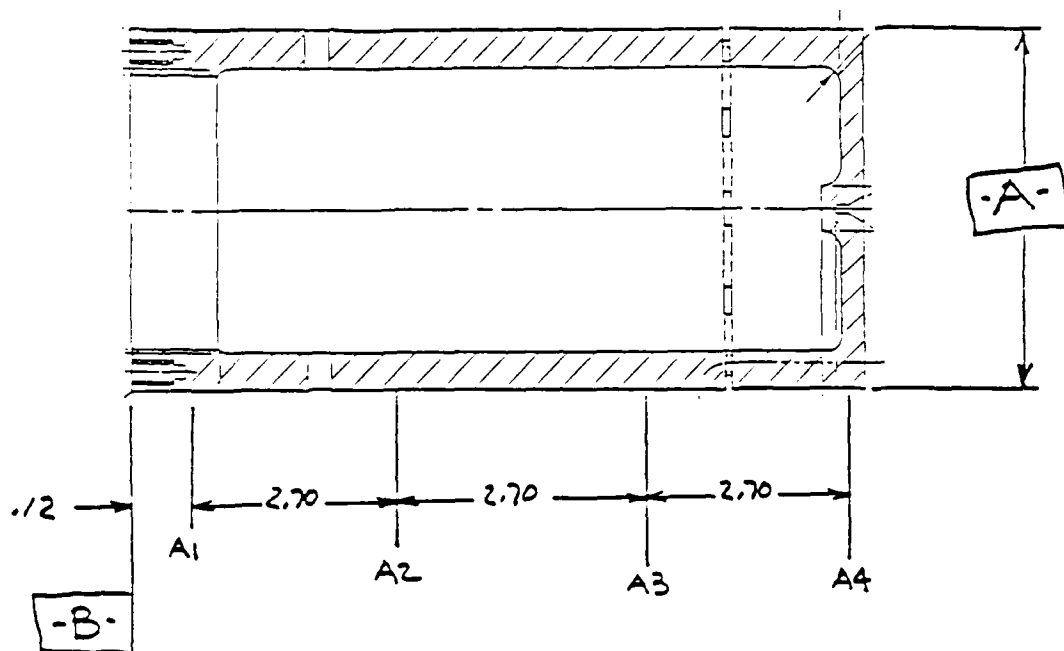
.0003 .0001 FIM (4 DECIMAL PLACE ACCURACY)

TOTAL RUNOUT SURFACE -B- W.R.T DIA-A-

.0005 .0006 FIM (ACCURATE TO 4 DECIMAL PLCS)



PISTON P/N 1010D06-0010 S/N 2



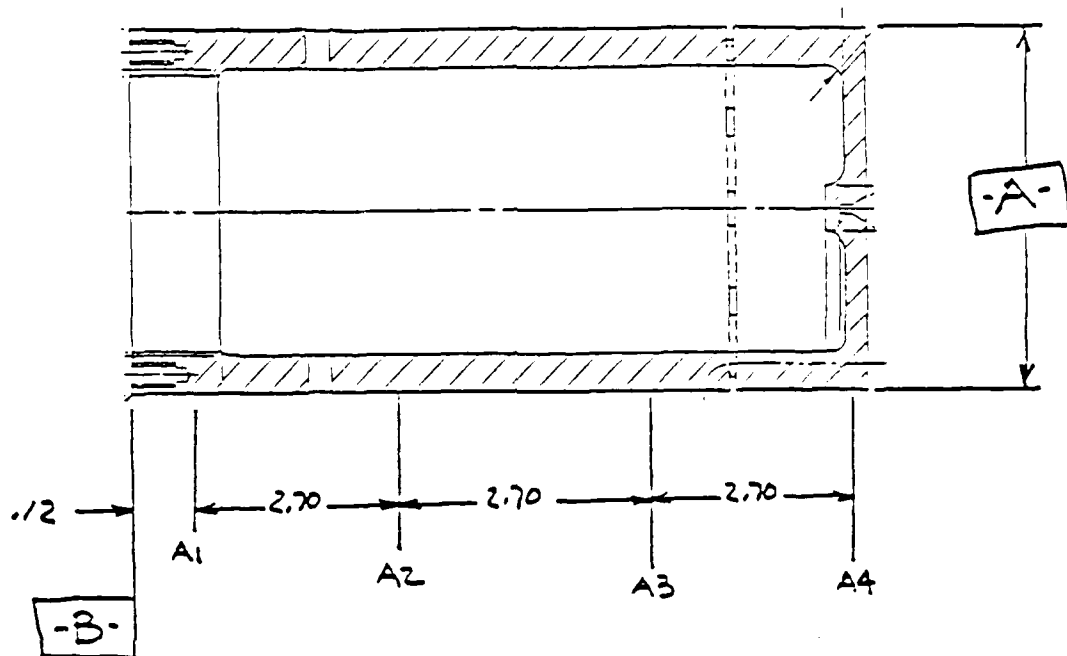
STA NO	DIA-A- (MEASURED 3 PLCS .120" APART W/ 4 DECIMAL PLACE ACCURACY)		
A1	<u>4.20055</u>	<u>4.20074</u>	<u>4.20048</u>
A2	<u>4.20036</u> ^{out}	<u>4.20045</u>	<u>4.20037</u>
A3	<u>4.20033</u>	<u>4.20045</u>	<u>4.20047</u>
A4	<u>4.20105</u>	<u>4.20110</u>	<u>4.20110</u> ^{out}

STRAIGHTNESS OF DIA-A- BETWEEN STA 1 & STA 4
.0001 FIM (4 DECIMAL PLACE ACCURACY)

TOTAL RUNOUT SURFACE -B- W.R.T DIA-A-
.0004 FIM (ACCURATE TO 4 DECIMAL PLCS)



S/N 3

PISTON P/N 1010DDG-0010

STA NO	DIA-A- (MEASURED 3 PLS. 120° APART W/ 4 DECIMAL PLACE ACCURACY)		
A1	<u>4.20100</u>	<u>4.20090</u>	<u>4.20090</u>
A2	<u>4.20085</u>	<u>4.20085</u>	<u>4.20085</u>
A3	<u>4.20085</u>	<u>4.20085</u>	<u>4.20085</u>
A4	<u>4.20085</u>	<u>4.20085</u>	<u>4.20085</u>

STRAIGHTNESS OF DIA-A- BETWEEN STA 1 & STA 4

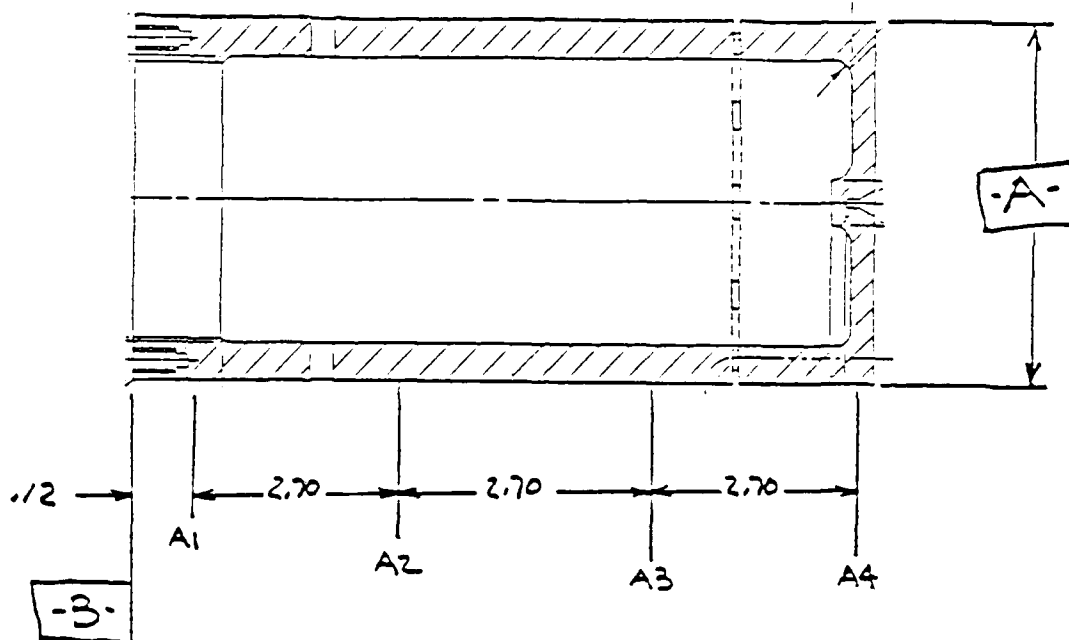
.0001 FIM (4 DECIMAL PLACE ACCURACY)

TOTAL RUNOUT SURFACE -B- W.R.T DIA-A-

.0005 FIM (ACCURATE TO 4 DECIMAL PLCS)

PISTON P/N 1010D06-0010

S/N 4



STA NO	DIA-A- (MEASURED 3 PLS. 120° APART W/ 4 DECIMAL PLACE ACCURACY)		
A1	<u>4.20010</u>	<u>4.20040</u>	<u>4.20035</u>
A2	<u>4.19990</u>	<u>4.20000</u>	<u>4.19995</u>
A3	<u>4.19975</u>	<u>4.19990</u>	<u>4.19990</u>
A4	<u>4.19990</u>	<u>4.19985</u>	<u>4.19985</u>

STRAIGHTNESS OF DIA-A- BETWEEN STA 1 & STA 4

.0001 FIM (4 DECIMAL PLACE ACCURACY)

TOTAL RUNOUT SURFACE-B- W.R.T DIA-A-

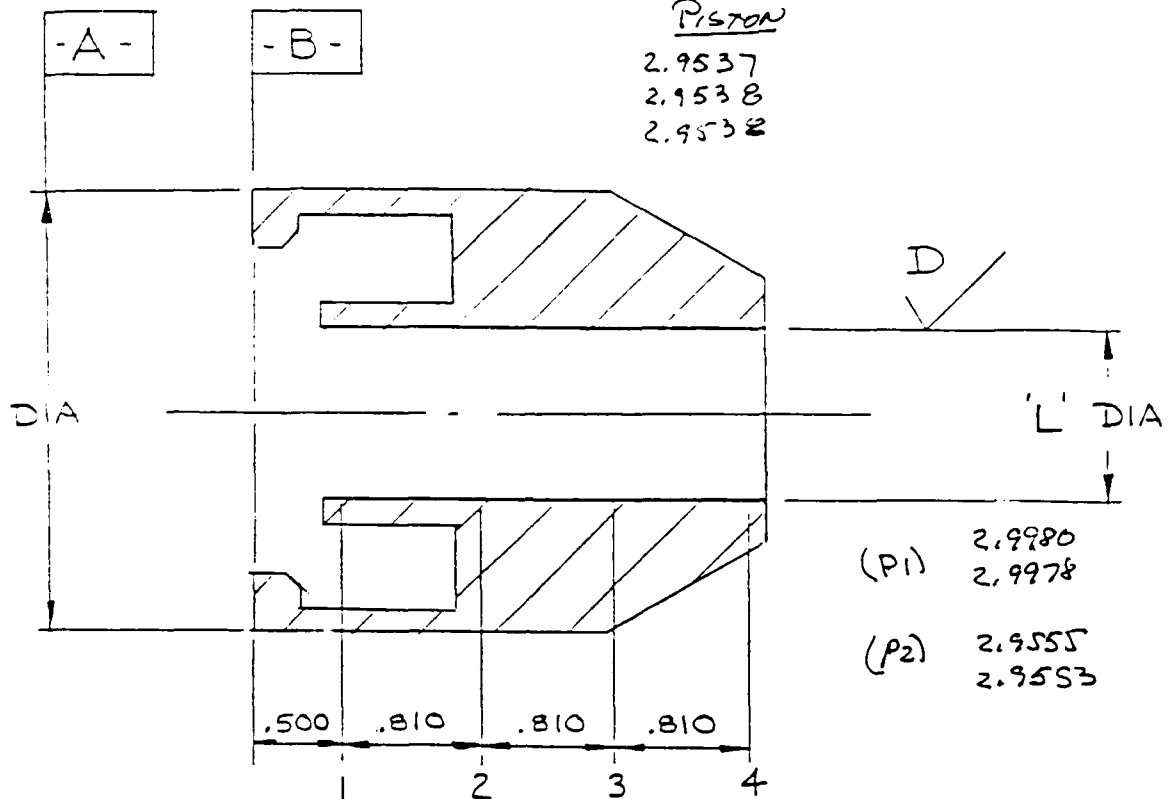
.0001 FIM (ACCURATE TO 4 DECIMAL PLCS)



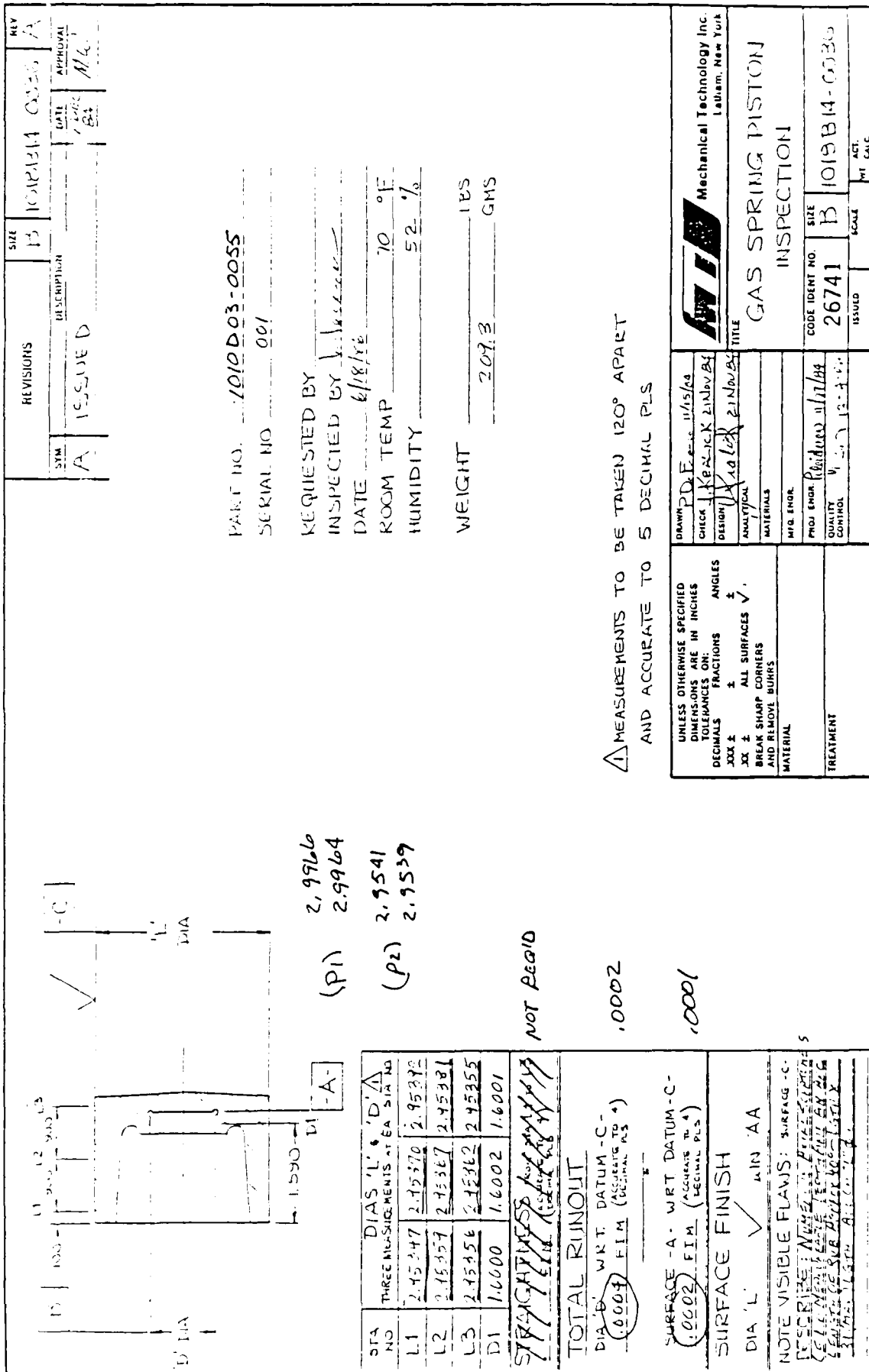
MEASURED 27 June 66 *AK*

PISTON


2.9537
2.9538
2.9538



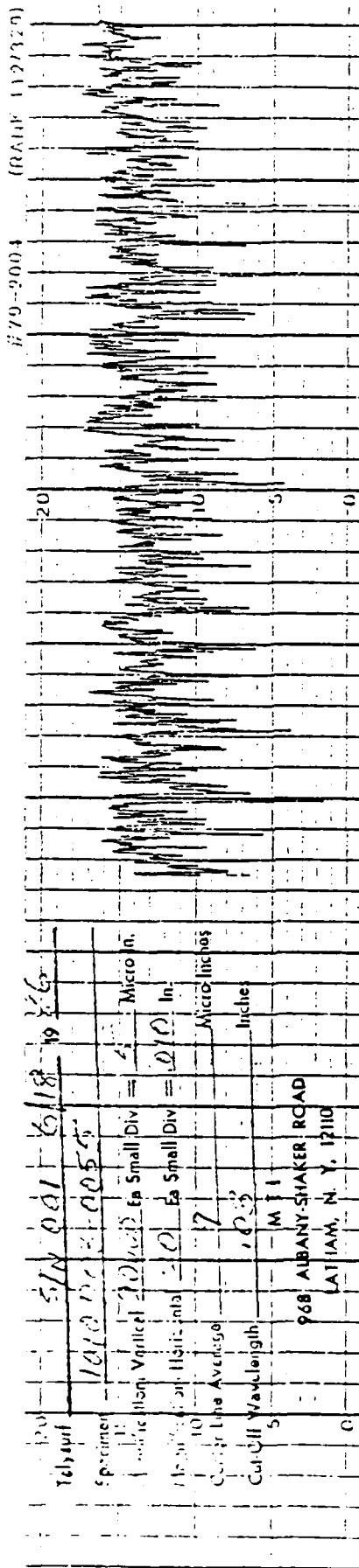
STA NO	DIA 'L' * THREE MEASUREMENTS 120° APART AT EA STA & ACCURATE TO 5 DECIMAL PLS.			NOTE VISIBLE FLAWS (DIA L)
1	2.9536	2.9543	2.9536	DESCRIBE: <u>Light axial</u>
2	2.9536	2.9541	2.9537	<u>Scratches in area between</u>
3	2.9537	2.9541	2.9538	<u>Sta #3 & 4</u>
4	2.9537	2.9539	2.9538	
PERPENDICULARITY DIA 'L' W.R.T. SURFACE -B- .0001 FIM (ACCURATE TO 4 DECIMAL PLS)				
SURFACE FINISH (DIA D) 20 μIN AA				* 0° ± 5/N



△ MEASUREMENTS TO BE TAKEN 120° APART AND ACCURATE TO 5 DECIMAL PLS

UNLESS OTHERWISE SPECIFIED DIMENSIONS ARE IN INCHES TOLERANCES ON:		DRAWN <i>P.D.F.</i> <i>11/15/88</i>		 Mechanical Technology Inc. Latham, New York
DECIMALS	FRACTIONS	CHECK <i>11/15/88</i>		
XXX ±	ALL SURFACES ✓	DESIGN <i>11/15/88</i>		
XXX ±	BREAK SHARP CORNERS AND REMOVE BURRS	ANALYSIS <i>11/15/88</i>		
MATERIAL		MATERIALS		
		MTQ. ENGR.		
TREATMENT		PROJ. ENGR. <i>11/15/88</i>		
		QUALITY CONTROL		
		CODE IDENT NO. 26741		
		SIZE B	SCALE	ACT. DATE
		1019 B14-0036		
		ISSUED		

BRUNING, JOSEPH



DATE 4/21/86		ORDER NO. 11R#28180	INSPECTION RECORD		QUANTITY 1	MATERIAL	UWG NO.	INV.
SHEET NO. 1 OF 1		0384-46167-161	HEAT TREAT		PLATING OR COATING		DWR NO.	
NAME OF PART 1010 CUB-0045		S/N 1	ACTUAL DIMENSION					
ADM Displacer Rod			ZONE	0°	120°	180°	270°	
DRAWING DIMENSIONS								
1	1.59995-1.60005 Ø @ 3/4 S.E.			1.59930	1.59933	1.59928		
2								
3	1.59995-1.60005 Ø @ 2 1/2 S.E.			1.59950	1.59948	1.59952		
4								
5	1.59995-1.60005 Ø @ 3/4 L.E.			1.59938	1.59940	1.59942		
6								
7	1.59995-1.60005 Ø @ 2 1/2 L.E.			1.59945	1.59948	1.59952		
8								
9								
10								
11								
12								
13								
14								
15								
16								
17								
18								
19								
20								
21								
22								
23								
24								
25								

Wood
11/5/84

TYPE OF INSPECTION
☐ RECEIVING
☐ IN PROCESS - AT STATION
☐ OTHER

COPIES EACH TO
 QC FILE PROD FILE PROD CONT

COMPANY INSPECTION
 T. J. [Signature]
 SOURCE INSPECTION

DATE 4/24/86
 PART OR LOT
 ACCEPT
 REJECT



DATE 4/21/86		ORDER NO. MR# 28180	INSPECTION RECORD		QUANTITY 1	MATERIAL	UWG NO.	REV
SHEET NO. 1 OF 1		0384-46167-161	HEAT TREAT 120°		ACTUAL DIMENSION	PLATING OR COATING	QWR NO.	
NAME OF PART 1010 J003-0016		S/N 1	ZONE	ACTUAL DIMENSION	REJECT	ACCEPT	REJECT	
DRAWING DIMENSIONS								
1	160085-160085φ @ 1/2" S.E.	160079	160082	160073				
2								
3	160095-160085φ @ 2" S.E.	160093	160105	160103				
4								
5	160095-160085φ @ 1/2" L.E.	160068	160067	160073				
6								
7	160085-160085φ @ 2" L.E.	160103	160100	160106				
8								
9								
10								
11								
12								
13								
14								
15								
16								
17								
18								
19								
20								
21								
22								
23								
24								
25								

TYPE OF INSPECTION
☐ RECEIVING
☐ IN PROCESS - AT STATION
☐ OTHER

CONES LEACH TO
 QC FILE PROJ FILE PROD CONT

COMPANY INSPECTION
 T. B. BARTLEY
 SOURCE INSPECTION

DATE

4/21/86

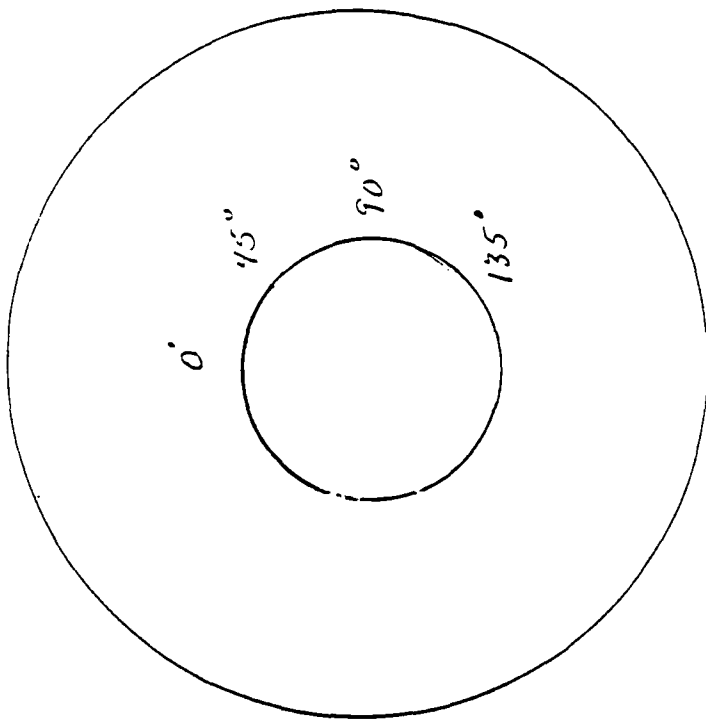
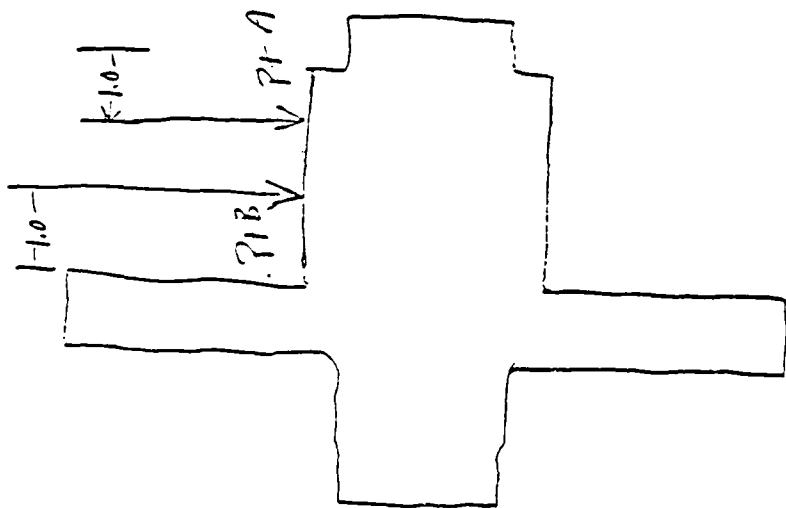
PART UNIT

ACCEPT

REJECT

Nov 1/86 R21780





	0	45	90	135
P1 A	3.06973	3.06973	3.06983	3.06983
P1 B	3.06969	3.06963	3.06975	3.06978

ADM Post & Flange

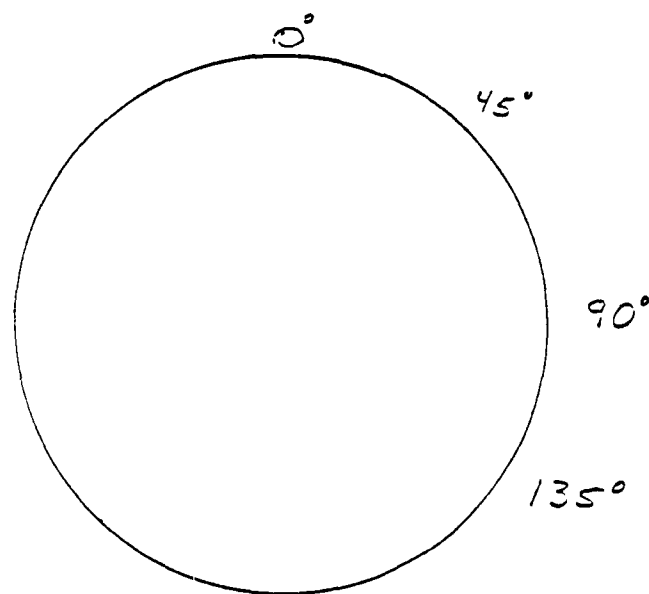
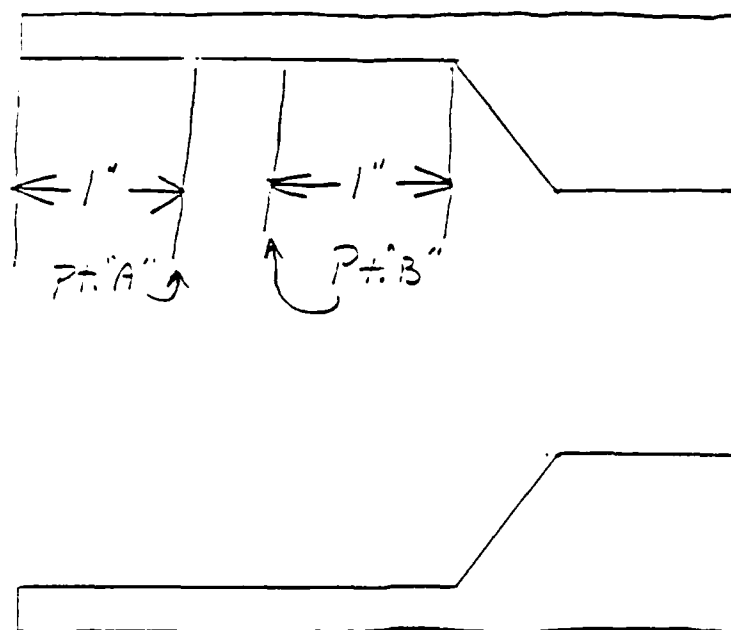
P/N 1010D03-0046

1/11/86

TB 4/3/86

7/27/86 TB

ADM Displacer (1010 D03 - 0042)
~~(1010 D03 - 0042)~~ S/N 002



	0°	45°	90°	135°
Pt A	3.07270	3.07275 ^{Max}	3.07130	3.07120
Pt B	3.07195	3.07270	3.07075	3.07045 ^{min}



DISPLACEMENT PROBE CALIBRATION

PARAMETER:

X_D

TEST CELL: #2 ADM

DVM: MT-10999

PROBE TYPE: KD-2350-24B SPL

SENSITIVITY: 10mm /VDC

OTHER INSTRUMENTS:

DIAL INDICATOR

NOTES	POSITION WRT		PROBE: X _{D1}	PROBE: X _{D2}	SUMMATION	% DEV.
	MIDSTROKE		S/N: 0-33386	S/N: 0-33323	OUTPUT	FROM ST.
	Ins.	MM's	CHAN:	CHAN:	CHAN: EX _D	LINE
	+0.5	+12.70				
UP	+0.45	+11.43	-1.139	-1.134	+1.136	-1.6
A	+0.4	+10.16	-1.021	-1.017	+1.019	+1.3
I	+0.3	+7.62	-1.765	-1.767	+1.767	+1.7
	+0.2	+5.08	-1.502	-1.505	+1.505	-1.6
	+0.1	+2.54	-1.250	-1.251	+1.253	-1.4
	0	0	-1.004	+1.000	+1.002	
	-0.1	-2.54	+1.248	+1.253	-1.250	-1.6
V	-0.2	-5.08	+1.500	+1.505	-1.501	-1.4
DN	-0.3	-7.62	+1.763	+1.767	-1.764	+0.3
	-0.4	-10.16	+1.013	+1.017	-1.014	-0.2
	-0.45	-11.43	+1.141	+1.133	-1.139	-0.3
	-0.5	-12.70				
	0	0				
	+0.01	+0.254				
	+0.02	+0.508				
	+0.03	+0.762				
	+0.04	+1.016				
	+0.05	+1.270				
	+0.06	+1.524				
	+0.07	+1.778				
	+0.08	+2.032				
	+0.09	+2.286				
	+0.10	+2.540				
	+0.11	+2.794				
	+0.12	+3.048				

REMARKS:

*Resistor used; check all voltages from E circuit
gain to next calibration.*

PERFORMED BY:

DATE:

J. K. Smith

9/27/26



DISPLACEMENT PROBE CALIBRATION

PARAMETER:

X_{A,P}TEST CELL: F₂ ADM

DVM: MTE 10999

PROBE TYPE: KD-2350-248 SPL

SENSITIVITY: 10mm/1VDC

OTHER INSTRUMENTS: DIAL

INDICATOR

INCH	POSITION WRT		PROBE: X _{A,P1}	PROBE: X _{A,P2}	SUMMATION	% DEV.
	MIDSTROKE		S/N: 0-33385	S/N: 0-33390	OUTPUT	FROM ST. LINE
MM	INS.	MM'S	CHAN:	CHAN:	CHAN: 2X _{A,P}	
	+0.55	+13.97	-1.378	-1.397	-1.389	-0.6
	+0.5	+12.70	-1.256	-1.271	-1.264	-0.5
	+0.45	+11.43	-1.147	-1.159	-1.153	+0.9
	+0.4	+10.16	-1.019	-1.025	-1.021	+0.5
	+0.3	+7.62	-.735	-.733	-.734	-3.7
	+0.2	+5.08	-.483	-.483	-.483	-4.9
	+0.1	+2.54	-.238	-.239	-.239	-5.9
	0	0	+1.006	+1.008	+1.009	
	-0.1	-2.54	+1.257	+1.258	+1.258	+1.6
	-0.2	-5.08	+1.503	+1.502	+1.506	-0.4
	-0.3	-7.62	+1.755	+1.747	+1.754	-1.0
	-0.4	-10.16	+1.007	+1.993	+1.003	-1.3
	-0.45	-11.43	+1.132	+1.119	+1.129	-1.2
	-0.5	-12.70	+1.258	+1.245	+1.256	-0.1
	-0.55	-13.97	+1.420	+1.378	+1.389	-0.6
	0	0				
	+0.01	+0.254				
	+0.02	+0.508				
	+0.03	+0.762				
	+0.04	+1.016				
	+0.05	+1.270				
	+0.06	+1.524				
	+0.07	+1.778				
	+0.08	+2.032				
	+0.09	+2.286				
	+0.10	+2.540				
	+0.11	+2.794				
	+0.12	+3.048				

REMARKS: Calibration OKPERFORMED BY: Hubert
DATE: 9-2-81

DISPLACEMENT PROBE CALIBRATION

PARAMETER:

XA₂P

TEST CELL: ADM #2

DVM: MTI-10999

PROBE TYPE: KD-2350-24B SFL

SENSITIVITY: 10 mm / INDC

OTHER INSTRUMENTS: DIAL

INDICATOR

NOTES	POSITION WRT		PROBE: XA ₂ P	PROBE: XA ₂ P ₂	SUMMATION	% DEV.
	MIDSTROKE		S/N: 0-33388	S/N: 0-33387	OUTPUT	FROM ST.
	INS.	MM'S	CHAN:	CHAN:	CHAN: XA ₂ P	LINE
	+0.55	+13.97	-1.393	-1.402	-1.399	+1
	+0.5	+12.70	-1.260	-1.264	-1.263	-1.6
↑	+0.45	+11.43	-1.153	-1.153	-1.154	+1.0
↓	+0.4	+10.16	-1.020	-1.016	-1.018	+0.2
↖	+0.3	+7.62	-0.754	-0.746	-0.752	-1.3
	+0.2	+5.08	-0.495	-0.498	-0.496	-2.4
	+0.1	+2.54	-0.247	-0.245	-0.246	-3.1
	0	0	0.00	-0.00	0.00	
	-0.1	-2.54	+0.257	+0.248	+0.253	-0.4
	-0.2	-5.08	+0.511	+0.500	+0.505	-0.6
↘	-0.3	-7.62	+0.761	+0.758	+0.760	-0.3
↙	-0.4	-10.16	+1.018	+1.008	+1.012	-0.4
↓	-0.45	-11.43	+1.136	+1.128	+1.133	-0.9
↖	-0.5	-12.70	+1.263	+1.260	+1.262	-0.6
	-0.55	-13.97	+1.420	+1.423	+1.421	+1.7
	0	0				
	+0.01	+0.254				
	+0.02	+0.508				
	+0.03	+0.762				
	+0.04	+1.016				
	+0.05	+1.270				
	+0.06	+1.524				
	+0.07	+1.778				
	+0.08	+2.032				
	+0.09	+2.286				
	+0.10	+2.540				
	+0.11	+2.794				
	+0.12	+3.048				

REMARKS:

Bearings Fixed

PERFORMED BY:
DATE:Tech. Smt
7/2/26

TESTED WITH STANDARDS REFERENCED TO
NATIONAL BUREAU OF STANDARDS



DATE - AUG. 6, 1986 PAGE - 1 OF - 7
 ORDER NO. - 353 I.D. - P6SH-1
 TEST ITEM PRESSURE TRANSDUCER
 CO. - DRUCK ANALOG DEVICES
 MOD - PDCR 200 2831-J
 S/N - 1901
TRANS. AMPL.
 LOCATION FREE PISTON TEST CELL # 2
N.E.R.

OPERATOR U.G. SPADNIEWSKI
 CALIB. FOR - M. DHAR
 Traceability Data

CALIBRATOR DAVID WIT. PRESSURE TESTER
 CO. PMETER
 MOD DMT-50
 S/N 10672

ADDITIONAL INSTRUMENTS -
 1. DIGITAL MULTIMETER
H.P. MCD-3465B S/N-1530 AO 3095

SIGNED: [Signature]

CALIBRATION LABORATORY - NER PLANT

MECHANICAL TECHNOLOGIES INCORPORATED
LATHAM, N.Y.

STANDARD			TEST ITEM		
	PSI	CALC.	VOLTS	ERROR	
			D.C.	VOLTS	
1.	0	0.100	0.100	0	
2.	200	1.470	1.477	.002	
3.	400	2.850	2.854	.005	
4.	600	4.220	4.234	.004	
5.	(*) 800	5.617	(*) 5.615	.002	
6.	1000	6.997	6.997	0	
7.					
8.					
9.					
10.					
11.					

NOTES: ☒ CALIBRATION DUE FEB. 6, 1987
☒ RECALIBRATION - PREVIOUS CALIB.
WAS ON JAN. 29, 1986
☒ (*) AMPLIFIER SET POINT: @ 800 PSI

M. DHAR
CALIBRATION LAB

H. SHORT
T. RUSSELL

COPIES TO:



TESTED WITH STANDARDS REFERENCED TO
NATIONAL BUREAU OF STANDARDS



DATE - AUG. 6, 1986 PAGE - 2 OF - 7
FOLDER NO. - 354 I.D. - PDGS
TEST ITEM PRESSURE TRANSDUCER
QD. - DRUCK | ANALOG DEVICES
MOD - PD-R 200 | 2831J
SN - 1902
| TRANS. | AMPL.
LOCATION FREE PISTON TEST CELL # 2
N.E.R.
OPERATOR W.G. SPIDNEWSKI
CALIB. FOR - M. DHAR
Traceability Data
CALIBRATOR DEAD WT. PRESSURE TESTER
CO. PMETEK
MOD DNT-50
SN 10672

ADDITIONAL INSTRUMENTS -
1. DIGITAL MULTIMETER
H.P. MOD-3465B S/N-1530 AD 3095
2. _____
3. _____
4. _____
5. _____
6. _____
7. _____
8. _____
9. _____
10. _____
11. _____

STANDARD				TEST ITEM	
	PSI		CALC.	VOLTS	52802
				VOLTS	D.C. " VOLTS
1.	0	0.100	0.092		.002
2.	200	1.470	1.474		.005
3.	400	2.857	2.851		.008
4.	600	4.222	4.234		.004
5.	(+) 800	5.617	(+) 5.617		0
6.	1000	6.997	6.992		.001
7.					
8.					
9.					
10.					
11.					

NOTES: 1. CALIBRATION DUE FEB. 6, 1987
2. RECALIBRATION - PREVIOUS CALIB.
WAS ON JAN. 8, 1986
3. (+) AMPLIFIER SET POINT: @ 800 PSI

SIGNED: [Signature]

CALIBRATION LABORATORY - IHR PLANT

MECHANICAL TECHNOLOGY INCORPORATED
LATHAM, N.Y.



M. DHAR
CALIBRATION LAB

H. SHORT
J. RUSSELL

COPIES TO



TESTED WITH STANDARDS REFERENCED TO
NATIONAL BUREAU OF STANDARDS



DATE - AUG 6, 1926 PAGE - 3 OF - 7
 ORDER NO. - 380 I.D. - PM
 TEST ITEM PRESSURE TRANSDUCER
 CO. - ENTRAN ANALOG DEVICES
 MOD - 9939 || 2831J
 SN - 12W4X-M9-9
TRANS. AMPL.
 LOCATION FREE PISTON TEST CELL # 2
N.E.R.
 OPERATOR W.G. SPADNEWSKI
 CALIB. FOR M.DHAR
Traceability Date
 CALIBRATOR DEAD WT. PRESSURE TESTER
AMETEK
 CO. DMT-50
 MOD 10672

ADDITIONAL INSTRUMENTS -

1. DIGITAL MULTIMETER
H.P. MOD-34653 S/N-1530 AD 3095

STANDARD		TEST ITEM	
PSI	CALC.	VOLTS	52202
		D.C. " VOLTS	
0	0.100	0.100	0
200	1.450	1.461	.018
400	2.850	2.834	.025
600	4.222	4.220	.018
(+) 800	5.617	(+) 5.615	.002
1000	6.997	7.015	.018

NOTES: ☒ CALIBRATION DUE FEB. 6, 1926
☒ RECALIBRATION - PREVIOUS CALIB.
 WAS ON JAN. 8, 1926
☒ (+) AMPLIFIER SET POINT: 0.000 PSI

SIGNED: M.D. HARR

CALIBRATION LABORATORY - NER PLANT



MEDICAL TECHNOLOGIES INCORPORATED
LAUREL, MD.

M.D. HARR
CALIBRATION LAB

H. SHORT
T. RUSSELL

COPY TO



TESTED WITH STANDARDS REFERENCED TO
NATIONAL BUREAU OF STANDARDS



DATE - AUG. 6, 1986 PAGE - 4 OF - 7
 INSTRUMENT NO. - 236 I.D. - DSSH-2
 DESCRIPTION - PRESSURE TRANSDUCER
 CO. - KULITE ANALOG DEVICES
 MOD. - YTM-190-2000 || 2831J
 S.N. - I6-46
 TYPE - TRANS. || AMPL.
 LOCATION FREE PISTON TEST CELL # 2
M.R.
 OPERATOR W.G. SPADNEWSKI - D.S.
 CALIB. FOR M.DHAR
Traceability Data
 CALIBRATOR DEAD WT. PRESSURE TESTER
AMETEK
 CO. DMT-50
 S.N. 10672

ADDITIONAL INSTRUMENTS -
 1. DIGITAL MULTIMETER
HP 1102-3465B S/N-1530 AO 3095
 2. _____
 3. _____
 4. _____

STANDARD				TEST ITEM	
	PSI	CALIB.		VOLTS	ERROR
				D.C.	VOLTS
1.	0	0.100	0.100	0	0
2.	200	1.470	1.495	0.016	
3.	400	2.850	2.880	0.021	
4.	600	4.232	4.254	0.016	
5.	(+)	800	5.617	(+)	5.617
6.	1000	6.997	6.971	0.026	
7.					
8.					
9.					
10.					
11.					

NOTES: 1. CALIBRATION DUE FEB 6, 1986
 2. RECALIBRATION - PREVIOUS CALIB.
WAS ON JAN. 29, 1986
 3. (+) AMPLIFIER SET POINT: @ 800 PSI

SIGNED: M.DHAR

CALIBRATION LABORATORY - NEW PLANT

MECHANICAL TECHNOLOGY, INC. INCORPORATED
LATHAM, N.Y.



M.DHAR
CALIBRATION LAB

H. SHORT
T. RUSSELL

COPIES

TO:





Ch. F. Johnson

CALIBRATION LABORATORY - HER PLANT

LABORATORY INCORPORATED
LABORATORY

田

11. D. HAR

713557212
L20454
H. SHORT

COPIES

STANDARD		TEST ITEM	
	PSI	CALC.	VOLTS
		VOLTS	D.C. " VOLTS
1.	0	0.102	0.092 .002
2.	200	1.470	1.493 .014
3.	400	2.859	2.870 .020
4.	600	4.232	4.254 .016
5.	(+) 800	5.617 (+)	5.619 .002
6.	1000	6.997	6.970 .027
7.			
8.			
9.			
10.			
11.			
12.			
13.			
14.			
15.			
16.			
17.			
18.			
19.			
20.			
21.			
22.			
23.			
24.			
25.			
26.			
27.			
28.			
29.			
30.			
31.			
32.			
33.			
34.			
35.			
36.			
37.			
38.			
39.			
40.			
41.			
42.			
43.			
44.			
45.			
46.			
47.			
48.			
49.			
50.			
51.			
52.			
53.			
54.			
55.			
56.			
57.			
58.			
59.			
60.			
61.			
62.			
63.			
64.			
65.			
66.			
67.			
68.			
69.			
70.			
71.			
72.			
73.			
74.			
75.			
76.			
77.			
78.			
79.			
80.			
81.			
82.			
83.			
84.			
85.			
86.			
87.			
88.			
89.			
90.			
91.			
92.			
93.			
94.			
95.			
96.			
97.			
98.			
99.			
100.			

NOTES: [] CALIBRATION DUE FEB 6, 1986
[] RECALIBRATION - PREVIOUS CALIB.
WAS ON JAN. 31, 1986
(+) AMPLIFIER SET POINT: @ 250 PSI



TESTED WITH STANDARDS REFERENCED TO
NATIONAL BUREAU OF STANDARDS



DATE - AUG 6, 1986 PAGE - 6 OF - 7
FOLDER NO. - 286 I.D. - P-226
TEST ITEM PRESSURE TRANSDUCER
CO. - KULITE ANALOG DEVICES
MOD - YTM-190-2000 2831J
S/N - B7-49
TRANS. AMPL.
LOCATION FREE PISTON TEST CELL # 2
N.E.R.
OPERATOR W.G. SPADNIEWSKI - D.S.
CALIB. FOR M.D.HAR
Traceability Data
CALIBRATOR DEAD WT. PRESSURE TESTER
CO. AMETEK
MOD DMT-50
S/N 10672

ADDITIONAL INSTRUMENTS -

1. DIGITAL MULTIMETER
H.P. MOD-3465B S/N-1530 AO 3095

	STANDARD		TEST ITEM	
	PSI	CALIB.	VOLTS	ERROR
			VOLTS	D.C. VOLTS
1.	0	0.100	0.100	0
2.	200	1.470	1.472	.001
3.	400	2.850	2.856	.003
4.	600	4.232	4.236	.002
5.	(*) 800	5.617	(*) 5.616	.001
6.	1000	6.997	6.997	0
7.				
8.				
9.				
10.				
11.				

NOTES: ☒ CALIBRATION DUE FEB 6, 1986
☒ RECALIBRATION - PREVIOUS CALIB.
WAS ON JAN. 8, 1986
☒ (*) AMPLIFIER SET POINT: @ 200 PSI

SIGNED: [Signature]

CALIBRATION LABORATORY - NER PLANT

MECHANICAL TECHNOLOGICAL INCORPORATED
LATHAM, N.Y.



M.D.HAR
CALIBRATION LAB

H. SHORT
T. RUSSELL

COPIES
101



TESTED WITH STANDARDS REFERENCED TO
NATIONAL BUREAU OF STANDARDS



DATE - AUG 6, 1986 PAGE - 7 OF - 7
 FORMER NO. - 164 I.D. - PLGS
 TEST ITEM PRESSURE TRANSDUCER
 Q.D. - KULITE ANALOG DEVICES
 MOD - YTM-190-2000 2831J
 S/N - A5-32
TRANS. AMPL.
 LOCATION FREE PISTON TEST CELL # 2
N.E.R.
 OPERATOR U.G. SPADNEWSKI - D.S.
 CALIB. FOR - M.D.HAR
 Traceability Data
 CALIBRATOR DEAD WT. PRESSURE TESTER
 CO. AMETEK
 MOD DMT-50
 S/N 10672

ADDITIONAL INSTRUMENTS -
 1. DIGITAL MULTIMETER
H.P. MCD-34658 S/N-1530 AO 3095
 2.

STANDARD		TEST ITEM	
PSI	CALC.	VOLTS	53802
		D.C.	VOLTS
1.	0	0.100	0
2.	200	1.470	1.492
3.	400	2.850	2.874
4.	600	4.220	4.249
5.	(+) 800	5.617	(+) 5.614
6.	1000	6.997	6.980
7.			
8.			
9.			
10.			
11.			

NOTES: ☒ CALIBRATION DUE FEB 6, 1986
☒ RECALIBRATION - PREVIOUS CALIB.
WAS ON JAN. 31, 1986
☒ (+) AMPLIFIER SET POINT: @ 200 PSI
☒ APPLIED EPOXY AROUND CONNECTION

SIGNED: [Signature]

CALIBRATION LABORATORY - NER PLANT



MECHANICAL TECHNOLOGY INCORPORATED
LATHAM, N.Y.

Y-1735
 M.D.HAR
 CALIBRATION LAB

H. SHORT
 F. RUSSELL

COPYED
 TO



TESTED WITH STANDARDS REFERENCED TO
NATIONAL BUREAU OF STANDARDS



DATE - JAN 13, 1986 PAGE - 1 OF - 4
FOLDER NO. - 56 I.D. - DP - AIR
TEST ITEM PRESSURE TRANSDUCER
CO. - VALIDDYNE M.T.I.
MOD - DP-45-26 D.O.E. COMB.
S/N - 42706 CH. NO. 2
TRANS AMPL.
LOCATION FREE PISTON TEST CELL # 2
N.K.R.
OPERATOR W.G. SPODNEWSKI - D.S.
CALIB. FOR 6 KOESTER
Traceability Data
CALIBRATOR DIGITAL PRESS. INDICATOR
CO. DRUCK
MOD DPI-600
S/N 600/0128

ADDITIONAL INSTRUMENTS -

1. DIGITAL MULTIMETER
H.P. MOD - 3465R, S/N - 1530 A03095
2. _____

STANDARD				TEST ITEM	
	H ₂ O	CALC.		VOLTS	ERROR
		VOLTS		D.C.	VOLTS
1.	0	0		0.000	0
2.	2	2.0		1.961	.039
3.	4	4.0		4.020	.020
4.	(*) 6	6.0	(*)	6.028	.028
5.	8	8.0		8.083	.083
6.	10	10.0		10.041	.041
7.					
8.					
9.					
10.					
11.					

NOTES: ☒ CALIBRATION DUE JULY 1, 1986

- ☒ REGALIBRATION - LAST ON: 2/26/85
- ☒ CALIBRATED (+) PORT - NORMAL POSITION
- ☒ (+) AMPL. SETTINGS: ZERO - 371 SPAN - 250
- ☒ DO NOT TOUCH TRANS. HOUSING SCREWS

SIGNED: [Signature]

CALIBRATION LABORATORY - INK PLANT

MECHANICAL TECHNOLOGY INCORPORATED
LATHAM, N.Y.



S. KOESTER
CALIBRATION LAB

H. SHORT
T. RUSSELL

COPY 8



TESTED WITH STANDARDS REFERENCED TO
NATIONAL BUREAU OF STANDARDS



DATE - JAN 13 1986 PAGE - 2 OF - 4
FOLDER NO. - 57 I.D. - DP - FUEL
TEST ITEM PRESSURE TRANSDUCER
CO. - VALIDYNE M.T.I.
MOD - DP-45-26 D.O.E. COMB.
S/N - 42705 CH. NO. 1
TRANS AMPL.
LOCATION FREE PISTON TEST CELL # 2
N.K.R.
OPERATOR W.G. SPODNEWSKI - D.S.
CALIB. FOR G. KOESTER
Traceability Data
CALIBRATOR DIGITAL PRESS. INDICATOR
CO. DRUCK
MOD DPI-600
S/N 600/0128

ADDITIONAL INSTRUMENTS -
1. DIGITAL MULTIMETER
H.P. MOD - 3465B S/N - 1530 A03005
2. _____
3. _____
4. _____

STANDARD				TEST ITEM	
	H ₂ O	CRG	CRG	VOLTS	ERROR
				D.C.	VOLTS
1.	0	0	0	0.046	0.46
2.	2	2.0	2	2.023	0.23
3.	4	4.0	4	4.013	0.13
4.	(*) 6	6.0	(*) 6	6.006	0.06
5.	8	8.0	8	8.042	0.42
6.	10	10.0	10	10.050	0.50
7.					
8.					
9.					
10.					
11.					

NOTES: ☒ CALIBRATION DUE JULY 1, 1986
☒ REGALIBRATION - LAST ON: 2/26/85
☒ CALIBRATED (+) PORT - NORMAL POSITION
☒ (+) AMPL. SETTINGS: ZERO - 456 SPAN - 724

SIGNED: W. Spodnewski

CALIBRATION LABORATORY - NKR PLANT



MECHANICAL TECHNOLOGY INCORPORATED
LATHAM, N.Y.

G. KOESTER
CALIBRATION LAB

H. SHORT
T. RUSSELL

COPIES TO:



TESTED WITH STANDARDS REFERENCED TO
NATIONAL BUREAU OF STANDARDS



DATE - JAN. 13, 1986 PAGE - 4 OF - 4
FOLDER NO. - 384 I.D. - P-AIR
TEST ITEM PRESSURE TRANSDUCER
CO. - DYNISCO SELF CONTAINED
MOD - APT 320J-25
S/N - 142570
TRANS. AMPL.
LOCATION FREE PISTON TEST CELL # 2
N.K.R.
OPERATOR W.G. SPODNEWSKI - D.S.
CALIB. FOR G. KOESTER
Traceability Data
CALIBRATOR DIGITAL PRESS. INDICATOR
CO. DRUCK
MOD DPI-600
S/N 600/0122
ADDITIONAL INSTRUMENTS -
1. DIGITAL MULTIMETER
H.P. MOD-34652, SN-1530 AD 3095

SIGNED: [Signature]

CALIBRATION LABORATORY - IHR PLANT



MECHANICAL TECHNOLOGY INCORPORATED
LATHAM, N.Y.

	STANDARD		TEST ITEM		
	PSI	CALC.	VOLTS		ERROR
			VOLTS	D.C.	VOLTS
1.	0	2.9	2.900		0
2.	1	3.1	3.101		.001
3.	2	3.3	3.300		0
4.	3	3.5	3.502		.002
5.	4	3.7	3.700		0
6.	5	3.9	3.902		.002
7.	10	4.9	4.896		.004
8.					
9.					
10.					
11.					

NOTES: ☒ CALIBRATION DUE JULY 1, 1986
☒ RECALIBRATION - NO RECORD
☒ CALIBRATED (+) POST-NORMAL POSITION

G. KOESTER
CALIBRATION LAB

H. SHOOT
T. RUSSELL

COPIES TO:



TESTED WITH STANDARDS REFERENCED TO
NATIONAL BUREAU OF STANDARDS



DATE - JAN. 13, 1986 PAGE - 3 OF - 4
FOLDER NO. - 383 I.D. - P-FUEL
TEST ITEM PRESSURE TRANSDUCER
CO. - DYNISCO SELF CONTAINED
MOD - DPT 320J-25
S/N - 142571
TRANS. AMPL.
LOCATION FREE PISTON TEST CELL # 2
N.K.R.
OPERATOR W.G. SPODNEWSKI - D.S.
CALIB. FOR - G. KOESTER
Traceability Data
CALIBRATOR DIGITAL PRESS. INDICATOR
CO. DRUCK
MOD DPT-600
S/N 600/0122

ADDITIONAL INSTRUMENTS -
1. DIGITAL MULTIMETER
H.P. MOD-3465B, S/N-1530A03095
2. _____
3. _____

STANDARD			TEST ITEM		
	PSI	CALC.	VOLTS	ERROR	
		VOLTS	D.C.	VOLTS	
1.	0	2.9	2.900	0	
2.	1	3.1	3.100	0	
3.	2	3.3	3.300	0	
4.	3	3.5	3.500	0	
5.	4	3.7	3.700	0	
6.	5	3.9	3.900	0	
7.	10	4.9	4.895	.005	
8.					
9.					
10.					
11.					

NOTES: ☒ CALIBRATION DUE JULY 1, 1986
☒ RECALIBRATION - NO RECORD
☒ CALIBRATED (+) PORT - NORMAL POSITION

SIGNED: [Signature]

CALIBRATION LABORATORY - NKR PLANT

MECHANICAL TECHNOLOGY INCORPORATED
LATHAM, N.Y.



G. KOESTER
CALIBRATION LAB

H. SHORT
T. RUSSELL

COPIES

PI TOI



END

DATED

FILM

8-88

Dtic